Inaugural Dissertation

for

obtaining the doctoral degree

of the

Combined Faculty of Mathematics, Engineering and Natural Sciences

of the

Ruprecht -Karls- University

Heidelberg

Presented by

Sridhar Kandala

Master of Science, Medical Biotechnology

Born in Hyderabad, India

Oral examination: January 24th,2023

Chronic chromosome instability induced by Plk1 results in immune suppression in breast cancer

Referees

Prof. Dr. Hans Reimer Rodewald

Prof. Dr. Benedikt Brors

Prof. Dr. Sylvia Erhardt

Dr. Guoliang Cui

ఈ పని నా ప్రియమైన తల్లిదండ్రులకు అంకితం చేయబడింది

నాగమణి కందాళ మరియు సత్యనారాయణ మూర్తి కందాల,

మరియు నా భార్యకు

సుస్మిత నెట్టు

This work is dedicated to my beloved parents

Nagamani Kandala and Satyanarayana Murthy Kandala,

and to my wife

Susmitha Nettu

Division of Molecular Thoracic Oncology (B220)
Head of Division: Prof. Dr. Rocio Sotillo
German Cancer Research Center (DKFZ)
Heidelberg, Germany

Contributions

This thesis was performed in collaboration with the group of Prof. Dr. Benedikt Brors from the division of Applied Bioinformatics (B330) at the Deutsches Krebsforschungszentrum (DKFZ), Heidelberg, Germany. The group helped us with the analysis of single cell sequencing data which is presented in the thesis. I am also thankful for the suggestions received from the following people who have been acknowledged appropriately in the prepared manuscript.

Contributions:

Design of the project and experiments: Sridhar Kandala[1,2], Rocio Sotillo[1,4]

Performing experiments: Sridhar Kandala[1,2], Sara Chocarro[1,2], Maria Ramos[1,2]

Sorting: Sridhar Kandala[1,2] and Yuanyuan Chen[1]

Bioinformatic analysis: Lena Voith von Voithenberg[3], Anand Mayakonda[2,5], Sridhar Kandala[1,2], Charles D. Imbusch[3].

Affiliations:

[1]Division of Molecular Thoracic Oncology, German Cancer Research Center (DKFZ), Heidelberg, Germany

[2]Faculty of Biosciences, Heidelberg University, 69120, Heidelberg, Germany

[3]Division of Applied Bioinformatics, German Cancer Research Center (DKFZ), Heidelberg, Germany

[4]Translational Lung Research Center Heidelberg (TRLC), German Center for Lung Research (DZL)

[5]Division of Cancer Epigenomics (DKFZ), Heidelberg, Germany

The results presented in the thesis are integrated into the manuscript “Chronic chromosome instability induced by Plk1 results in immune suppression in breast cancer”, which is presently in bioRxiv (https://doi.org/10.1101/2022.06.16.496429). The author of the present thesis, Sridhar Kandala, is the first author of the above-mentioned research article and contributed significantly to the design of the project, data analysis, data interpretation and manuscript writing. Contributions from co-authors are acknowledged in the figure/table legends wherever necessary.

Declarations

Declarations according to § 8 (3) b) and c) of the doctoral degree regulations:

a) I hereby declare that I have written the submitted dissertation myself and, in this process, I have used no other sources or materials than those expressly indicated.

b) I hereby declare that I have not applied to be examined at any other institution, nor have i used the dissertation in this or any other format at any other institution as an examination paper, nor submitted it to any other faculty as a dissertation.

Sridhar Kandala

Table of Contents

Summary

Chromosomal instability (CIN), the failure of cells to segregate chromosomes correctly during cell division, is a typical feature of solid and hematopoietic tumors. By fostering intratumor heterogeneity and facilitating therapy resistance CIN aids in the growth of tumors. Natural killer (NK) cells have been shown to recognize and destroy cells with complex karyotypes in *in vitro* experiments. Contrarily, immunosuppressive phenotype has also been noted in human malignancies with high levels of CIN. However, which CIN-associated genetic characteristics influence immune recognition during tumor progression still remains to be elucidated. Previous research from our group demonstrated that overexpression of Polo-like kinase 1 (Plk1) in Her2-positive mammary tumors, resulted in increased CIN levels along with a delay in tumor initiation. Using the same mouse model, I demonstrate that Her2-Plk1 tumors induce a senescence-associated secretory phenotype (SASP) and mediate immune evasion by upregulating PD-L1 and CD206 and inducing non-cell-autonomous NF-kB signaling (RELB). Immune cells from early-stage induced mammary glands were sequenced and the results disclosed the presence of $Arg1^{+}$ macrophages with EMT signatures, NK cells ($CD11b^{-}CD27^{+}$) with reduced effector capabilities along with increased infiltration of resting regulatory T cells during development of Her2-Plk1 tumors compared to tumors with low CIN. Thus, immune modulation in tumors possessing high CIN happens very early during tumor development with multiple arms of the immune system playing an important role. We further corroborate similar findings in human breast tumors expressing high levels of PLK1 and find upregulation of gene sets associated with SASP, NF-kB signaling and immune suppression. In conclusion, the results presented from *in vivo* experiments aid in understanding the interaction between different levels of CIN and the immune system. The study also highlights the need for novel adjuvant therapies such as anti-PDL1 or RELB inhibition in the context of chromosomally unstable tumors expressing PLK1.

Zusammenfassung

Chromosomeninstabilität (CIN), also das Versagen von Zellen bei der korrekten Segregation von Chromosomen während der Zellteilung, ist ein typisches Merkmal solider und hämatopoetischer Tumoren. Indem sie die Heterogenität innerhalb des Tumors fördert und die Therapieresistenz erleichtert, unterstützt CIN das Wachstum von Tumoren. Natürliche Killerzellen (NK-Zellen) haben in In-vitro-Versuchen gezeigt, dass sie Zellen mit komplexem Karyotyp erkennen und zerstören können. Umgekehrt wurde auch bei menschlichen Malignomen mit hohem CIN-Gehalt ein immunsuppressiver Phänotyp festgestellt. Die Frage, welche CIN-assoziierten genetischen Merkmale die Immunerkennung während der Tumorprogression beeinflussen, muss jedoch noch geklärt werden. Frühere Forschungsarbeiten unserer Gruppe haben gezeigt, dass die Überexpression von Polo-like kinase 1 (Plk1) in Her2-positiven Brusttumoren zu erhöhten CIN-Werten und einer Verzögerung der Tumorentstehung führt. Anhand desselben Mausmodells zeige ich, dass Her2-Plk1-Tumore einen Seneszenz-assoziierten sekretorischen Phänotyp (SASP) induzieren und durch Hochregulierung von PD-L1 und CD206 sowie Induktion der nicht-zellautonomen NF-kB-Signalisierung (RELB) eine Immunevasion vermitteln. Immunzellen aus induzierten Brustdrüsen im Frühstadium wurden sequenziert, und die Ergebnisse enthüllten das Vorhandensein von Arg1+-Makrophagen mit EMT-Signaturen, NK-Zellen (CD11b-CD27+) mit reduzierten Effektor-Fähigkeiten zusammen mit einer erhöhten Infiltration ruhender regulatorischer T-Zellen während der Entwicklung von Her2-Plk1-Tumoren im Vergleich zu Tumoren mit niedrigem CIN. Die Immunmodulation in Tumoren mit hohem CIN findet also schon sehr früh während der Tumorentwicklung statt, wobei mehrere Arme des Immunsystems eine wichtige Rolle spielen. Wir bestätigen ähnliche Ergebnisse in menschlichen Brusttumoren, die hohe PLK1-Konzentrationen aufweisen, und finden eine Hochregulierung von Gensätzen, die mit SASP, NF-kB-Signalen und Immunsuppression in Verbindung stehen. Zusammenfassend lässt sich sagen, dass die vorgestellten Ergebnisse aus In-vivo-Experimenten dazu beitragen, die Interaktion zwischen verschiedenen Ebenen von CIN und dem Immunsystem zu verstehen. Die Studie unterstreicht auch die Notwendigkeit neuer adjuvanter Therapien wie Anti-PDL1- oder RELB-Inhibition im Zusammenhang mit chromosomal instabilen Tumoren, die PLK1 exprimieren.

List of Figures

List of Tables

Acronyms

Acronym	Definition
CIN	Chromosomal instability
MEF	Mouse embryonic fibroblast
FISH	Fluorescence insitu hybridization
GFP	Green fluorescence protein
PLK1	Polo like kinase
MAD2	Mitotic arrest deficient
MudPIT	Multidimensional protein identification technology
SILAC	Stable isotope labelling by aminoacids in culture
HCT116	Human colorectal carcinoma
MHC	Major histocompatibility complex
UPS	Ubiquitin proteasome system
ROS	Reactive oxygen species
DSB	Double strand break
SAC	Spindle assembly checkpoint
RPE1	Retinal pigment epithelial cells
MPS1	Monopolar spindle
BUB1	Budding uninhibited by benzimidazoles
ITH	Intra tumor heterogeneity
5-FU	5-Fluorouracil
APC	Adenomatous polyposis coli
CiMKi	Cre inducible MPS1 knock in
PTEN	Phosphatase and tensin homolog
REST	RE1 silencing transcription factor
SUZ12	Suppressor of Zeste
ZNF98	Zinc finger protein
MMTV	Mouse mammary tumor virus
rtTA	Reverse tetracycline controlled transactivator
CDK	Cyclin dependent kinase
PCNA	Proliferating cell nuclear antigen
PRR	Pattern recognition receptor
PAMP	Pathogen associated molecular patterns
HMGB1	High mobility group box1
TCR	T cell receptor
TNF	Tumor necrosis factor
IL-1	Interleukin
SCNA	Somatic copy number alterations
TCGA	The cancer genome atlas

GSEA	Gene set enrichment analysis
CRC	Colorectal cancer
IRF	Interferon
GZM	Granzyme
cGAS	Cyclic GMP-AMP synthase
STING	Stimulator of interferon response CGAMP interactor1
ULBP	UL16 binding protein
MICA	MHC class1 polypeptide related sequence A
MICB	MHC class1 polypeptide related sequence B
NKG2D	Natural killer group 2D
cGAMP	Cyclic guanosine monophosphate- adenosine monophosphate
TBK	Tank binding kinase
ISG	Interferon stimulated genes
MDA-MB-231	MD Anderson metastatic breast 231
EMT	Epithelial to mesenchymal transition
NF-KB	Nuclear factor kappa light chain enhancer of activated B cells
BRCA	Breast cancer gene
HER2	Human epidermal growth factor receptor 2
ER^+	Estrogen receptor
PR^+	Progesterone receptor
FACS	Fluorescence activated cell sorting
PCR	Polymerase chain reaction
HCL	Hydrochloric acid
NAOH	Sodium hydroxide
DEG	Differentially expressed genes
GO	Gene ontology
SDS	Sodium dodecyl sulphate
FBS	Fetal bovine serum
DMEM	Dulbecco's modified eagle medium
DTT	Dithiothreitol
TME	Tumor microenvironment
TIL	Tumor infiltrating lymphocyte
MCF	Michigan cancer foundation
CAL51	Centre antoine lacassagne
PCA	Principle component analysis
MMP	Matrix metalloproteases
CXCL	Chemokine ligand
KIF	Kinesin superfamily proteins

JAK	Janus kinase
STAT	Signal transducer and activator of transcription
TAM	Tumor associated macrophages
IDO1	Indoleamine 2,3 dioxygenase
PDCD1	Programmed cell death protein 1
VEGF	Vascular endothelial growth factor
TIMP	Tissue inhibitors of metalloproteinases
TCF	T cell factor
HAVCR	Hepatitis virus A cellular receptor 1
TIGIT	T cell immunoreceptor with Ig and ITIM domains
LAG	Lymphocyte activation gene
LUSC	Lung squamous cell carcinoma
TGCT	Tenosynovial giant cell tumor
STAD	Stomach adenocarcinoma
GBM	Glioblastoma
ESCA	Esophageal carcinoma
KIRC	Kidney renal clear cell carcinoma
THCA	Thyroid carcinoma
THYM	Thymoma
BLCA	Bladder urothelial carcinoma
LIHC	Liver hepatocellular carcinoma
TNFRSF	Tumor necrosis factor receptor superfamily

1. Introduction

1.1 Chromosomal instability (CIN) and methods to detect CIN

Chromosomal instability (CIN) is a condition in which cells experience chromosome segregation errors during mitosis, resulting in aneuploidy. Aneuploidy is associated with chromosome copy number changes and structural modifications like deletions, amplifications, insertions etc. Large-scale tumor analysis shows that 86% of solid tumors and 72% of hematopoietic tumors are aneuploid and have high missegregation rates (Zasadil et al., 2013). Although CIN and aneuploidy are sometimes used interchangeably, it's important to understand the difference between the two. Aneuploidy is a genetic condition while CIN is a cellular state that leads to aneuploidy. Ongoing CIN beginning from a euploid state results in various missegregation events (Figure 1). However, cells can also be aneuploid without displaying characteristics of CIN (Trisomy 21) and these are termed as stably aneuploid, as they carry the same number of chromosomes in every cell division. Stable aneuploid cell lines are used *in vitro* to study the effects of aneuploidy in the absence of CIN.

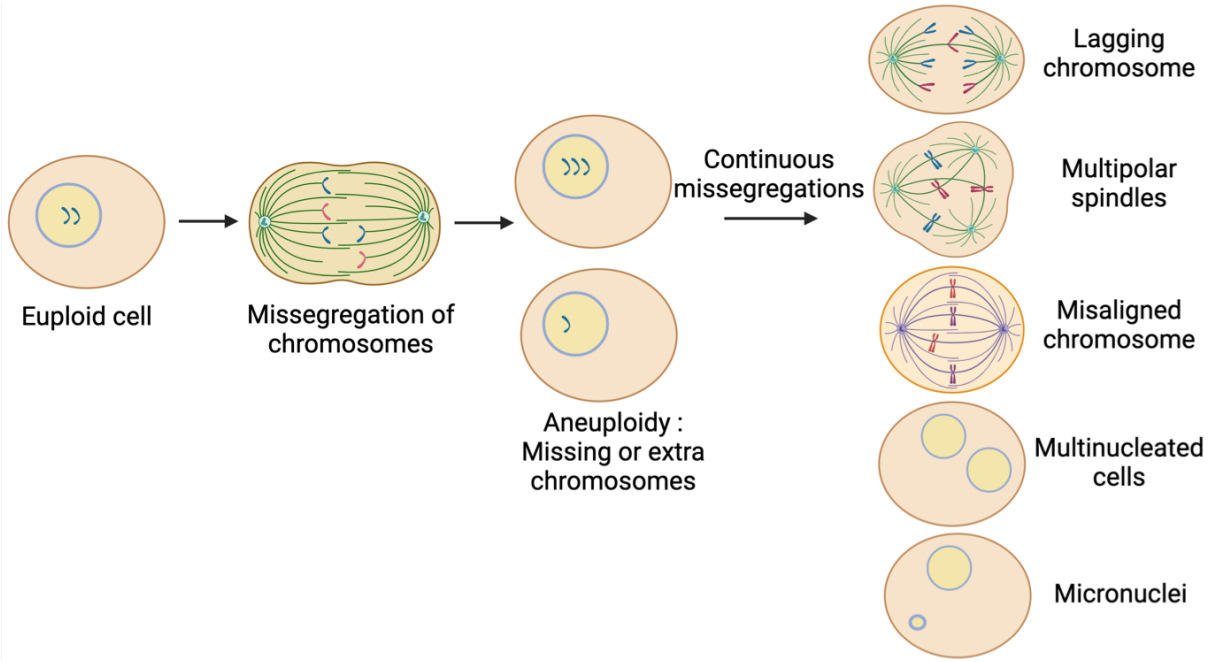

Figure 1: Different missegregation events generated as a consequence of ongoing chromosomal instability beginning from a euploid state in a cell. *Created with Biorender.com*

There are many ways in which CIN can be studied both *in vitro* and *in vivo*. The effect of CIN is mainly influenced by the rate of missegregation and also the type of missegregation induced. Mouse embryonic fibroblast cells (MEFs), primary tumor cells and organoids isolated from

mouse models of genetically induced CIN are primarily used in the *in vitro* setting to quantify rates of CIN. *In vitro* quantification of CIN is mainly done through fluorescence in-situ hybridization (FISH), immunofluorescence or immunohistochemistry of fixed cells in mitosis. There are drawbacks associated with using *in vitro* models. Firstly, the ability to determine the actual rate of missegregation (takes a snapshot of mitosis). Secondly, the absence of a microenvironment involving the immune, nervous and endocrine systems and lastly the influence of cell culture conditions on CIN behavior as different cell types respond differently to CIN *in vitro* (Thompson et al., 2010). *In vivo* measurements include the use of single-cell DNA sequencing, time-lapse microscopy (mouse models expressing H2B-GFP) or intra-vital imaging to monitor missegregation in mitosis over time. Overexpression of mitotic checkpoint proteins like Plk1, Mad2 etc in different tumor models are predominantly used as genetic models to understand the consequences of CIN in tumorigenesis. However, the only disadvantages associated with *in vivo* measurements include the technical difficulty of creating H2B-GFP animal models and high cost of sequencing. Therefore, in most cases levels of aneuploidy are used as an end point measurement to quantify CIN levels in a particular cell type.

1.2 Physiological consequences of chromosome missegregations

CIN induces both direct and indirect effects on the transcriptome. Gene dosage effects are the direct consequence of chromosome copy numbers, where the RNA expression is proportional to chromosome gains or losses (Williams et al., 2008). Besides the direct effects, it is also shown in yeast that aneuploidy causes upregulation of 43-78% downstream genes located on other chromosomes which are targets of the genes encoded on aneuploid chromosomes (Pavelka et al., 2010; Rancati et al., 2008). To further see if changes in transcriptome translate to protein level, Pavelka et al., 2010 and Torres et al., 2010 used multidimensional protein identification technology (MudPIT) and stable isotype labeling with amino acids in cell culture (SILAC) based mass spectroscopy to show that protein levels do corelate with DNA copy numbers in yeast. Interestingly, it is found to be less pronounced in human cells because of dosage compensation. SILAC analysis on HCT116 cells showed a 1.6-fold increase in protein levels for genes encoded on chromosome 5 with tetrasomy compared to cells diploid for chromosome 5 (Stingele et al., 2012). However, such a reduction in protein levels in not because of a decrease in translation but increase in protein degradation levels. Also seen in aneuploid cells is the upregulation of genes corresponding to MHC complex, antigen presentation, metabolic pathways and ER, Golgi and lysosome related pathways (Durrbaum et al., 2014). However, the

degree of stress depends on various factors like ploidy level, cell type and tissue of origin. Different types of stress induced by aneuploidy are elucidated below:

Proteotoxic stress: Unbalanced gene expression often results in proteotoxic stress due to defective protein folding and homeostasis (Deshaies et al., 2014, Morimoto et al., 2008). Cells exhibiting CIN overproduce proteins that go beyond the ability of chaperones to fold them or proteasome to remove misfolded or damaged proteins (Donnelly and Storchova et al., 2015). Apart from upregulation of genes associated with ubiquitin proteasome system (UPS), aneuploid cells show lysosome dependent activation of autophagy through increased LC3 and p62 expression (Stingele et al., 2012). However, the ability of chromosomally unstable cells to tolerate extra proteins differs from karyotype to karyotype.

Metabolic stress: Malfunctioning of a particular set of enzymes and their regulators leads to an imbalance in metabolic homeostasis. Aneuploidy induced altered metabolism causes changes in glutamine and glucose uptake (Williams et al., 2008). Other studies show downregulation of proteins involved in RNA, DNA and carbohydrate metabolism while upregulation of mitochondrial metabolism in tetrasomic HCT116 cells (Stingele et al., 2012). Metabolic defects are also associated with increase in Reactive oxygen Species (ROS) levels (Apel et al., 2004) causing further DNA damage and proteotoxicity.

Replication stress: Stalling of replication fork progression during DNA replication induces replication stress (Mazouzi et al., 2014). Replication stress leads to cell cycle arrest as a result of cell cycle checkpoint activation. Inability to repair the halted replication fork induces DNA damage in the form of double stranded breaks (DSB). In addition to DNA damage, replication stress also induces senescence and immunological detection of aneuploid cells (Adriani et al., 2016; Santaguida et al., 2017).

Mitotic stress: Copy number changes lead to altered ratio of protein machinery involved at the spindle assembly checkpoint (SAC), thus contributing to karyotype diversity. Classic example of this comes from the treatment of RPE-1 cells with MPS1 inhibitor to generate cells with different levels of aneuploidy (Santaguida et al., 2017). Followed by the removal of MPS1 and in the presence of SAC, the daughter cells show high levels of mitotic aberrations like lagging chromosomes and micronuclei during mitosis as observed by live cell imaging. Thus, mitotic stress persisting in cells harboring aneuploidy contribute to further chromosomal instability.

1.3 Chromosomal instability (CIN): A Hallmark of Cancer

The loss or gain of chromosomes can cause phenotypic differences due to changes in expression of genes, as described previously. This is the key reason why CIN promotes tumor heterogeneity and is linked with poor patient survival in many tumor types. Majority of chromosome missegregations are caused by abnormalities in the mitotic process such as amplification of centrosomes, pre-mitotic replication stress, incorrect microtubule-kinetochore attachments and dysregulation of mitotic checkpoint (Holland et al., 2009; Vitre et al., 2012). Both loss of function and hyper activation of the spindle assembly checkpoint proteins lead to missegregations, with low rate of missegregations associated with loss of function phenotype (Janssen and Medema et al., 2013). Studies from mouse models have shown that tumors overexpress checkpoint proteins such as Plk1 (de Carcer et al., 2018), Mad2 (Sotillo et al., 2007), Bub1 (Ricke et al., 2011), BubR1 (Baker et al., 2013). The consequence of overexpression results in cell cycle arrest in G1 phase due to activation of DNA damage signaling or further missegregations resulting in micronuclei (Rowald et al., 2016) or binucleated cells (de Carcer et al., 2018) in Mad2 and Plk1 breast tumors respectively.

The role of CIN in tumor evolution remains very complex. The prevalence of CIN in tumors generates new karyotypes promoting intra-tumor heterogeneity (ITH) and selecting advantageous karyotypes. Interestingly, by looking at the levels of CIN in tumors, intermediate levels induce tumor growth, while high and very high levels of CIN impair tumor growth and also show good prognosis (de Carcer et al., 2018; Silk et al., 2013; Zasadil et al., 2016). One theory put forward to support the tumor suppressive effects of CIN is the high production of nonviable karyotypes or activation of p53 activity (Ohashi et al., 2015; Thompson et al., 2010, Soto et al., 2017). Furthermore, CIN correlates with resistance to cytotoxic chemotherapy drugs such as taxol in tumor-derived cell lines and human tissues (Bakhoum et al., 2011, Swanton et al., 2009). Reciprocally, chromosome missegregations also sensitize glioblastomas to radiation treatment and ovarian and breast tumors to cisplatin and 5-fluorouracil (5-FU) therapies (Roylance et al., 2011; Swanton et al., 2009). Thus, it can be understood that CIN could have profound effects not only on cancer cells but other cell types in the tumor microenvironment. These can be termed as non-cell autonomous effects. Nevertheless, to say, tumors having high levels of CIN such as triple-negative breast cancer, pancreatic cancer, lung cancer, anaplastic thyroid cancer, poorly differentiated sarcomas and colorectal cancer show more propensity towards therapy resistance, immune evasion, metastasis with decreased overall survival (Bielski et al., 2018, Carter et al., 2012).

Furthermore, understanding how different levels of CIN in different tissues affect tumor formation is very important. Hoevenaar et al., 2020 used Cre-inducible *CiMKi* knock-in model carrying conditional T649A(TA) or D637A (KD) kinase-dead mutation in spindle assembly checkpoint kinase *Mps1* to induce different levels of CIN (in the intestine, *CiMKi: Villin-Cre*) ranging from mild to very high. CIN lead to early and spontaneous tumor initiation, with the strongest effect in animals with moderate CIN levels (multiple low-grade adenomas in the small intestine and colon). To further understand the impact of CIN on tissues already predisposed to cancer, Hoevenaar et al, used *CiMKi* mice with a mutant APC allele and found that moderate to high CIN substantially increased the number of adenomas in the colon and small intestine, with tumors appearing in the distal part of the colon, as seen in humans. Moderate to high CIN accelerated tumor growth and initiation compared to low and very high (embryonic lethal) levels of CIN and a similar phenotype was seen in organoids cultured from the tumors. In humans, adenomas from the distal part of the colon are highly aneuploid, and sc-KaryoSeq of the adenomas in the distal part of the colon induced by moderate to high CIN (mutant APC allele) also showed elevated levels of aneuploidy and heterogeneity. These data suggest that tumor formation and karyotype heterogeneity primarily depend on the degree of CIN and the tissue of origin. Further studies, involving the use of mouse models with varying degrees of CIN to induce spontaneous/inducible tumors in different tissues will add more value to the existing evidence and determine the site-dependent effect of CIN.

1.4 Plk1 and its role in Tumorigenesis

Plk1, also known as polo-like kinase 1 is a serine/threonine protein kinase that mediates G2/M transition during the cell cycle and also phosphorylates various substrates as the cell transitions through different phases of mitosis until cytokinesis (Barr et al., 2004). Besides, Plk1 also plays a crucial role in regulating the spindle assembly, centrosome maturation, chromosome segregation and DNA replication etc (Liu et al., 2010; Song et al., 2011). The role of Plk1 remains ambiguous as studies show both the oncogenic and tumor-suppressive ability of this gene. The oncogenic effects of Plk1 have been associated with the modulation of tumor suppressors like PTEN (phosphorylating at Ser385), REST (phosphorylation at Ser1030), SUZ12 (phosphorylation at Ser539, Ser541), ZNF98 (phosphorylation at Ser303, Ser305, Ser309) preventing its localization to the nucleus (Li et al., 2014) or favoring protein degradation by the proteasome (Karlin et al., 2014). On the contrary, Plk1 is known to phosphorylate histone methyltransferase MLL2 at Ser4822 to activate tumor suppressors downstream of the Estrogen receptor (ER) (Wierer et al., 2013). Furthermore, overexpression

of Plk1, reduced tumor incidence in Her2 (50%) and Kras (85%) breast tumor models (Rowald et al., 2016; de Carcer et al., 2018). Moving beyond breast tumors, Plk1 knockdown in combination with mutant APC allele increases the incidence of colorectal polyps (Raab et al., 2018). Since this thesis focuses on the role of Plk1 in breast cancer, I will elaborate more on the phenotype associated with Plk1 expression in the mammary glands.

de Carcer et al, showed the *in vivo* effects of Plk1 overexpression in malignant transformation by using an *in vivo* mouse tumor model that overexpresses Her2 (Neu) and Plk1 in an inducible manner under the control of mammary gland tumor virus promoter (MMTV-rtTA). Plk1 overexpression in mammary tumors caused a delay in tumor initiation with first palpable tumors appearing after 349 days compared to Her2 tumors with tumors appearing in 112 days after doxycycline administration. These Her2-Plk1 tumors exhibited high percentage of somatic copy number alterations and aneuploidy as seen by low coverage whole genome sequencing (WGS) and fluorescence insitu hybridization (FISH). Further phenotypic validation revealed that these tumors cells were arrested in the G1 phase of the cell cycle expressing high levels of the CDK inhibitor p21 and p16 with reduced expression of proliferation markers such as Ki67 and PCNA. Interestingly, time-lapse microscopy of these cells showed abnormal chromosome missegregations and cytokinesis failure resulting in polyploidy (binucleated cells). In summary, a few key points to consider when talking about Plk1 expression in tumors: Firstly, Plk1 expression by itself does not function as an oncogene. Secondly, Plk1 can act as a tumor suppressor when combined with oncogenes like Her2 or Kras (de Carcer et al., 2018) and induces significantly high mitotic aberrations leading to CIN and lastly like many other cell cycle checkpoint genes, Plk1 is also commonly overexpressed in different cancer types and is associated with bad prognosis (Ramani et al., 2015; Tut et al., 2015; Zhang et al., 2015). This comes from the fact that several genes associated with the CIN70 signature (proliferation/cellcycle) are frequently upregulated in cancers and Plk1 is a component of the CIN70 signature (Maleki et al., 2017). Plk1 inhibitors (Volasertib, BI2536) are also presently being tested clinically for various solid and hematopoeitic tumors. So far the cellular effects of Plk1 overexpression in tumor development have been described, however the immune responses associated with Plk1 overexpression still remain to be eluciated.

1.5 Innate and adaptive immune system

The human immune system includes both innate and adaptive immune responses. The innate immune system comprises of anatomical barriers (epithelial skin layers and glandular tissue surfaces) along with cellular responses (phagocytosis and inflammation) to infection. It is made up of cells like Macrophages, Natural Killer cells (NK), Dendritic cells, Mast cells, Neutrophils, Basophils and Eosinophils. The innate immune system functions primarily by recruiting immune cells to the site of infection by releasing cytokines and by activation of the complement system. The complement system triggers the recruitment of inflammatory cells and tags the surface of infected cells with proteins called opsonins. The infected cells coated with opsonins are then phagocytized by scavenger cells like macrophages. Inflammation is a key cellular response to infection, mediated by macrophages, neutrophils, mast cells etc. They present exclusive receptors called pattern recognition receptors (PRRs) which recognize molecules present on pathogens and damaged cells and mediate the release of inflammatory cytokines. The molecules present on damaged cells are often referred to as pathogen-associated molecular patterns (PAMPs) or damage-associated molecular patterns (DAMPs). Cytokines released during inflammation include TNFa, IL-1, HMGB1 etc (Turner et al., 2014).

On the other hand, the adaptive system, also called as acquired immunity is a slower response compared to innate immunity, but is highly specific to the encountered pathogen and creates immunological memory. It is comprised of B cells and T cells that develop from multipotent hematopoietic cells in the bone marrow (Fischer et al., 2020). As the name suggests, B cells develop and mature in the bone marrow. Naïve B cells circulate in the lymphatic system until they encounter an antigen and once the appropriate antigen is bound to the membrane bound antibody receptor, B cells are activated to differentiate to plasma cell (producing antibodies) or memory B cells. The diversity of B and T cell receptors is facilitated by somatic recombination of gene segments resulting in a wide array of antigen specific receptors. Various immune cell subsets are shown below (Figure 2).

Similarly, T cells migrate and mature in the thymus (Schmitt et al., 1995). In the thymus T cells express T cell receptors (TCRs) along with CD4 or CD8. Unlike B cells, T cell receptors recognize antigen bound to MHC I or MHC II (major histocompatibility complex) molecules. These MHC receptors are present on the surface of antigen-presenting cells like macrophages and dendritic cells. For efficient functioning of T cells, they also undergo positive selection (ensures MHC restriction) and negative selection (maintenance of self-tolerance). After the

selection process, mature T cells are classified into three types: Helper T cells (express CD4 and aid in the activation of B cells and other immune cells), Cytotoxic T cells (express CD8 and aid in the removal of infected cells or pathogens) and Regulatory T cells (express CD4, CD25 and aid in reducing the risk of autoimmune diseases by distinguishing self and nonself molecules).

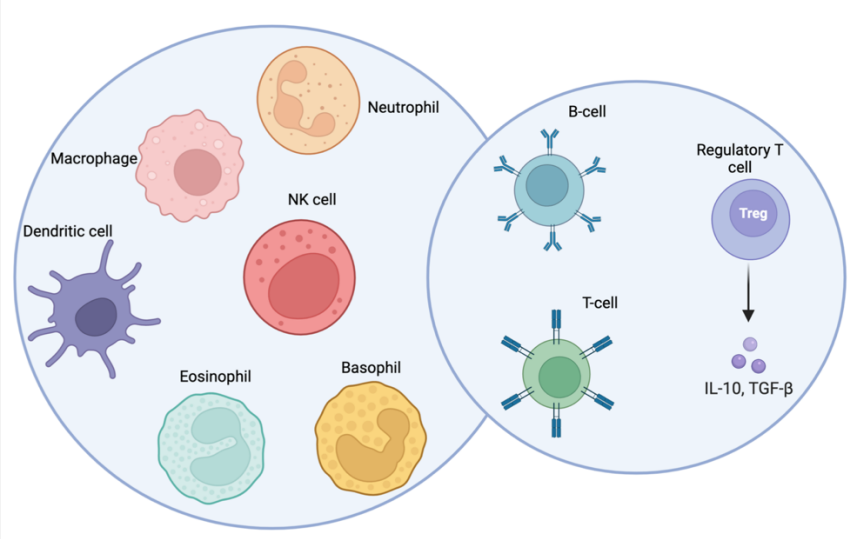

Figure 2: Various cell types of the innate (left) and adaptive immune system (right). *Created with Biorender.com*

1.6 Immune Responses to Chromosomal Instability

A key question in the field of aneuploidy is how an ongoing CIN shapes tumor evolution and affects immune cell infiltration in the context of high and low CIN tumors. Several studies have so far attempted to address this question through *in silico* studies and *in vitro* models along with the identification of pathways mediating immune surveillance. One of the earliest computational studies done by Davoli et al., 2017 showed the relationship between somatic copy number alterations (SCNA) levels, mutations, immune cell markers and mitosis/cell cycle genes in multiple tumor types. The study showed a positive correlation between SCNA levels and number of mutations in 8 out of 12 TCGA tumor types, except for colorectal (CRC) and endometrial carcinoma (UCEC) which showed a statistically negative correlation. The positive correlation between high SCNA levels and mutations was seen in passenger genes (not predicted to be cancer drivers) but not in driver genes (tumor suppressor genes and oncogenes). Secondly, gene set enrichment analysis (GSEA) of tumors with high aneuploidy (SCNA levels > 70th percentile) showed downregulation of genes associated with the immune system. Gene

sets associated with T cell and B cell receptors (*CD3E, CD3D, CD247,* Igα, Igβ), cytotoxic functions of T cells and NK cells (*GZMA, GZMB, GZMK, GZMM* etc), IFN-δ pathway (*JAK2, IRF1, IRF2, GBP4*) and genes corresponding to cytokine production (*IL-1β, IL-16, IL-18, CCL3, CCL7, CCL22* etc) were downregulated compared to tumors with low aneuploidy (SCNA levels < 30th percentile). Similarly, clinical trial data from anti-CTLA-4 blockade in melanoma patients (Van allen et al., 2015) shows that long-term survival post-immunotherapy is dependent on tumor SCNA levels and thereby acts as an independent prognostic factor that determines overall survival.

Moving forward to *in vitro* studies, there are several ways for inducing chromosome mis-segregation. Compounds that disrupt microtubule function or microtubule-kinetochore attachment, induce missegregation through delay in mitosis. Some of the common ways include the use of DNA damaging agents (induce double-stranded breaks by interfering with DNA synthesis), spindle poisons like taxanes (effect microtubule dynamics), vinca alkaloids (depolymerization of microtubules), inhibition of mitotic proteins (Plk1, Mad2, Aurora B etc) or chemical inhibitors like reversine (MPS1 inhibitor) and nocodazole (effect microtubule polymerization). Santaguida et.al., 2017 used hTERT immortalized RPE1 cells treated with reversine or NMS-P175 to induce chromosome missegregations. Cells were separated into those that were dividing with low levels of missegregations (mostly euploid) and those that experienced G1 arrest because of multiple chromosome gains and losses (aneuploid). These arrested cells showed features of senescence (elevated levels of CDK inhibitors p16 and p21), increased cytokine production and subsequent elimination by NK cells (Figure 3). Moving to immune responses, arrested cells with complex karyotypes (aneuploid cells) upregulated gene sets corresponding to inflammation and immune response along with cGAS-STING pathway and proinflammatory cytokines like IL6, IL8 and CCL2 compared to cycling RPE1 cells (euploid cells). The trigger for immunogenecity (NK cell activation) in aneuploid cells came from the activation of cell surface proteins like MICA, MICB and NKG2D ligands ULBP1, ULBP2. Likewise, upregulation of CD112 and CD155 on aneuploid RPE1 cells mediated NK cell interaction with aneuploid cells. Furthermore, co-culture of both aneuploid and euploid karyotypes with NK-92 cells showed that NK cells were efficient in killing cells with high levels of aneuploidy 6-12 hours post incubation through the activating receptor NKG2D.

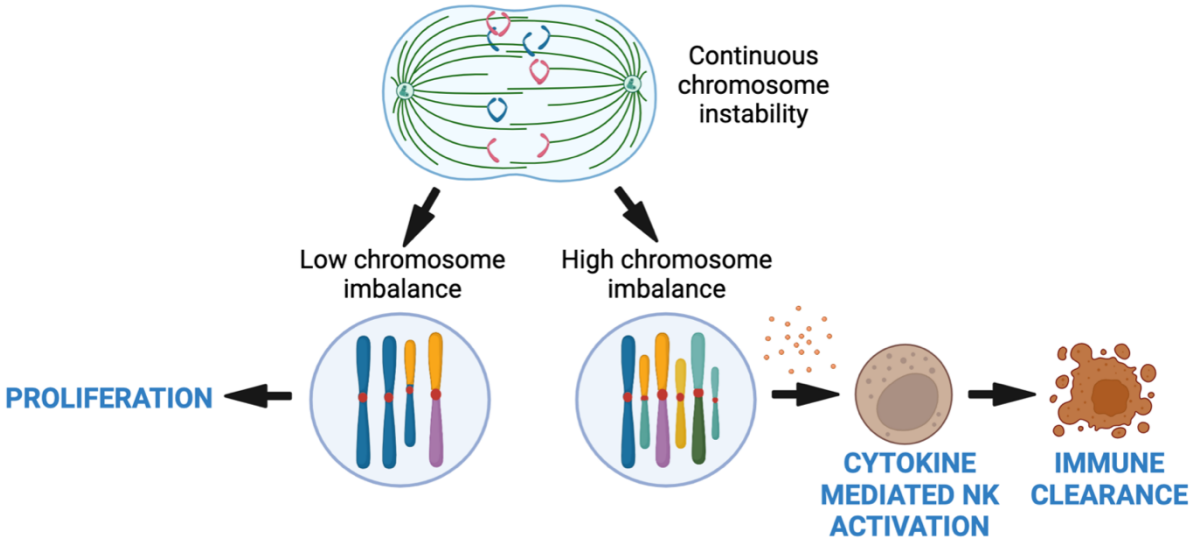

Figure 3: Ongoing chromosome missegregation creates complex karyotypes with high chromosomal instability, which are eliminated by NK cells *invitro*. Modified from Santaguida et.al. 2017. *Created with Biorender.com*

Wang et al., 2021, further explored mechanisms that contribute to NK cell-mediated elimination of aneuploid cells, and identified the NF-kB pathway to be crucial for contributing to immunogenecity (Figure 4). Several factors like G1 arrest associated with characteristics of senescence, activation of both canonical and non-canonical NF-kB signaling, combination of proteotoxic, oxidative and genotoxic stress associated with aneuploidy state appear critical for NK cell-mediated cytotoxicity in aneuploid arrested cells. The study also shows that the levels of aneuploidy positively correlated with NF-kB in transformed cancer cells, but concluded that there are other factors acting in parallel to diminish NK cell-mediated immune response compared to non-transformed cells.

1.7 cGAS-STING pathway in chromosomal instability: Friend or Foe

The cGAS-STING pathway is part of the innate immune system, that detects and responds to cytosolic DNA by the release of inflammatory cytokines (Decout et al., 2021). It plays a pivotal role by mediating communication between tumor cells with chromosomal instability (release of micronuclei into the cytoplasm) and the surrounding tumor microenvironment. Upon binding to dsDNA in the cytoplasm, cGAS produces cGAMP via the C-terminal domain (Sun et al., 2013).

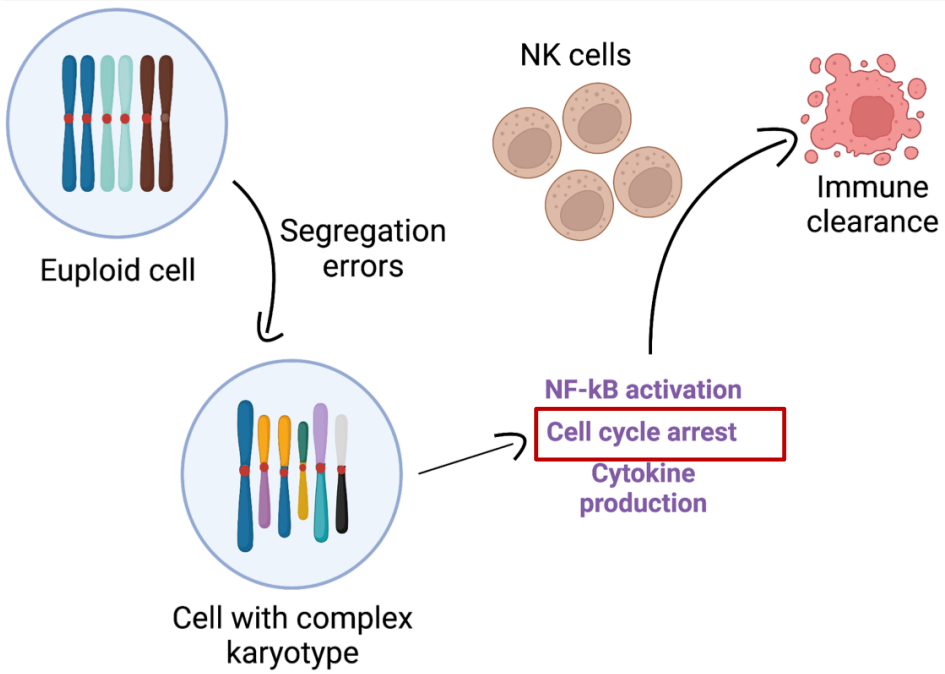

Figure 4: Cells with complex karyotypes are eliminated by NK cells invitro through the activation of NF-kB signaling. Modified from Wang et.al. 2021. *Created with Biorender.com*

cGAMP then binds to STING (Stimulator of interferon genes), helping in the translocation of STING from ER to Golgi (Ishikawa et al., 2008). In the golgi STING recruits TBK1 and IRF3 (Mukai et al., 2016) resulting in the phosphorylation of IRF3 and translocation into the nucleus leading to the activation of Type1 interferon genes and IRF3 target genes (Tanaka et al., 2012). This activation of cGAS-STING and Type1 interferon pathways leads to the recruitment of NK cells to eliminate cells with CIN (Santaguida et al., 2017). Besides, it is also known that larger fragments of DNA activate cGAS more effectively compared to short fragments (Luecke et al., 2017).

Moreover, activation of cGAS-STING by antigen-presenting cells like dendritic cells and macrophages during phagocytosis of cancer cells promotes recruitment and expansion of tumor-specific T cells through interferon upregulation (Deng et al., 2014; Wang et al., 2017). Likewise, STING-deficient mice also showed reduced infiltration of tumor-specific CD8 T cells and activation factors like CD40, CD86 and IL12 (Woo et al., 2014). Furthermore, cGAS also acts as a tumor suppressor by instigating mitotic cell death during prolonged cell cycle arrest by suppressing caspase activation and inhibiting MOMP (Zierhut et al., 2019). Thus, it can be understood that cGAS-STING pathway modulates both innate and adaptive immune responses to suppress tumor growth by activation of IFN signaling and other interferon-stimulated genes (ISG). What remains interesting is the fact that, cGAS-STING levels vary

significantly between tumor types and in breast, prostate and head and neck tumors there is increased expression as a result of decreased methylation at promoter regions (Bakhoum et al., 2018; Konno et al., 2018).

On the contrary, the activation of cGAS-STING is also associated with tumor-promoting effects. One classical example comes from the study of Bakhoum et al., 2018 where MDA-MB-231 breast cancer cells in the presence or absence of a CIN phenotype were transplanted into immunocompromised mice for monitoring metastasis. Mice with CIN phenotype showed decreased average survival, increased in EMT and inflammatory genes and higher metastatic burden. Interestingly, when STING was knocked down in high CIN MDA-MB-231 cells, the cells showed reduced metastatic burden, downregulation of EMT genes and reduced non-canonical NF-kB signaling. Furthermore, cGAS is also known to suppress homologous recombination-mediated DNA repair to promote tumorigenesis (Liu et al., 2018). In addition to this, p38MAPK stress signaling also silences cGAS-STING mediated downstream effects by inhibiting IFN production in the context of chromosomal instability (Dou et al., 2017). The effects of cGAS-STING in the context of CIN are summarized below (Figure 5). Therefore, it can be well understood that cGAS-STING signaling can be modulated for the treatment of cancers in the context of chromosomally unstable tumors. But how the tumor activates or deactivates this pathway is still under investigation.

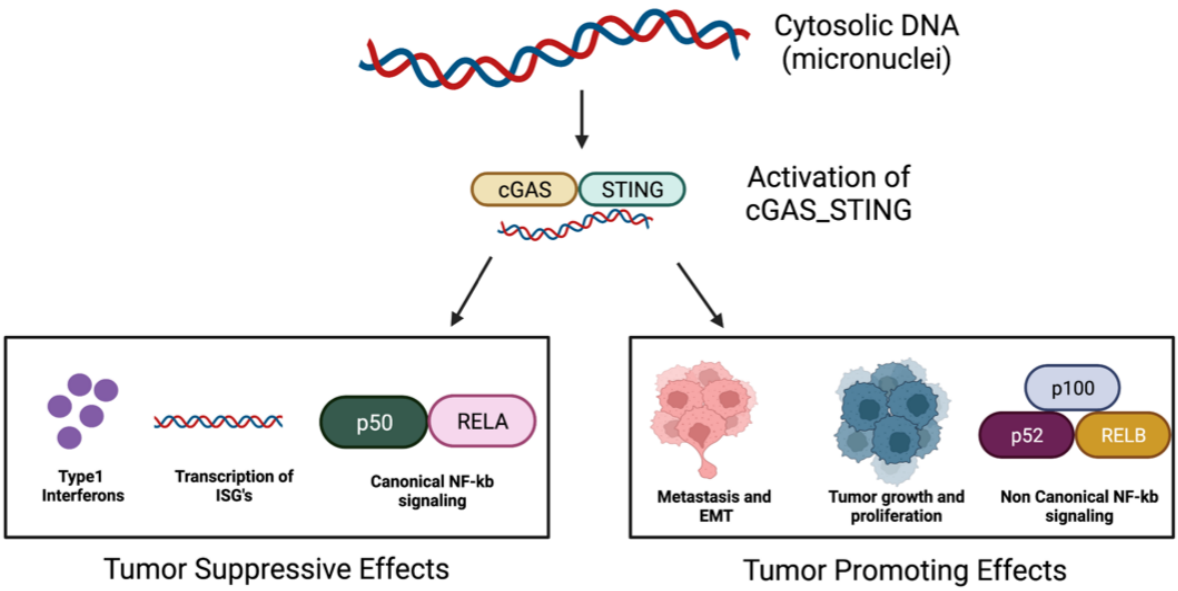

Figure 5: Two faces of cGAS-STING signaling associated with chromosomal instability. *Created with biorender.com*.

1.8 Breast Cancers and need for novel adjuvant therapies in the context of CIN

Breast cancer is the most frequent cause of cancer death in women with statistics showing 264,121 new cases reported in 2019 with 42,280 deaths (www.gis.cdc.gov). For every 100,000 women there are 130 new cases reported in the United States. Risk factors include age, genetic mutations (BRCA1 and BRCA2), familial history of breast cancer, reproductive history, obesity etc. However, the highest incidence is seen in women with familial history and mutations in BRAC1 and BRCA2 genes (Petrucelli et al., 2016). A high frequency of cell turnover increases the probability of chromosomal abnormalities and incorrect DNA replication which also increases the risk of cancer occurrence (Ashford et al., 2015). Different types of breast cancers are determined by specific cells from which the cancer arises. Ductal carcinomas arise from the milk ducts while lobular carcinomas arise from the lobules of the breast (site of milk production). They are further classified as *in situ* vs *invasive* based on whether the cancer spread across the surrounding breast tissue or not. Other types include triple-negative and inflammatory breast cancers. Treatment for breast cancers include surgery which is done preliminarily to remove the tumor (lumpectomy) or the entire mammary glands (mastectomy) based on the size and staging of the tumor. It is often followed by chemotherapy, radiotherapy, immunotherapy or targeted therapy in case of tumors expressing estrogen receptor (ER^+), progesterone receptor (PR^+) and human epidermal growth factor receptor 2 ($Her2^+$) (Burstein et al., 2014; Moasser & Krop., 2015; Goel et al., 2016).

CIN has been at the pinnacle in conferring resistance to many anti-cancer therapies (Lukow et al., 2021). Firstly, slower proliferation as a result of G1 cell cycle arrest and presence of higher somatic copy number alterations in cancer cell lines is associated with resistance to chemotherapeutics like cisplatin and paclitaxel (Swanton et al., 2009). Similarly, missegregations induced (treatment with reversine) in cancer cell lines and exposing them to chemotherapeutics revealed that survival of cancer cells was through karyotype evolution with changes in dosage of specific genes associated with drug efflux pumps and metabolic enzymes thereby selecting favorable karyotypes (Ippolito et al., 2021). On the other hand, studies have identified molecules that could be responsible for resistance to chemotherapeutics in the context of CIN.

Firstly, patient-derived xenografts generated from triple negative and luminal breast cancers treated with paclitaxel and docetaxel showed no effect on tumor growth, however targeting p38a in these tumors made them sensitive to chemotherapeutics with aggressive tumor regression (Canovas et al., 2018). One explanation is that inhibition of p38a increases DNA damage, further elevates CIN levels beyond DNA repair. Secondly, activation of downstream NF-kB signaling as a result of CIN is known to promote cellular invasion and metastasis besides triggering resistance to both chemotherapy and radiation therapy in cancer cells (Gupta et al., 2015). Considering the off-target effects associated with inhibition of signaling pathways like NF-kB and p38, it remains crucial to identify various immunological targets for tumors with high levels of CIN, which are discussed in the result section of the thesis.

All in all, to consider aneuploidy and CIN as an independent prognostic factor, it is important to understand that aneuploidy plays a context dependent role in various tissues and targeting the aneuploidy state/aneuploidy drivers and immune cells in the microenvironment *per se* aids in recognition and eliminating of aneuploid tumor cells. Therefore, the use of *in vivo* models to address these questions become more relevant from a clinical perspective. These results remain critical in the development of novel adjuvant therapies for treatment of high CIN tumors including breast cancer.

2. Objectives and Aims of the Thesis

It is still unclear how aneuploid tumor cells interact with the tumor microenvironment in the context of chromosomal instability. During the last decade, an enormous effort has been made to identify if and how chromosomally unstable cells are sensed by the immune system during the course of tumor progression. Whereas *in vitro* studies have demonstrated that aneuploidy triggers an innate immune response, human malignancies with high levels of CIN have also been reported to have an immunosuppressive phenotype. A crucial question in the field is to understand this controversy and how different levels of CIN influence this phenomenon. The majority of the studies shed light on conclusions from *in vitro* models where chromosome missegregation was induced chemically. Hence, the translational impact of the relation between aneuploid tumor cells and the immune system *in vivo* still remains to be understood. The current thesis addresses these issues by utilizing mouse models and omics data generated for different immune cell subsets during early and late stages of tumor development in high and low CIN breast cancers.

2.1 Consequence of Plk1 overexpression in Her2^{+} breast tumors:

PLK1 overexpression has been found in many human tumors and is often associated with poor prognosis and increased metastatic potential. To design effective immunotherapy strategies, it remains essential to understand the immune phenotype of Plk1 overexpressing tumors. Here we address the following from our *in vivo* experiments in end stage tumors:

- Identifying the gene expression profile of high and low CIN tumors.
- Quantifying immune cells in spleens and tumors along with the identification of immune suppression markers.
- Understanding the signaling mechanisms associated with high CIN tumors expressing Plk1.
- Corroborating immune cell phenotypes with TCGA-BRCA end stage human tumors expressing high levels of PLK1.

2.2 Innate and Adaptive immune cells during early stages of tumor development in Her2^{+} breast tumors with different levels of CIN:

The oncogenic effects of CIN/aneuploidy are well established. Contrarily, CIN induced by Plk1 expression also delays mammary tumor initiation in both Her2 and Kras mouse models. Thus, it appears as if these chromosomally unstable cells are detected during early stages (due to delay in tumor initiation) but eventually evade the immune system. To address this question and to see if immune suppression is an early event during tumor initiation in Plk1 overexpressing high CIN tumors compared to Her2 tumors with low CIN, we address the following:

- Determining somatic copy number alterations (SCNA) in early-stage Her2 and Her2-Plk1 tumors.
- Understanding the relative percentage, gene expression profile including activation/inhibition markers, phenotype and genes affecting functional development of different subtypes of innate and adaptive immune cells at early stages during tumor development through single-cell sequencing.

3. Materials and Methods

3.1 Overview of the PLK1 transgenic mouse model

At the ColA1 locus of KH2 embryonic stem cells (Beard et al., 2006), a FLAG-tagged human PLK1 cDNA cassette was inserted under the regulation of the tetracycline response element by homologous recombination using the FLP-FRT system (Figure 6). The ES cells were selected using a hygromycin resistance cassette and ColA1-Plk1 animals were then bred with MMTV-rtTA (Gunther et al., 2002), TetO-rat-Her2 (Moody et al., 2002), and H2B-GFP (Hadjantonakis & Papaioannou., 2004) to carry all four transgenes. When doxycycline is administered to the animals, it binds to the transcription factor rtTA which further binds to the promoter region enabling gene expression.

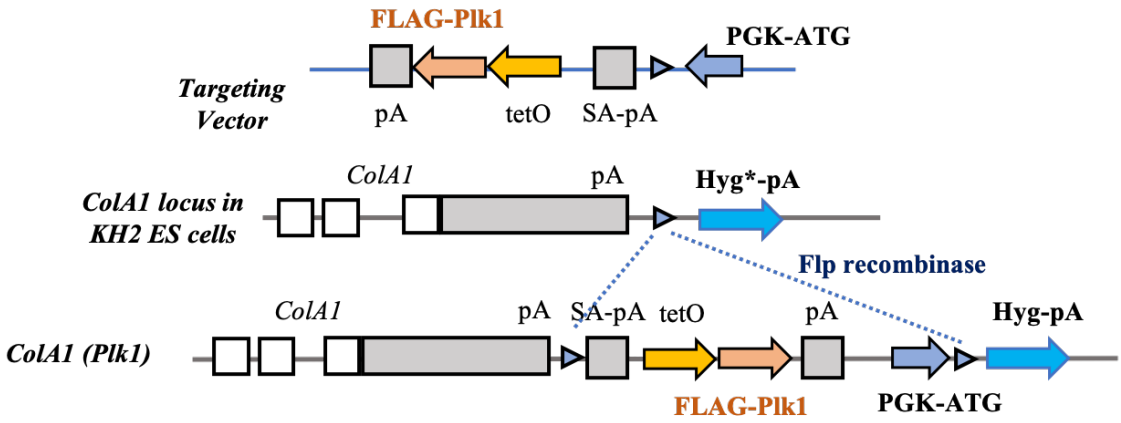

Figure 6: Schematic representation of human FLAG-PLK1 cDNA inserted into ColA1 locus of KH2 ES cells via FLP-FRT system. Modified and *created with Biorender.com*

3.2 Breeding of mice and monitoring of the disease

Pathogen-free (SPF) environment with 12-hour day-night cycles and a median temperature of 21°C, was used to house all the experimental mice. All breeding and experimental methods were carried out in accordance with the animal protocol (G231/15) and G-18/21 at the DKFZ, Heidelberg, Germany. Food pellets (625 mg/kg, Harlan-Teklad) containing doxycycline (stable tetracycline analog) was used to induce expression of transgenes in adult female mice (8-10 weeks) Tumor progression was monitored twice a week after the onset of the tumor, and measurements were taken with vernier calipers. When the tumors surpassed 1.5 cm, mice were

sacrificed by cervical dislocation method. Mice on FVB background were used for all the experiments.

3.3 Stages of mouse estrous cycle

Before feeding mice with the Dox diet, Pap smears were conducted to assess the estrous phase of the mice. Autoclaved distilled water, PBS, and 0.1 percent crystal violet were used for the experiment. Vaginal lavage was performed by injecting 50ul of 1x PBS into the mouse's vaginal canal. After aspirating 4-5 times to obtain sufficient quantity of cells, the cells were resuspended and spread out on a superfrost slide to dry. The slides were stained with Crystal Violet (Sigma) for 1 minute, then washed with water for 2-3 minutes. They are then air dried and examined under a microscope for stage identification (Figure 7).

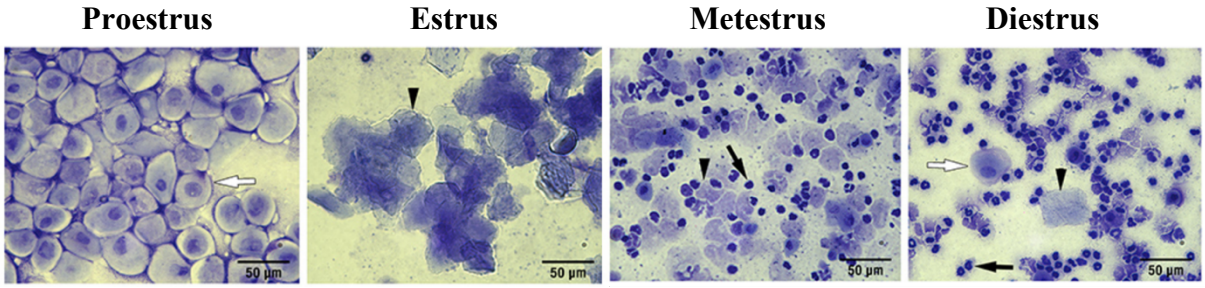

Figure 7: Different stages in the mouse estrous cycle. Ratio of three cell types i.e. nucleated epithelial cells, squamous epithelial cells and leukocytes (shown in arrows) are used in the identification process of each stage. *Source of the figure*: Mclean et al., 2021.

3.4 Animal necropsy and removal of mammary glands

Prior to the process, the necropsy tools and other ancillary equipment was sanitized with 70% ethanol. Externally, the mice were checked and obvious abnormalities were noted. Mice were sacrificed via cervical dislocation. To open up the mammary glands on the flanks, a vertical incision was made across the torso and the skin was pulled back. Mammary glands in positions L1, R1, L2/3, R2/3, L4, and R4 (L=left, R=right) were collected (Figure 8). The tissue samples were either snap frozen with liquid nitrogen for DNA and RNA analysis or processed in 10% formalin (Sigma) for processing of histology slides or FACS buffer (PBS+5%FBS) used in the preparation of single-cell suspension for flow cytometry analysis of immune cells.

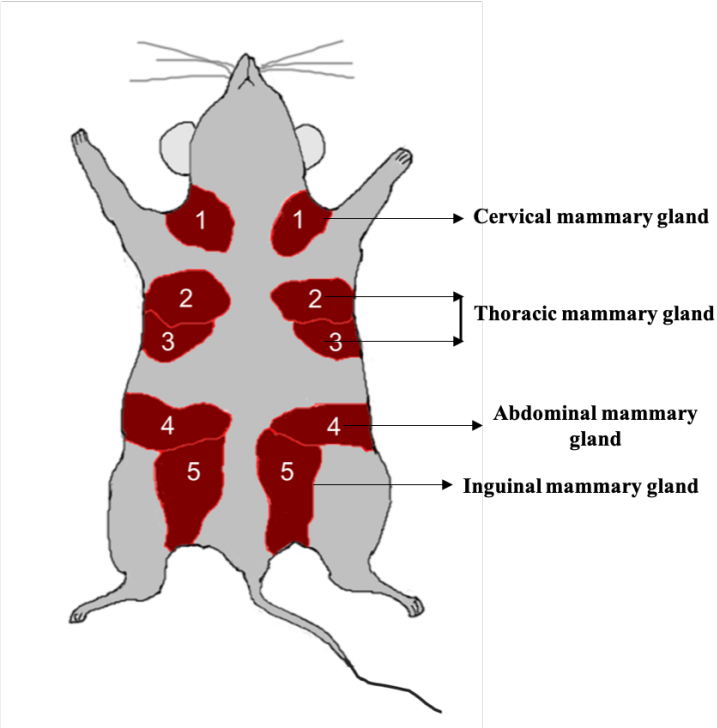

Figure 8: Schematic showing different mammary glands in mice. Adapted and modified from Meng-Chieh Lin et al., 2017.

3.5 Genotyping

21 days after birth, mice are weaned, and ear punches are taken for genotyping. DNA was recovered from the ear punches after 1.5 hours of incubation in 200µL 0.05M NaOH at 98ºC and neutralization with 20µL 1M Tris HCl at pH7.5. 1µL of extracted tail DNA and 19µL of PCR mastermix was diluted in an appropriate volume of dH2O and used in the PCR experiment. Dream Taq green buffer (Thermo Scientific) 1X, 200µM dNTPs, Taq polymerase-1U/20µl, 0.25pmol/µl forward primer, and 0.25pmol/µl reverse primer make up the mastermix. All genes were subjected to the below mentioned PCR program conditions: initial denaturation (94°C for 2 min), exponential amplification for 30 cycles [95°C for 30 s, 60°C for 30 s, 72°C for 30 s], and a final denaturation (94°C for 2 min). The primers used for the identification of various transgenes are listed below:

Gene	Primer Name	Sequence
ColA1-Plk1	Primer Coll frt A	GCACAGCATTGCGGACATGC
	Primer Coll frt B	CCCTCCATGTGTGACCAAGG
	Primer Coll frt C1	GCAGAAGCGCGGCCGTCTGG
MMTV-rtTA	CMV-rtTA F	GTGAAGTGGGTCCGCGTACAG
	CMV-rtTA R	GTACTCGTCAATTCCAAGGGCATCG
TetO-Neu	TAN-IRES 3528F	GACTCTCTCTCCTGCGAAGAATGG
	TAN-IRES 3914B	CCTCACATTGCCAAAAGACGG
H2B-GFP	H2B EGFP (F)	CAAGGGCGAGGAGCTGTT
	H2B EGFP (R)	AAGTCGTGCTGCTTCATGTG

Table 1: Genotyping PCR Primers

3.6 Immunohistochemistry (IHC) of tissue sections

The formalin-fixed paraffin-embedded sections were used to perform IHC on mouse tumor tissues. After deparaffinization with xylene, the samples were rehydrated with graded ethanol. Antigen retrieval was done in a steamer for 30 minutes with 0.09 percent (v/v) unmasking solution (Vector Labs). Endogenous peroxidases were inactivated for 10 minutes with 3% hydrogen peroxide (Sigma). VECTASTAIN Elite ABC kits were used for secondary antibody staining and biotin-streptavidin incubation (Vector Labs). For antibody detection, a DAB Peroxidase Substrate kit (Vector Labs, SK-4100) was used. Bio-Optica and Vector Labs provided the hematoxylin used for DNA counterstaining for the detection of nuclei. Anti-Plk1(1:20) [Trakala et al., 2015], anti-PD-L1(1:150) [catalog: cellsignaling-64988T], and anti-CD206(1:500) [catalog: R&D systems, AF2535] were employed as primary antibodies. The sections were then incubated with the mentioned biotinylated secondary antibodies and avidin/biotinylated enzyme reagents (ABC kit (PK-6101; PK-61-04)) in a sequential order. StrataQuest software (Tissue-Gnostics) was used to perform the slide scanning and quantification for PD-L1 and CD206. The total sum area of positive cells is determined.

3.7 Bulk RNA sequencing

According to the manufacturer's instructions, complete RNA was extracted from mammary tumor tissues with the help of RNeasy Mini kit (Qiagen), buffer RLT and RNeasy spin columns (Qiagen, Venlo, The Netherlands). Libraries were created using the Illumina TruSeq Stranded mRNA Library Prep (Illumina, San Diego, California, USA). With the help of HiSeq 4000 (Illumina), the libraries were sequenced as 50 base pair (bp) single-end reads and Kallisto v0.46.1 was used to align the sequenced reads to Mm10 reference genome (Bray et al., 2016).

Differentially expressed genes (DEGs) were calculated using DEseq2 package in after raw counts were adjusted (Love et al., 2014). With the help of R packages ClusterProfiler, enrichplot (Wu et al., 2021) and pathview (Luo & Brouwer., 2013), differentially expressed genes were subjected to GO analysis and GSEA for the identification of signaling pathways. A statistically difference between groups was measured with a significance of $P<0.05$.

3.8 Western Blotting

MCF7 and Cal51 cells with and without the overexpression of Plk1 (rtTA-Plk1) were lysed in Laemmli lysis buffer (0.25 M Tris-HCl pH 6.8, 2.5% glycerol, 1% SDS, and 50 mM DTT) for the extraction of proteins from cell lines. Cells were scraped from the dish using a cell scraper and the lysate is collected in a microtube. For the extraction of proteins from tumor tissues (Her2/Her2-Plk1 and Her2-Mad2), the same buffer was used. Samples were put on a shaking incubator at 100^{o}C for 10 min and further centrifugation was done at 14000 rpm for 5mins to collect the protein sample. Tris-Glycine acrylamide gels were used for the separation of proteins (BioRad) and later transferred to nitrocellulose membranes (BioRad). The gels were probed with the following antibodies from cell signaling. Anti-PLK1(1:500) [catalog:4535S], anti-NF-kB-p65(1:1000) [catalog:8242S], anti-RELB (1:1000) [catalog:10544S], anti-p38a (1:1000) [catalog:9218S] anti-GAPDH (1:2000) [R&D systems], anti-Actin (1:6000) [catalog: A2066 Sigma]. Signal detection was done using super-signal chemiluminescence substrate (Thermo-scientific) after incubation with anti-mouse/anti-rabbit secondary antibodies. Finally, iBright1500 system (Invitrogen) was used for taking the pictures of the blots.

3.9 Sorting and Single cell RNA sequencing

Single-cell suspensions of mammary glands from 16 (Her2) and 22 (Her2-Plk1) day mice after doxycycline administration was obtained through the disassociation of the tissue with the help of collagenase IV (100 U/ml) and DNase I (50 U/ml). gentleMACS Octo Cell Disassociator (Miltenyi Biotec) was used to incubate the cell suspension at 37°C with mild agitation. Cells were washed with RPMI-1640 medium to stop the reaction. After two rounds of filtering, samples were stained with anti-CD45 and anti-EpCAM antibodies in order to separate hematopoietic cells from mammary epithelial cells. Using the gating strategy that was previously described, sorting was done on FACS Aria II (Becton, Dickinson & Company) cell sorter. 10x Genomics platform was used for single cell sequencing. Reverse transcription and library preparation were done in accordance with the Chromium Next GEM sc 3 Reagent v3.1

protocol. Following this, Illumina NovaSeq 6000 S1 was used to carry out paired end sequencing runs. Processing of sequencing data was done using 10x Genomics Cell Ranger 3.0.0. (Zheng et al., 2017). The R package 'Seurat' was used to analyze the data (Butler et al., 2018). If a cell had more than 200 genes and a mitochondrial content of less than 10%, it was chosen for further investigation. The first 30 features based on principal component analysis and manual examination of the accompanying "Elbow graph" were chosen for downstream clustering and dimensionality reduction. With a resolution of 0.5, clusters were identified using a shared closest neighbor modularity optimization built using the Louvain algorithm (Waltman & Eck., 2013). Cells were annotated to a reference database (ImmGen) using the SingleR program (Aran D et al., 2019). A Wilcoxon Rank Sum test was used to assess the differences in gene expression between clusters as well as between samples within specific clusters. Using datasets for hallmark genes (H), curated genes (C2), gene ontology genes (C5), and immunologic signatures (C7) from MSigDB, gene set enrichment analysis was carried out with the help of R program clusterProfiler (Wu et al., 2012). The R program ggplot2 (Wickham H., 2016) as well as the Python utilities matplotlib and seaborn were used for data visualization (Waskom ML., 2021).

3.10 Invitro culture of MCF7 and Cal51 cells

Dulbecco's modified eagles medium supplemented with 10% FBS (Gibco), 1% penicillin/streptomycin (Life Technologies), non-essential amino acids (0.1mM), insulin (10 ug/mL), and sodium pyruvate (1mM, Life Technologies) was used to grow MCF7 cells. Similarly, DMEM (high glucose) supplemented with 10% FBS (Gibco), 1% Penicillin-Streptomycin (Life Technologies), and 1% glutamine (Life Technologies) was used for culturing of Cal51 cells. To generate PLK1-inducible cell lines, Puromycin (1g/ml) was used to select MCF7 cells following infection with lentivirus expressing rtTA. Selection based on GFP positive cells after infection was used for sorting Cal51 cells expressing rtTA. Second infection was done using Tet-ON lentivirus carrying the human PLK1 cDNA (pLenti CMVtight Hygro DEST) obtained from Addgene #26433). The infected cells are selected using hygromycin resistance (350 µg/ml). The cells were incubated in the presence and absence of doxycycline (5mg/ml) for 24, 48 and 72hrs to see the expression of NF-kB related genes.

3.11 TCGA data sets, pre-processing and TME cell type inference

Gene expression data in the form of Log_2 normalized counts+1 was obtained from the Xena browser (Goldman et al., 2020) for a total of 1108 breast cancer samples from TCGA. With the

help of expression data, I separated tumors as PLK1 high and PLK1 low based on the Z-score and identified 165 tumor samples as PLK1 low and 186 tumor samples as PLK1 high. Data was retrieved from the legacy archive of GDC, normalized and filtered with the help of R/Bioconductor package TCGAbiolinks version 2.22.3 (Colaprico et al., 2016) using GDCquery, GDCdownload, and GDCprepare functions for tumor types (level 3) and platform ("IlluminaHiSeq_RNASeqV2"). Unsupervised clustering using principle component analysis was used to identify the similarity between the PLK1 high and PLK1 low tumor cohorts. CIBERSORT v.1.06 (https://cibersort.stanford.edu/) was used to determine the corresponding fractions of 22 cell subsets within the tumor microenvironment (TME). lymphocyte populations were computed based on batch-normalized gene-expression patterns for every tumor sample. The application was run using the default LM22 reference matrix and total number of immune cells in both Plk1-high and Plk1-low cohorts were estimated.

3.12 Fluorescence in-situ hybridization (FISH)

FISH was carried out on formalin-fixed paraffin-embedded 5µm sections (Vector Labs, California, USA, NA). Deparaffinization, rehydration, and antigen retrieval using unmasking solution 0.09% (v/v) was done prior to starting the procedure. The BAC DNAs were tagged via nick translation according to instructions in the kit. 3µL of labeled probe and 7µL of Vysis LSI/WCP Hybridization buffer were used to make the probe mix. The following program was used to hybridize utilizing the Abbott Molecular Thermobrite system: Hybridization took place at 37 °C for 20–24 hours after denaturation at 76 °C for 5 minutes. Chr 16-RP23–290E4 and RP23–356A24 tagged with SpectrumOrange-dUTP (Vysis) and Chr 17-RP23–354J18 and RP23–202G20 tagged with SpectrumGreen-dUTP (Vysis) were used to make pan-centromeric probes (Vysis). In order to quantify the percentage of aneuploidy in both Her2 and Her2-Plk1 samples, a minimum of 400 cells from each sample and an average of 10 ROI (Region of Interest) from each sample were taken into consideration.

3.13 Fluorescence-activated cell sorting (FACS)

Her2 and Her2-Plk1 tumors were digested at 37 °C with 100 U/ml collagenase IV and 50 U/ml DNase-I. Spleen and tumor tissue single-cell suspensions were prepared to calculate immune cell subset percentages. The following antibodies from Biolegend, anti-CD45[catalog:103115], anti-Cd3[catalog:100320], anti-Ly6C[catalog:128007], anti-CD4[catalog:100537], anti-CD8[catalog:100714, anti-CD11c[catalog:117328], anti-MHCII[catalog:107606], anti-CD11b[catalog:101235], anti-Nk1.1[catalog:108709], anti-Nkp46[catalog:137611] and anti-

CD25[catalog:102011] and anti-Foxp3[catalog:FJK-16s] (eBioscience) were used to stain the cells. For intracellular staining, cells were treated with perm/fix solution (Foxp3 transcription factor staining buffer kit, eBioscience) for 4 to 5 hours. Following permeabilization they were stained with anti-Foxp3 to quantify intracellular Foxp3. Cells were acquired on a BD FACS Canto (Becton, Dickinson & Company) flow cytometer and FlowJo (Version 10.1) software was used to do the analysis.

3.14 Invivo NK cell depletion

NK cells in Her2 and Her2-Plk1 animals (6 weeks of age) were depleted by injecting 500 µg of anti-NK1.1 (PK136) on day 1 followed by 250 µg on day 2 and a third injection of 250 µg on day 10 until the time of doxycycline administration (8 weeks of age). The antibody was diluted in 200 µl PBS and administered intraperitoneal (ip) to the recipient mice. From the time the animals were put on doxycycline diet, a maintenance injection of 250 µg of anti NK1.1 (PK136) was given every week until a palpable tumor was formed. Mice were then sacked to perform necessary experiments. Cervical dislocation method was used to sacrifice the mouse and all the mice were on a FVB background.

3.15 Statistical analysis

I used GraphPad Prism 8 software for statistical analysis in all the experiments. However, appropriate R packages were used for determining statistical significance in single cell and bulk RNA-seq analysis.

4. Results

4.1 Immune response to Plk1 overexpression in the mammary glands

4.1.1 Plk1 overexpression results in increased overall survival in Her2 breast cancer model

One of the crucial mechanisms of immune evasion in malignancies is CIN (McGranahan et al., 2017, Burrell et al., 2013, Watkins et al., 2020, Bakhoum et al., 2018, Rosenthal et al., 2019, Davoli et al., 2017). Previous studies by de Carcer et al., 2018 showed the cell-autonomous effects of PLK1, where PLK1 overexpression resulted in a significant delay in breast tumor initiation with elevated levels of CIN (Average SCNA, Her2 = 2.3 and Her2-Plk1 = 4 per tumor). Similarly, Her2 tumors presented 24% mitotic errors in comparison to Her2-Plk1 cells which showed about 50% (de Carcer et al., 2018). To better comprehend how varied degrees of CIN shape and affect carcinogenesis, and to see the effects of PLK1 overexpression on the immune system, I used the same *in vivo* mouse tumor model that overexpresses either Her2 or Her2 in combination with Plk1 to see the expression of transgenes in mammary epithelial cells, under the influence of the mouse mammary tumor virus promoter (MMTV-rtTA) (Figure 9A). To confirm the phenotype, I followed up to see the overall survival in both the tumor groups and found that Her2-Plk1 tumors have a higher overall survival compared to Her2 tumors (Median survival of Her2 = 72 days and Her2-Plk1 = 134 days) (Figure 9B).

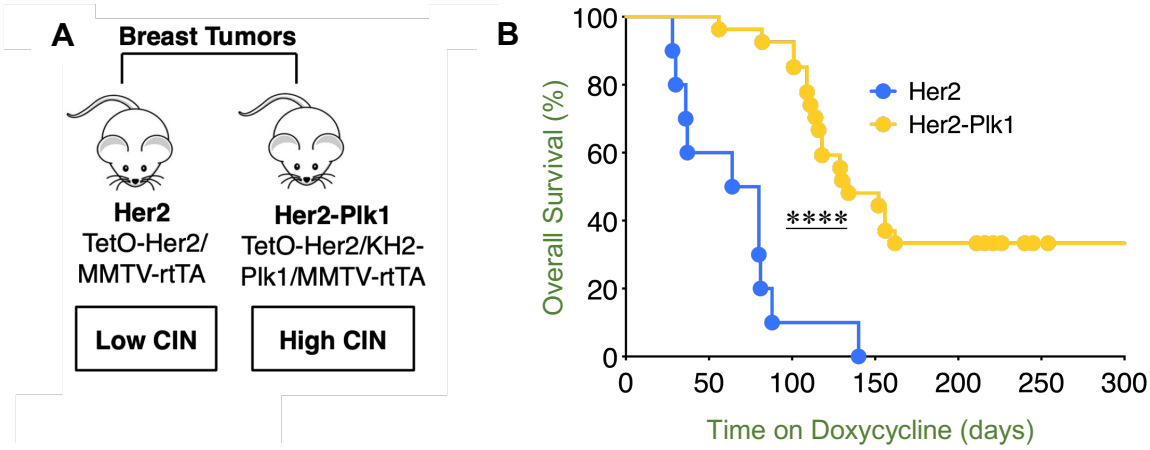

Figure 9: A) Schematic representation of the mouse models used in the study. **B)** Graph showing overall survival in mice after doxycycline administration for oncogene activation. ****P<0.0001, Mantel-Cox test.

4.1.2 Plk1 overexpression in Her2 tumors results in a senescence associated secretory phenotype (SASP)

To characterize the immune signatures associated with Plk1 overexpression, I investigated the entire transcriptome of Her2 and Her2-Plk1 breast cancers by bulk RNA sequencing at humane endpoint. Hierarchical clustering was used to determine the similarity between the two groups (Figure 10A). There were in total 2096 differentially expressed genes between the two groups as seen in the MA plot (Figure 10B). The results of differential expression analysis showed that Plk1 overexpression resulted in elevated levels of SASP (Senescence Associated Secretory Phenotype) markers. SASP was defined as a combination of inflammatory cytokines, chemokines such as *Tnfa, Cxcl12, Cxcl17, Cxcl15, S100a13, S100a4*, extracellular matrix ECM proteases such as *Mmp3, Mmp9, Mmp11* and molecules like *Ido1, Arg2* and *Relb*. Genes associated with cell cycle regulation

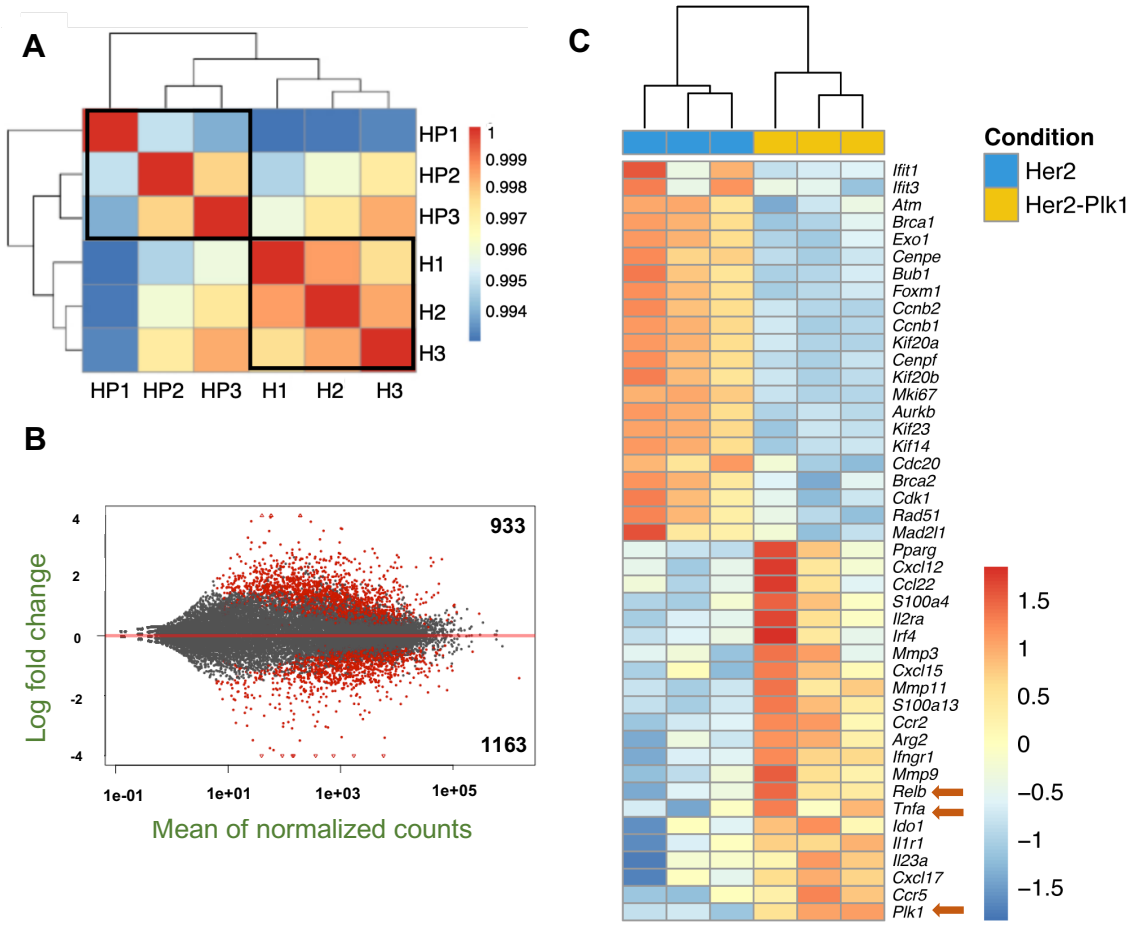

Figure 10: A) Heatmap of hierarchial clustering in Her2 (H) and Her2-PLK1 tumors (HP) samples (n=3). B) MA plot showing the number of differentially expressed genes between the groups. **C)** Bulk RNA sequencing of the entire transcriptome of Her2 and Her2-Plk1 tumors. Heatmap representing differentially expressed cell cycle and SASP genes (Fold change (FC) >1.5 or < 1.5, p=0.05, n=3 tumors per genotype). * Analyzed with assistance from Anand Mayakonda.

such as *Bub1, Kif20a*, *Kif20b*, *Cenpe*, *Aurkb*, *Mad2l1* and DNA damage repair genes *Brca1*, *Brca2*, *Atm*, *Exo1*, *Rad51* were downregulated (Figure 10C).

Her2-Plk1 tumor cells showed irreversible cell cycle arrest in G1 phase with the expression of cyclin dependent kinase inhibitor p21 along with decreased expression of proliferation marker PCNA. They are further characterized by flattened and enlarged morphology (de Carcer et.al). So, I asked the question whether these tumor cells are senescent and tumor lysates from Her2-Plk1 samples displayed increased ß-galactosidase activity when compared to Her2, confirming that Plk1 overexpression induces senescence (Figure 11A). Next, I performed functional analysis or over representation analysis to dissect pathways related to Plk1 expression and associated chromosomal instability. Gene set enrichment analysis (GSEA) showed enrichment of pathways related to NF-kB, JAK-STAT, MAPK, NK cell mediated cytotoxicity and T cell receptor signaling. Moreover, as predicted pathways related to cell cycle and DNA repair are downregulated (Figure 11B). Additionally, I used ClusterProfiler (Yu et al., 2012) to analyze GO terms associated with significant genes obtained from differential expression. The tool uses hypergeometric testing and performs enrichment analysis by considering the significant gene list and a reference gene list. The up and down regulated GO terms (biological pathways) in the context of PLK1 overexpression were plotted using a dotplot. Interestingly, pathways corresponding to immune suppression, angiogenesis, T cell activation, leukocyte activation and migration etc were upregulated and pathways related to DNA replication, mitosis, DNA repair and cell cycle etc were downregulated (Figure 14).

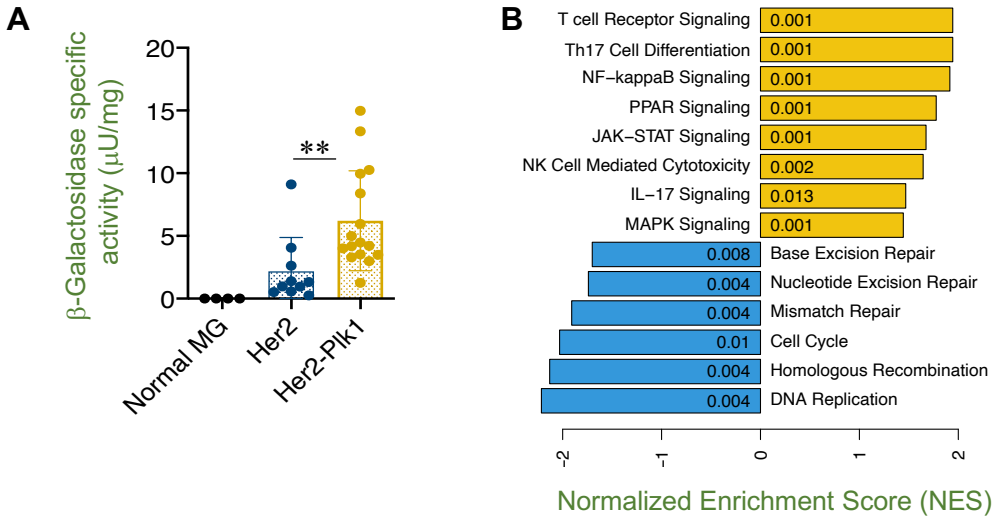

Figure 11: A) β-galactosidase activity in Her2 and Her2-Plk1 tumor lysates as measured by fluorometric analysis (Mann Whitney test p<0.005**, n=10 (Her2) and n=16 (Her2-Plk1). **B)** Gene set enrichment analysis using gene sets from KEGG pathways. Pathways overexpressed in Her2-Plk1 tumors are shown in yellow while Her2 tumors are displayed in blue.

4.1.3 SASP induction in Plk1 tumors leads to upregulation of cytokines associated with inflammation and increase of inflammatory monocytes

SASP is known to disrupt normal tissue function by producing inflammatory cytokines (Gorgoulis et al., 2019; Davalos et al., 2010). Similarly, inflammatory cytokines also suppress immune system function (Coppe et al., 2014; Ben-Baruch., 2006). To corroborate the findings from bulk RNA seq, I performed cytokine array analysis by extracting protein lysates from Her2 and Her2-Plk1 tumors and saw elevated concentrations of SASP associated inflammatory cytokines such as CXCL1, IL16 and anti-inflammatory IL1RN in the Her2-Plk1 group (Figure 12). CXCL1 and IL16 are known to mediate infiltration of neutrophils and T cells respectively to site of inflammation (Li et al., 2015; Sawant et al., 2015; Sawant et al., 2021; Laberge et al., 1998). Moreover, the upregulation of IL1RN serves to modulate the activity of IL1 family proteins and dampen the inflammatory responses arising due to Plk1 expression.

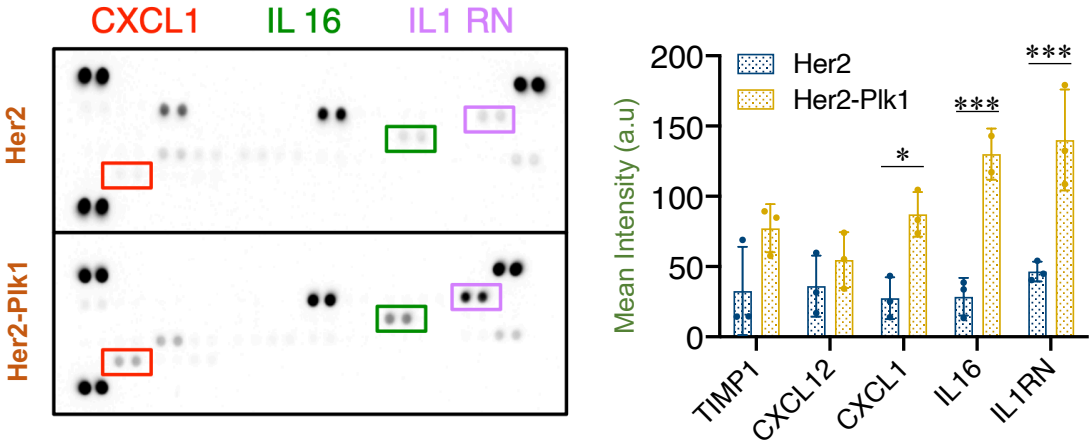

Figure 12: A) Cytokine array from Her2 and Her2-Plk1 tumor lysates displaying elevated levels of CXCL1, IL16 and IL1RN in the latter group. ($p<0.05$* $p<0.0005$***, 2-way ANOVA, Sidak's multiple comparison test, n=3).

Furthermore, I used flow cytometry to look at monocyte influx in response to SASP because inflammation results in recruitment of monocytes that extravasate along the bloodstream (Shi et al., 2011). Different types of macrophages/monocytes in the tumors were segregated based on the expression of Ly6C and MHCII (Georgoudaki et al., 2016) (Figure 13A). Live $CD45^+$ tumor cells were gated for the expression of CD11b. The $CD45^+Cd11b^+$ double-positive cells were then divided into four TAM (tumor-associated macrophage) subgroups based on the expression of Ly6C and MHCII. $Ly6C^{high}$ $MHCII^{low}$ are termed as inflammatory monocytes, $Ly6C^{int}$ $MHCII^{high}$ cells are termed as immature macrophages, $Ly6C^{low}$ $MHCII^{high}$ cells were

termed as M1 TAMs and Ly6C^{low} MHCII^{low} cells as M2 TAMs. I detected a notable increase in CD11b^{+}Ly6C^{high}MHCII^{low} inflammatory monocytes and a reduction in CD11b^{+}Ly6c^{low}MHCII^{high} M1 tumor-associated macrophages (TAMs) in the Her2-Plk1 cohort compared to Her2 alone (Figure 13B). Using the above classification M2 macrophages have been described to be immunosuppressive and M1 macrophages are inflammatory and have antitumor immunity. Thus, influx of inflammatory monocytes appears to be a consequence of SASP induced by Plk1 overexpression in Her2 tumors.

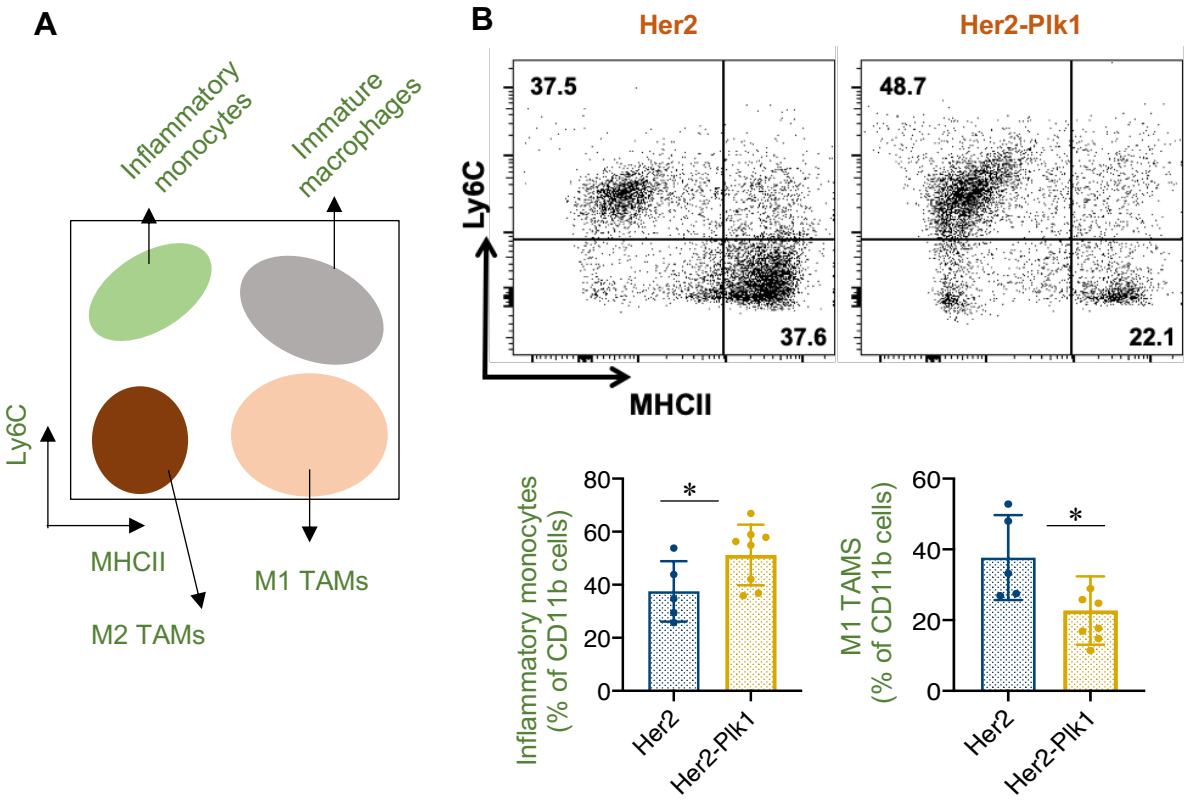

Figure 13: A) Schematic of gating monocyte populations based on the expression of Ly6C and MHCII **B)** Flow cytometric analysis of inflammatory monocytes (Ly6c^{high}MHCII^{low}) and M1 TAMs (Ly6c^{low}MHCII^{high}) in endpoint tumors (Mann Whitney test $p<0.05$*, n=5 (Her2) and n=8 (Her2-Plk1)).

4.1.4 Gene Ontology analysis with biological processes associated with overexpression of Plk1 in Her2 tumors

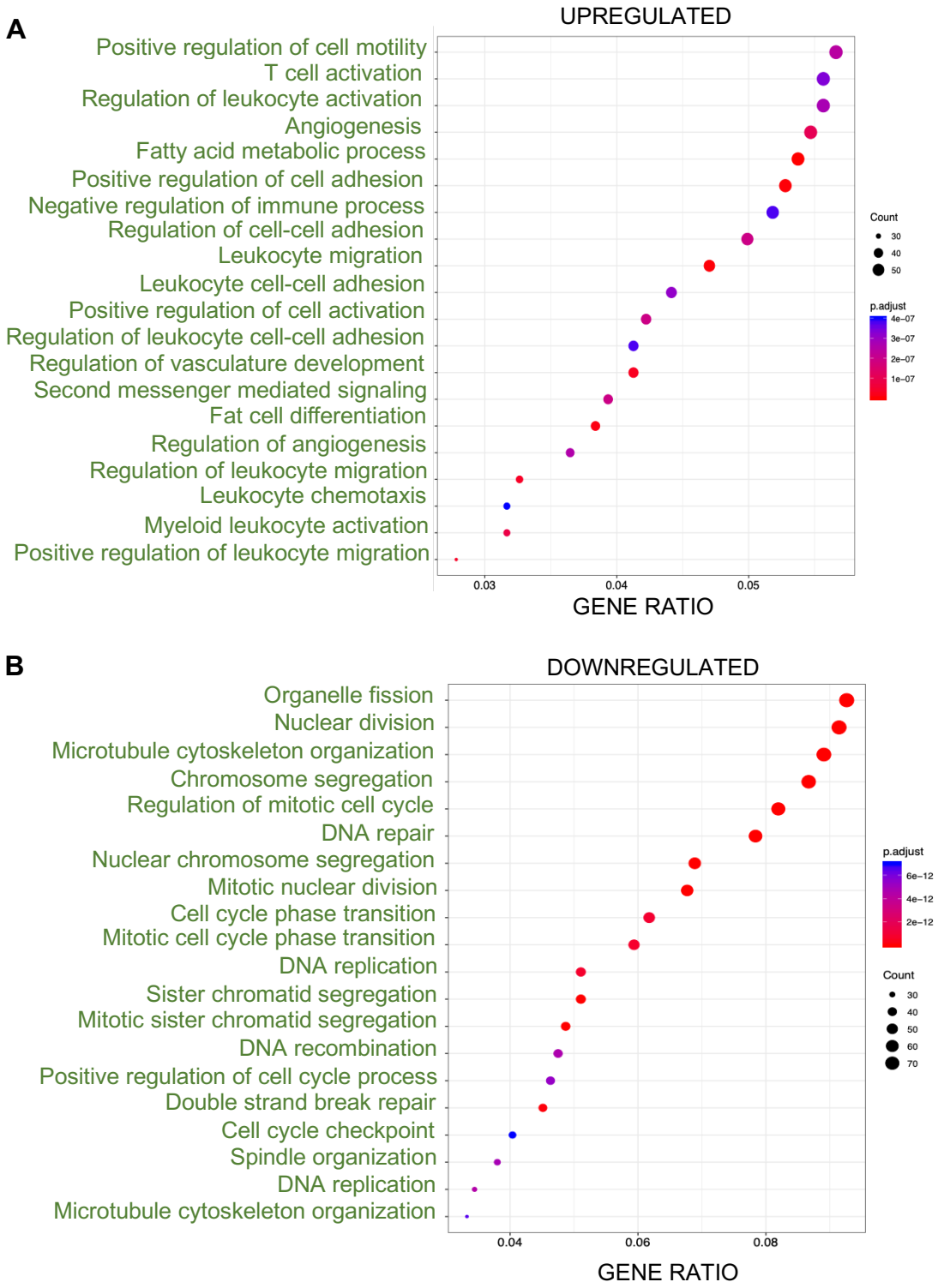

Figure 14: GO overrepresentation analysis of differentially expressed genes between Her2 and Her2-Plk1 tumor cohorts. The first 20 markedly (P<0.05) enriched GO terms from biological processes are shown. **A)** Upregulated and **B)** Downregulated. The pathway adjustment enrichment score is represented by color, and the dot size is depending on the number of genes enriched in the pathway

4.2 Validation of signaling pathways and immune suppression markers associated with overexpression of Plk1 in mammary tumors

4.2.1 High CIN activates NF-kB (canonical & non-canonical) signaling

Chronic stress, endogenous DNA damage, and the onset of senescence are all caused by chromosome missegregation (Scheltzer et al., 2016; He Q et al., 2018; Torres et al., 2007). Through the recruitment of NK cells, NF-kB: a principle transcription factor of senescence and inflammation (Hayden et al., 2008) promotes immunological detection of chromosomally unstable cells (Wang et al., 2021). Conversely, by facilitating migration, invasion, and metastasis, NF-kB also promotes immune escape (Bakhoum & Cantley., 2018). Similarly, p38 MAPK is shown to be activated where it acts upstream of p53 to initiate cell cycle arrest in response to prolonged mitosis or chromosome missegregations (Thompson & Compton., 2010; Uetake & Sluder., 2010). Further, p38 MAPK also plays a role in aneuploidy tolerance by acting as a stress sensor by responding to proteotoxic and oxidative stress (Cuadrado & Nebreda., 2010; Cuenda & Rousseau., 2007). As my previous results point towards a SASP phenotype with influx of inflammatory monocytes and upregulation of pro inflammatory cytokines, I asked the question whether there is any upregulation of NF-kB and p38MAPK in the context of high chromosomal instability induced by PLK1. Therefore, I performed western blotting of NFkb-p65 (RELA), RELB, p38α, Phospho-p38 and PLK1 from tumor lysates of both tumor

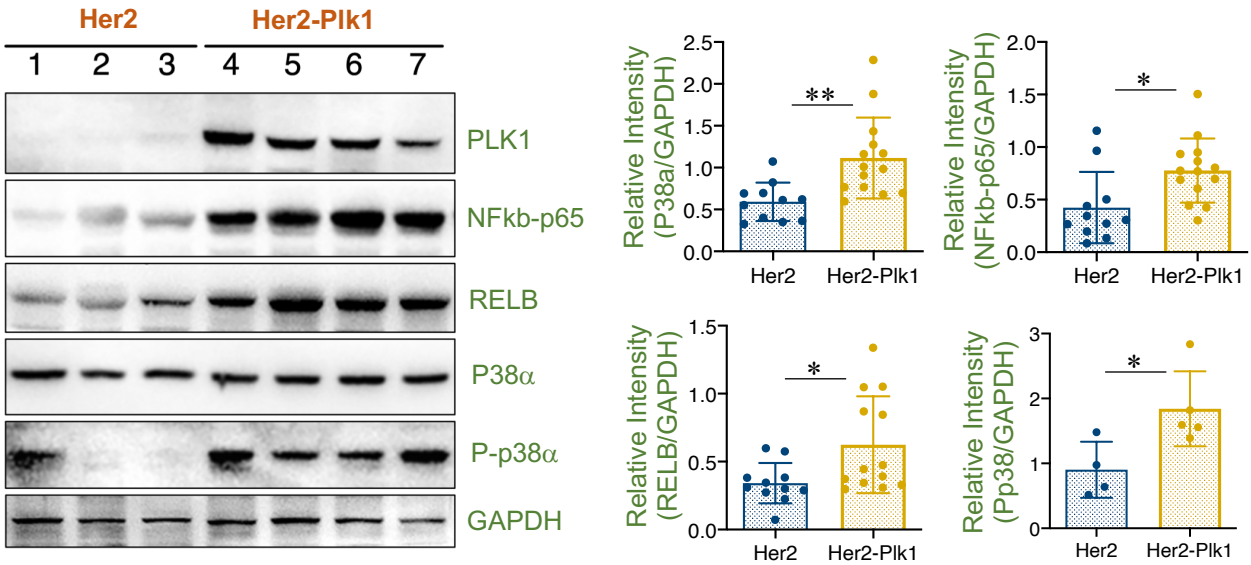

Figure 15: Protein levels of P38α, Phopsho-p38α, RELB and NF-kB-p65 by western blotting in Her2 and Her2-Plk1 mammary tumors. GAPDH is used as a loading control. Bar graphs denote the relative intensity of the signal with respect to GAPDH (* $p<0.05$, ** $p<0.01$, ns, not significant, Mann-Whitney test, n=11 (Her2), n=13 (Her2-Plk1); numbers represent different tumors). For P-p38, n=4 (Her2), n=5 (Her2-Plk1).

groups and found elevated protein levels of p-p38α, NFkb-p65 (canonical signaling) and RELB (non-canonical signaling) in the Her2-Plk1 group (Figure 15).

4.2.2 Plk1 overexpression results in upregulation of markers associated with immune suppression

Highly aneuploid tumors show reduction in markers associated with cytotoxic cells, decreased antigen presentation and elevated levels of anti-inflammatory cytokine production (Davoli et al., 2017; Tripathi et al., 2019; Xian Su et al, 2021). Moreover, NF-kB is known to regulate PD-L1 expression in tumor cells (Xu et al., 2019; Antonangeli et al., 2020). Therefore, to see if senescence and SASP induced by NF-kb upregulation alter the tumor microenvironment of tumor expressing high levels of Plk1, I preliminarily performed immunohistochemistry for PD-L1 (CD274) and CD206, a marker for M2 macrophages in mammary tumor sections from both groups. Her2-Plk1 tumors showed increase in expression of PD-L1 and CD206, indicating a suppressive microenvironment in these tumors (Figure 16).

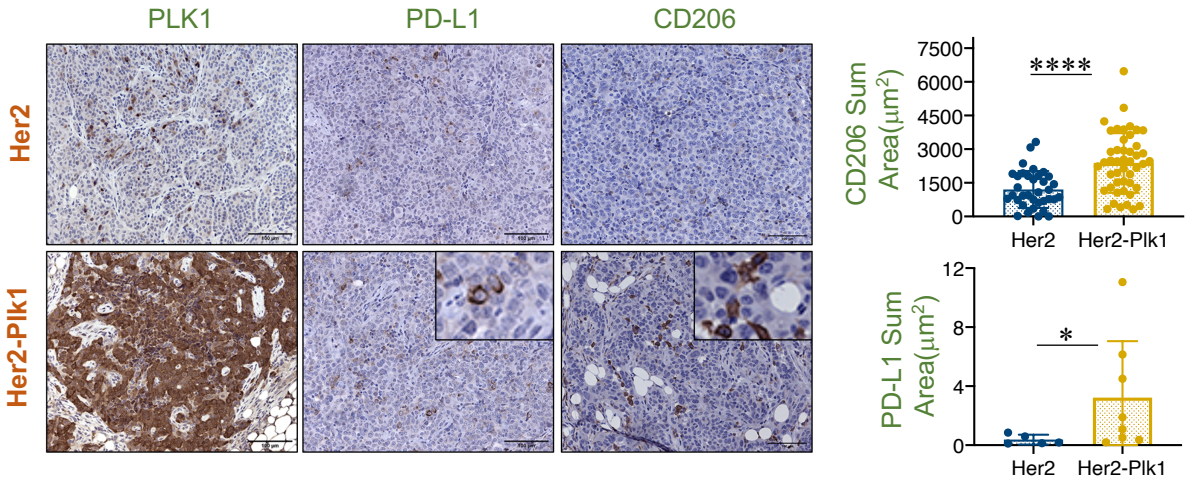

Figure 16: Immunohistochemistry showing expression of PLK1, PD-L1 and CD206 in Her2 and Her2-Plk1 tumor cohorts. Bar plots denote total sum area (µm^2). Positive regions are computed by dividing DAB positive area in each ROI to the total area of the ROI (region of interest). The total sum area (µm^2) of each sample is determined by adding positive regions from all the ROI's. Scale bar: 100µm. (*, $p<0.05$, **** $p< 0.0001$, Mann-Whitney test, n=5 (Her2), n=8 (Her2-Plk1).

4.2.3 Plk1 overexpression results in decreased infiltration of cytotoxic immune cells

Many studies have reported PLK1 to be oncogenic and associated with poor prognosis (Xun et al., 2020; Liu et al., 2022; Liu et al., 207; Dang et al., 2018; Hassan et al., 2018). Furthermore, correlation of tumor immunity with PLK1 expression in different cancer types showed tissue-specific effects (Li et al., 2018). Therefore, to see if there is an exclusion of cytotoxic immune cells from the high CIN microenvironment, I performed flow cytometry to quantify the immune cell populations (NK cells, CD4/CD8 T cells, Dendritic cells and Regulatory T-cells) in spleens and tumors of both Her2 and Her2-Plk1 cohorts. The schematic of the gating strategy is described below (Figure 17). FACS analysis of specific immune cell types from breast tumor tissues displayed elevated numbers of Tregs and dendritic cells in the Her2-Plk1 cohort characterized as $CD3^{+}CD4^{+}CD25^{+}Foxp3^{+}$ and $CD11c^{+}MHCII^{high}$ respectively. Similarly, these tumors also showed reduction in the total number of infiltrating NK cells which were characterized as $CD11c^{-}Nkp46^{+}/Nk1.1^{+}$ expressing cells (Figure 18). Interestingly, such a phenotype was not seen in the spleens of these mice (Figure 19). Thus, these results conclude that Plk1 expression inhibits cytotoxic tumor cell infiltration thereby effecting antitumor immunity.

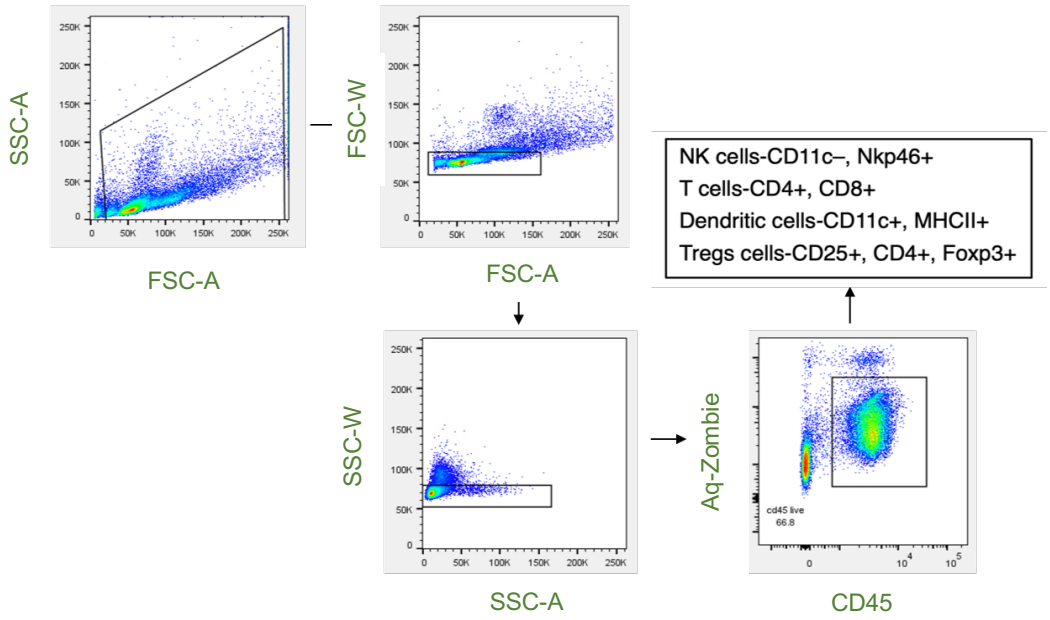

Figure 17: Schematic of strategy used for analyzing NK cells, T cells, Dendritic cells and Regulatory T cells (Tregs) in both Her2 and Her2-Plk1 tumors.

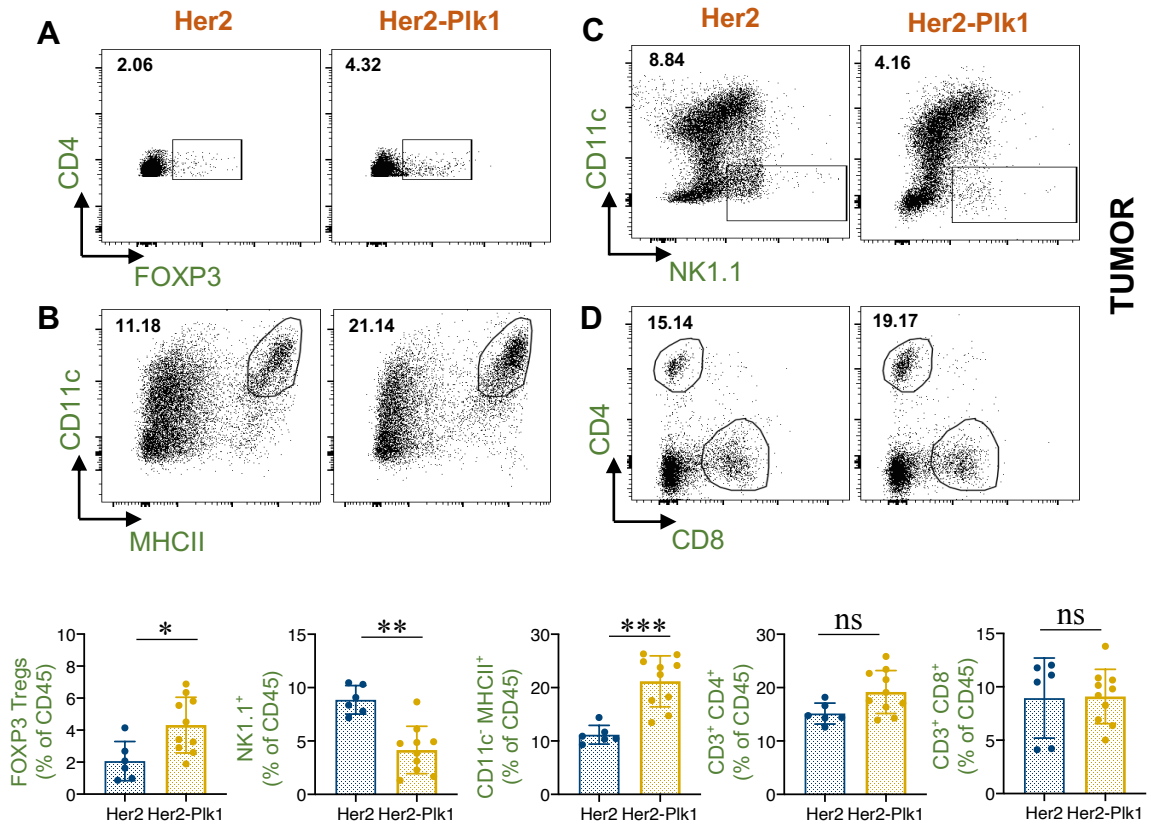

Figure 18: Quantification of tumor-infiltrating lymphocytes by two-parameter dot plots in Her2 and Her2-Plk1 tumors. **A)** Tregs ($CD25^+CD4^+Foxp3^+$), **B)** Dendritic cells ($CD11c^+MHCII^{high}$), **C)** NK cells ($CD11c^-Nkp46/Nk1.1^+$)) and **D)** T cells ($CD3^+CD4^+$, $CD3^+CD8^+$) in tumors (*, $p<0.05$, ** $p<0.005$, ***, $p< 0.0005$, Mann-Whitney test n=6 (Her2), n=10 (Her2-Plk1)) and bar plots are shown as % of CD45 positive cells. Percentage of each cell type is depicted in the boxes.

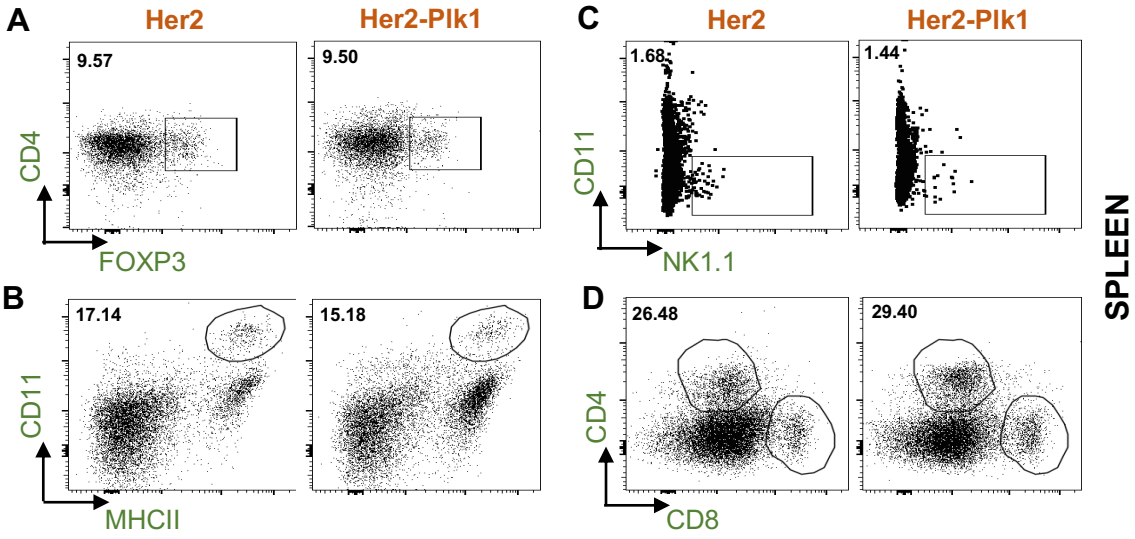

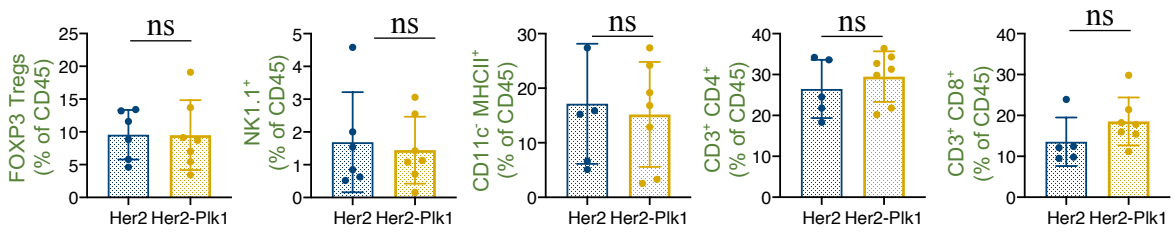

Figure 19: Quantification of tumor-infiltrating lymphocytes by two-parameter dot plots in Her2 and Her2-Plk1 spleens. **A)** Tregs ($CD25^+CD4^+Foxp3^+$), **B)** Dendritic cells ($CD11c^+MHCII^{high}$), **C)** NK cells ($CD11c^-Nkp46/Nk1.1^+$)) and **D)** T cells ($CD3^+CD4^+$, $CD3^+CD8^+$) in spleens (*, $p<0.05$, ** $p<0.005$, ***, $p< 0.0005$, Mann-Whitney test n=5 (Her2), n=7 (Her2-Plk1)) and bar plots are shown as % of CD45 positive cells. Percentage of each cell type is depicted in the boxes.

4.2.4 Activation of NF-kb signaling is a result of non-cell autonomous effects of Plk1 overexpression

To test whether the activation of NF-kB (canonical and non-canonical) and p38MAPK signaling is a direct consequence of Plk1 overexpression (cell-autonomous effect) or an indirect effect mediated by the presence of immune cells (non-cell autonomous effect) in the tumor microenvironment, I used human breast cancer cell lines MCF7 (expressing estrogen/progesterone receptor) and Cal51 (Triple negative) to test the hypothesis *in vitro*. Cells were cultured alone or infected with doxycycline-inducible PLK1 vector for 24, 48 and 72 hrs. I discovered that MCF7 and Cal51-rtTA cells infected with a doxycycline-inducible PLK1 vector and grown in isolation without a surrounding microenvironment (immune cells) did not exhibit significant differences in NF-kB-p65, RELB and p38α expression levels after doxycycline induction. This experiment suggests the importance of immune cells in the tumor microenvironment in activation of corresponding signaling pathways (Figure 20 A&B). Thus, this experiment underlines the importance of using *in vivo* mouse models for studying the consequences of chromosomal instability and also the significance of other cell types in the tumor microenvironment.

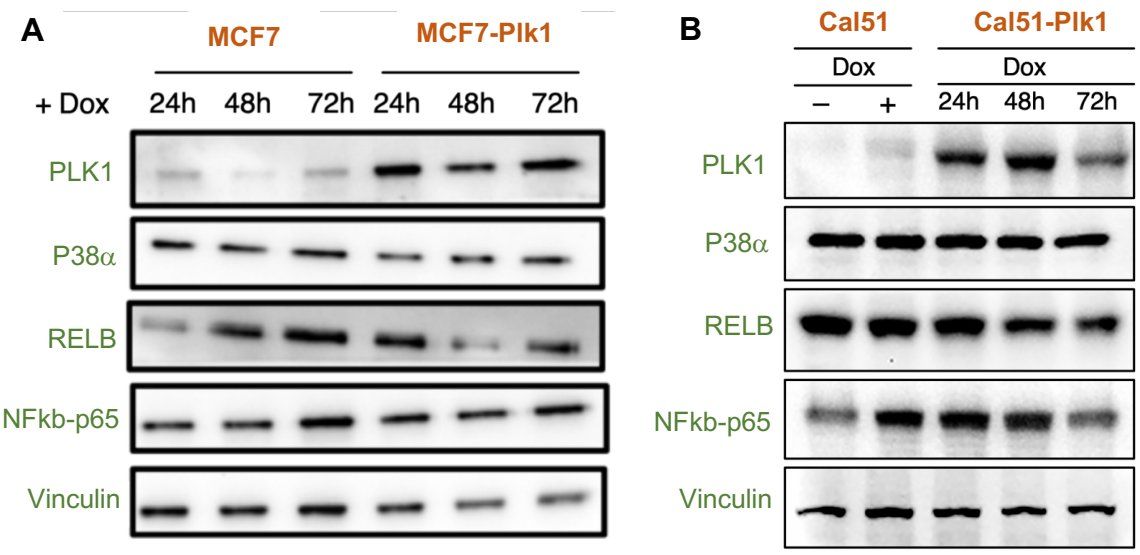

Figure 20: Protein levels of P38α, PLK1, RELB and NF-kB-p65 by western blotting in A) MCF7 and MCF-Plk1 and B) Cal51 and Cal51-Plk1 cells. The cells were incubated with doxycycline for 24, 48 and 72hrs. Vinculin was used as a loading control.

Next, to see if the activation of NF-kB (both canonical and non-canonical) signaling was merely due to Plk1 expression or a consequence of high CIN, with the assistance of my colleague Maria Ramos, we performed western blotting of the NF-kB family and p38MAPK proteins using another breast cancer mouse model, which overexpresses Mad2 instead of Plk1 in the mammary epithelial cells under the influence of the mouse mammary tumor virus promoter (MMTV-rtTA). MAD2 is an essential spindle checkpoint protein whose overexpression also induces CIN in mammary tumors predominantly by the formation of micronuclei (Rowald et al., 2016). Interestingly, I saw elevated expression of NF-kB-p-65, RELB and phospho-p38 in the tumors expressing Mad2 (Figure 21), concluding that this upregulation of NF-kB and p38MAPK pathways is a result of direct consequence of CIN induced by Plk1 and not due to increased levels of Plk1.

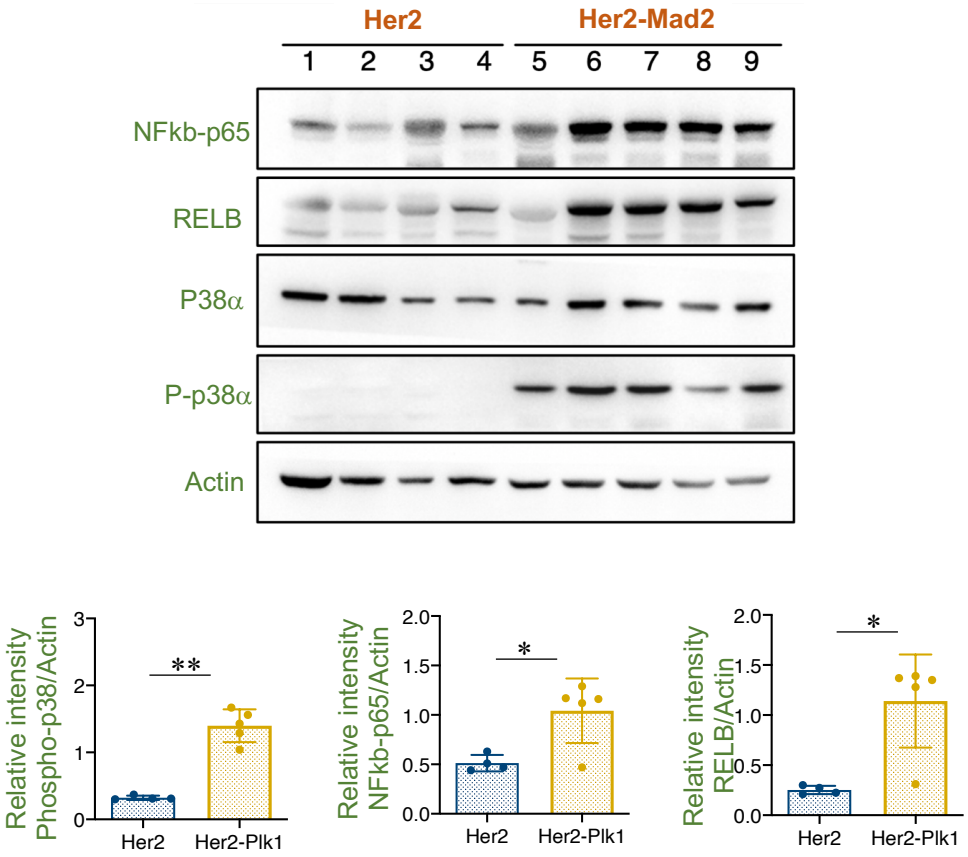

Figure 21: Protein levels of P38α, Phopsho-p38α, RELB and NF-kB-p65 from lysates of Her2 and Her2-Mad2 mice by western blotting. Actin was used a loading control. Bar plots denote the relative intensity of the signal with respect to actin (*, $p<0.05$, **, $P<0.01$, Mann-Whitney test, n=4 (Her2), n=5 (Her2-Plk1); numbers represent different tumors). * Western blot performed by Maria Ramos

4.3 Modulation of immune cells during early stages of high CIN tumor development

4.3.1 Somatic copy number alterations in early stage mammary glands expressing PLK1.

Chromosomally unstable (mitotically arrested) cells upregulate gene signatures associated with inflammation and cell surface proteins belonging to NKG2D family that are recognized by NK cells to eliminate them *in vitro* (Santaguida et al., 2017). However, my preliminary data showed that overexpression of Plk1 in mammary tumors resulted in reduced infiltration of cytotoxic immune cells and upregulation of PD-L1. This led to the hypothesis that chromosomally unstable cells are initially recognized by the immune system but at some point, evade anti-tumor immunity to facilitate tumor growth. Therefore, to comprehend how CIN alters the immunological microenvironment to cause suppression, I collected pre-malignant stage mammary glands from 16 days Her2 mice and 22 days Her2-Plk1 mice respectively (Figure 22A). Moreover, to determine the aneuploidy levels, I performed immunohistochemistry of Plk1 (Figure 22B) and my colleague Sara Chocarro performed fluorescence *in situ* hybridization (FISH) on the same sections (Figure 23 A&B). It is clear from these results that Plk1 expression induces higher levels of somatic copy number alterations very early during tumor development.

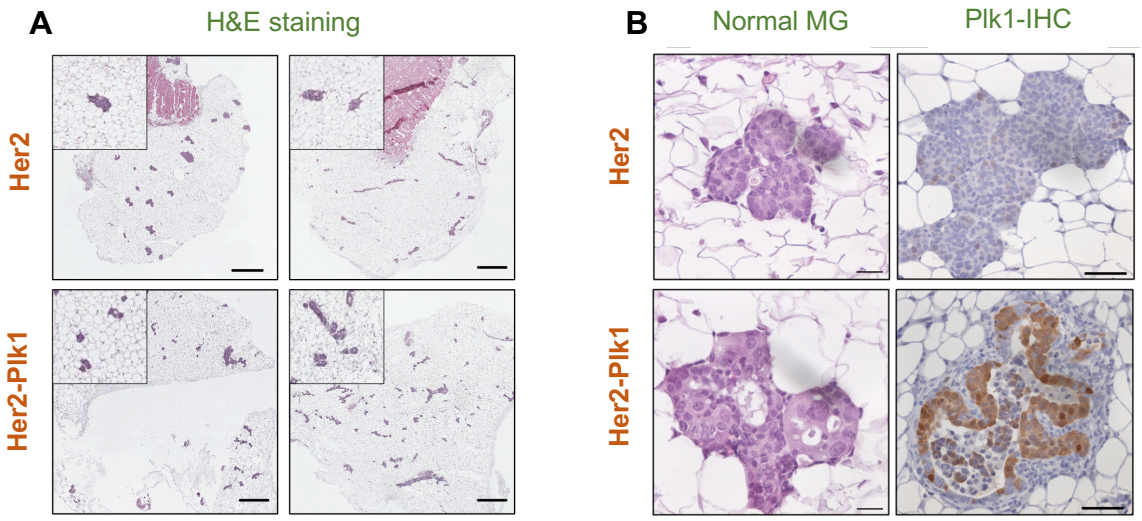

Figure 22: **A)** H & E staining of mammary glands from early stages in both Her2 and Her2-Plk1 mice. **B)** Immunohistochemistry showing expression of Plk1 in in both the cohorts.

4.3.2 Single cell sequencing of early stage Her2 and Her2-Plk1 tumors

To understand the phenotype of immune cells at these early time points, I performed single cell sequencing on 23120 sorted CD45^{+} cells from both the cohorts. The schematic of the sorting strategy is described below (Figure 24A). The Seurat package (Butler et al., 2018) was used to analyze the data, and cell-type annotation using SingleR and the ImmGen database was carried out to determine various populations of innate and adaptive immune cells. I identified 14 different immune cell subsets as shown in the UMAP below (Figure 24B). The analysis of single cell data was done with the help of Lena Voith von Voithenberg and I sincerely thank Charles Imbusch for his feedback and inputs during the discussions.

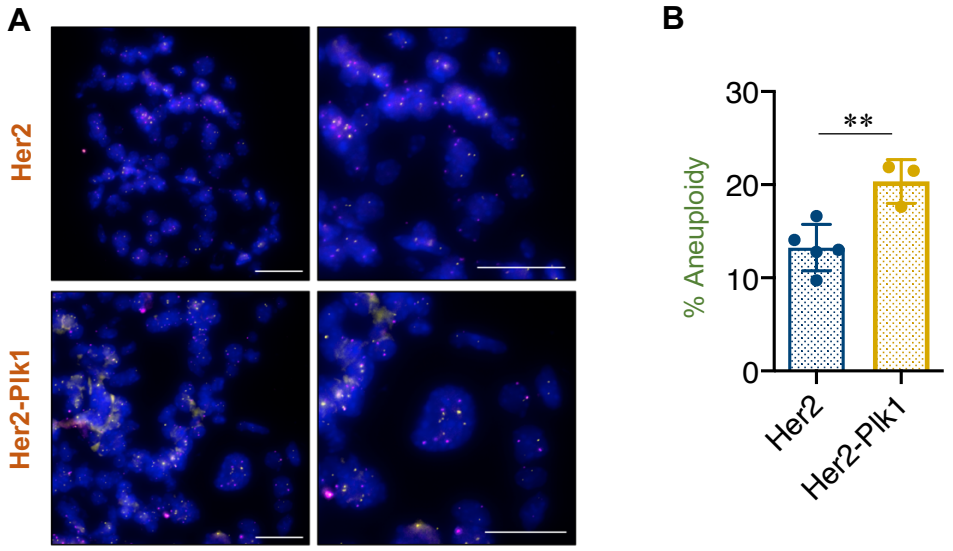

Figure 23: **A)** Using two centromeric probes against chromosomes 16 and 17, fluorescence in situ hybridization (FISH) of early stage mammary glands was performed. **B)** Aneuploidy percentage is represented by bar plots. P=0.0073**, unpaired t-test. Scale bar: 50µm. * Experiment performed by Sara Chocarro.

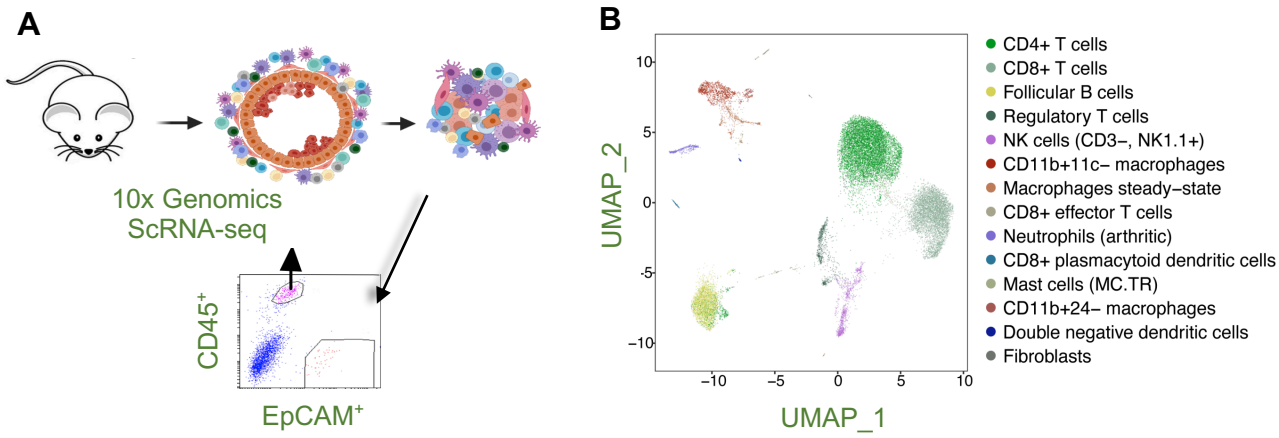

Figure 24: **A)** Schematic of FACS sorting to obtain CD45 hematopoietic cells at early stages in Her2 and Her2-Plk1 samples. Samples were extracted from three different mice per group. **B)** UMAP displaying immune cell populations from both cohorts in color coded fashion. *Sorting done with the assistance of Yuanyuan Chen.

Firstly, from the single cell analysis, the relative number of cells between the two groups is represented in the UMAP and bar plot below (Figure 25 A&B). It is clear that the tumor microenvironment of the two groups is dominated by T cells (approximately 60-70% of all cells) based on the composition of immune cells. At baseline, Her2-Plk1 group has a relatively larger fraction of T cells (CD4 T cells and Tregs) whereas macrophages and NK cells were found in lesser numbers. The total number of cells that were captured from each cell type is represented in the table below (Table 2).

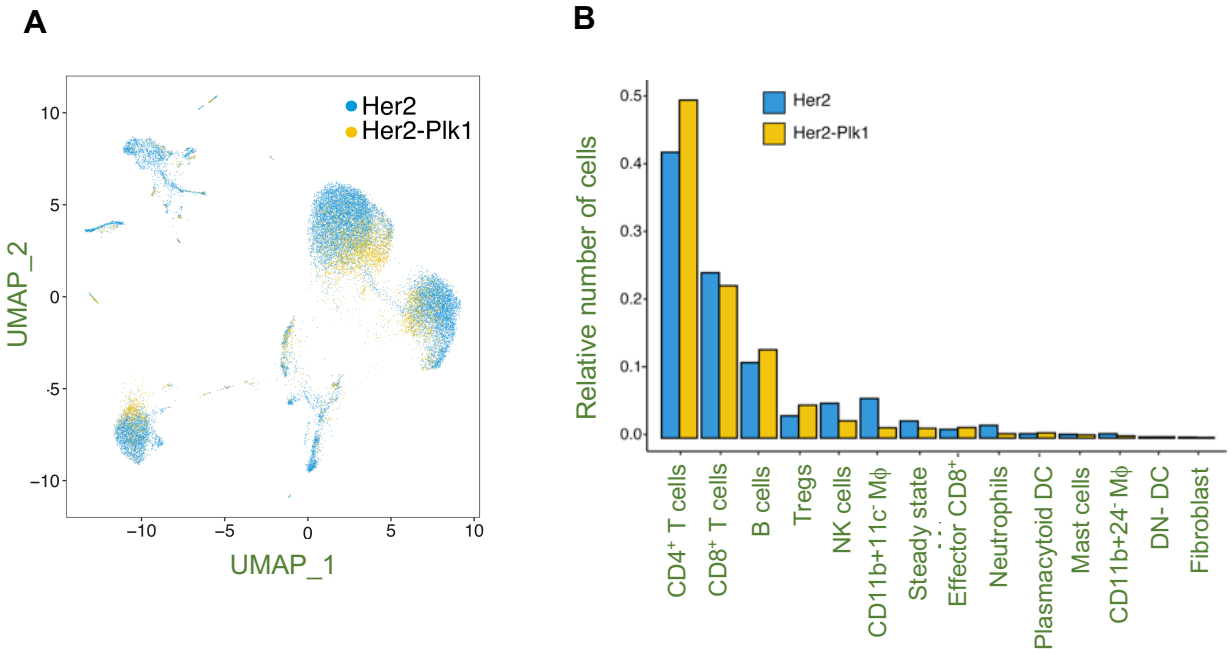

Figure 25: **A)** UMAP representing, total number of immune cells from each of the sample type Her2 and Her2-Plk1. **B)** Bar graph showing relative number of immune cells in Her2 and Her2-Plk1 early stage mammary glands.

Cell Type	Her2	Her2-Plk1	Total
Follicular B cells	2062	605	2667
CD4+ T cells	7808	2312	10120
Regulatory T cells	608	225	833
CD8+ T cells	4519	1043	5562
CD8+ effector T cells	239	73	312
CD11b+24^{-} macrophages	120	15	135
CD11b+11c- macrophages	1082	71	1153
Macrophages steady-state	468	67	535
Natural killer cells (CD3^{-}, NK1.1^{+})	950	118	1068
CD8+ plasmacytoid dendritic cells	121	36	157
Double negative dendritic cells (DN-DC)	34	9	43
Neutrophils (arthritic)	349	30	379
Mast cells (MC.TR)	106	22	128
Fibroblasts	24	4	28
Total	18490	4630	**23120**

Table 2: Total number of cells captured per sample and cell type respectively.

Cell type annotation in single cell analysis starts with identification of markers that define a cluster via differential expression. All the positive and negative markers in a single cluster are identified compared to all other cells. The same strategy is employed to find markers in all other remaining clusters. The features (markers) are detected based on a threshold: at a minimum percentage and differentially expressed (on average) at minimum amount between the groups. Finally, the cell type identity is determined by the expression of top 20-30 markers in each of the cluster compared to all other clusters. Below is the heatmap showing different cell types identified based on the expression of top markers in each cluster (Figure 26).

4.3.3 Cell type annotation for different immune cells in early stage Her2 and Her2-Plk1 tumors

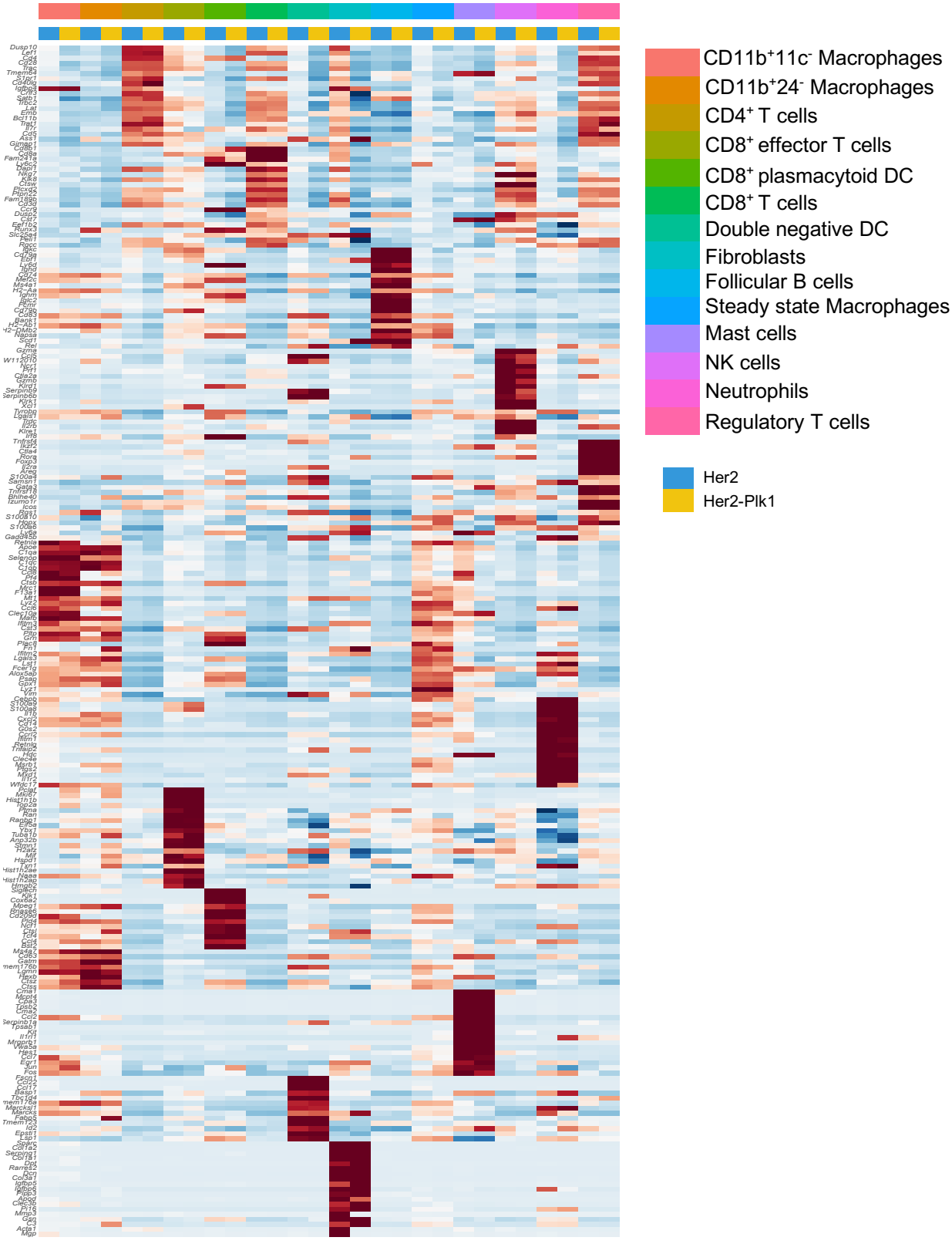

Figure 26: Identification of cluster-specific marker genes detected through differential expression analysis between the clusters. Heatmap representing normalized gene expression of different cluster specific markers.

4.3.4 Immune modulation in early stages of Her2-Plk1 tumors – effect on innate immune system (NK cells)

NK cells are innate immune cells that mediate cytolytic/anti-tumor effects against stressed cells such as those experiencing high levels of DNA damage or tumor cells. Cells with complex karyotypes exhibiting CIN are detected and eliminated by NK cells *in vitro* (Santaguida et al., 2017) and furthermore, *in vitro* NK cell killing systems demonstrate NF-kB upregulation central to eliciting a cytotoxic response in the context of CIN (Wang et al., 2021). To understand the phenotype *in vivo* in the presence of a tumor microenvironment, I analyzed the NK1.1 cluster of the sorted CD45^{+} cells. Firstly, I observed a stark difference in the expression of *Cd27* and *Itgam* (CD11b) when comparing NK cells of both cohorts (Figure 27A). Surface expression of *Itgam* and *Cd27* in mouse NK cells defines their maturation status and cytotoxic ability (Abel et al., 2018). This functional classification from the existing literature gave a hint that the NK cells from Her2-Plk1 cohort showed reduced cytotoxicity.

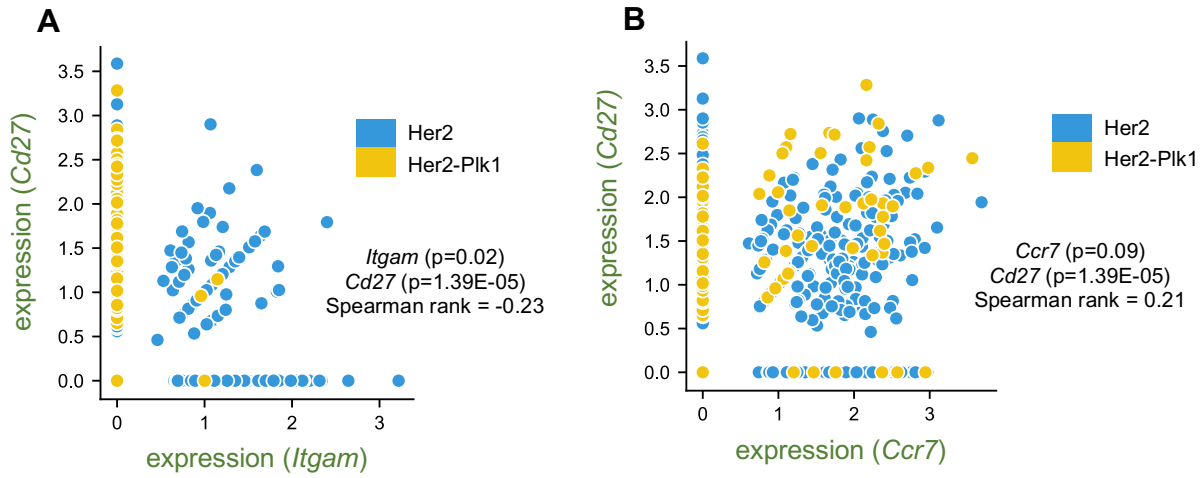

Figure 27: **A)** Scatter plots with normalized gene expression of *Cd27* versus *Itgam* (CD11b) and **B)** *Cd27* versus *Ccr7* in NK cells at the single cell level. The Spearman rank correlation coefficients and p-adjusted values for differential gene expression between Her2 and Her2-Plk1 samples are shown.

Expression of another chemokine *Ccr7*, which plays a key role in NK cell migration to lymph nodes (Campbell et al., 2001; Vitale et al., 2004) was seen in both the cohorts (Figure 27B). To assess the levels of cytotoxicity between NK cells of both the cohorts, I looked into the expression of key effector molecules like *Gzma*, *Gzmb* and *Prf1* and observed a trend with downregulation of NK-effector molecules in the Her2-Plk1 group (Figure 28B).

Secondly, other set of genes that aid in the activation of NK cells such as *Nkg7*, chemokines (*Ccl5, Ccl4, Ccl3)* and activating receptors (*Klrd1, Ncr1, Cd226, Klrb1c)* were upregulated in Her2 samples in comparison to Her2-Plk1 (Figure 28A). Surprisingly, activating receptor *Klrk1* (NKG2D) which is upregulated in the context of aneuploidy was not significantly different between both groups (Figure 28B), although both groups showed varying degrees of CIN.

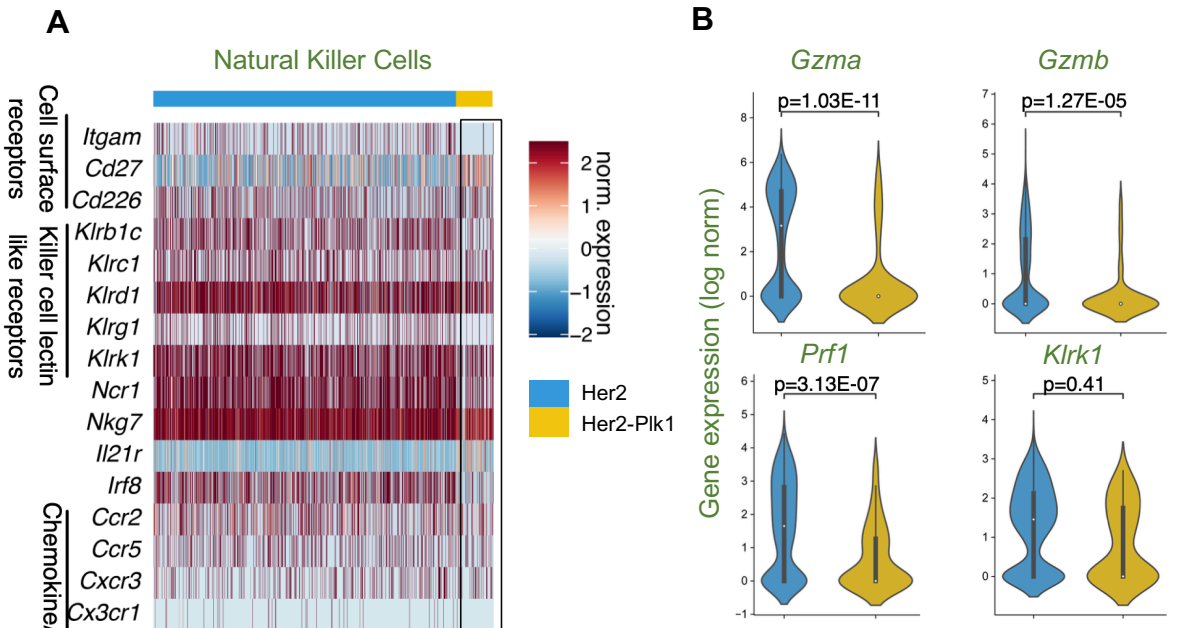

Figure 28: **A)** Heatmap showing normalized gene expression levels of differentially expressed genes in NK cells. Each line represents a single cell. **B)** Violin graphs showing the log-normalized gene expression values of *Gzma, Gzmb, Prf1, Klrk1* in NK cells of both the cohorts.

Apart from activating receptors and effector molecules, I looked to see if there are any additional genes that effect the functional maturation, development, and trafficking of NK cells within tumors exhibiting chromosomal instability and found upregulation of *Socs3* and downregulation of *Cx3cr1, Irf8* in the Her2-Plk1cohort (Figure 28A). However functional validation needs to be done to see the effect of up/down regulation of these specific genes/transcription factors on the phenotype of NK cells. Furthermore, gene set enrichment analysis of NK cells between the two cohorts showed downregulation of hallmark signatures associated with IFNα response, oxidative phosphorylation, and complement system in early stage mammary glands of Her2-Plk1 mice (Figure 33B).

Lastly, to corroborate some of the previous findings *in vivo*, and to validate whether NK cells mediate immune sensing of aneuploid tumor cells, I treated Her2 and Her2-Plk1 animals with an NK blocking antibody (anti-mouse NK1.1) intra peritoneally (ip) and monitored the survival of the animals. Even though, Her2 tumors proliferated more quickly after NK cell depletion, I found that this difference was not significant when compared to Her2-Plk1 animals, which had significantly shorter survival times (Figure 29 A&B). Interestingly, blocking NK cells besides reducing the survival time of high aneuploid tumors, also gave a hint on their reduced effector capabilities during early stages. Therefore, a possible explanation in this scenario is that CIN induced in early stages drives the tumor delay of Her2-Plk1 tumors (direct effect), while non-cell autonomous effects drive NK cells in conjunction with other immune cells to a suppressive state. Subsequent experiments aimed at elucidating the relationship between NK cells and tumor microenvironment during different stages of tumor progression would aid in a better understanding of their dual role in the context of CIN. Thus, it can be concluded based on this functional validation that cytotoxic abilities of NK cells are viable only until a certain level of CIN and beyond that threshold, non-cell autonomous effects of CIN kick in as a result of increased rate of missegregations and irreversible cell cycle arrest. This results in modulation of the activity of NK cells.

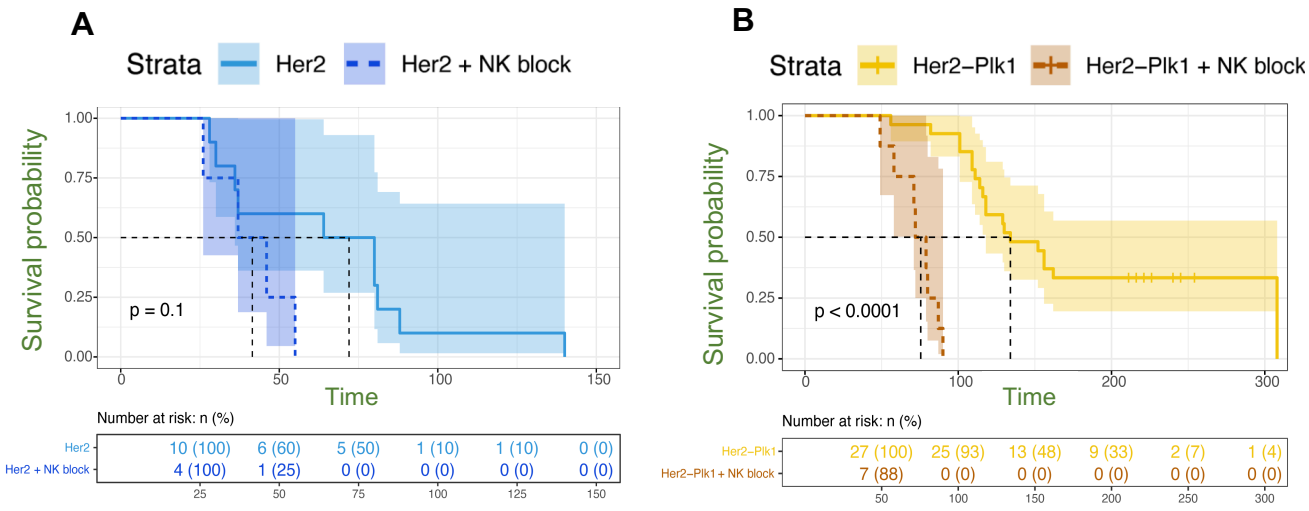

Figure 29: A &B) Survival curves of Her2 (n=4) and Her2-Plk1 (n=7) mice treated with NK1.1 blocking antibody. Survival probability and percentages of mice alive over time are displayed below the graph.

4.3.5 Immune modulation in early stages of Her2-Plk1 tumors – Effect on innate immune system (Macrophages)

Macrophages are specialized cells that help in phagocytosis and are considered an important component of the innate immune system. CIN attracts neutrophils and macrophages, which promotes the growth of tumors as a result of ongoing inflammation (Duijf & Benezra., 2013; Roschke & Rozenblum., 2013). Therefore, I considered looking at the phenotype of these cells in the context of CIN. Single-cell sequencing analysis showed the presence of two different populations of TAMs (Tumor associated macrophages). The first group of macrophages labelled as $CD11b^{+}CD11c^{-}$ expressed genes *Cd209d, Mrc1, Retnla/Fizz1, Selenop, F13a1, Igfbp4* and *Clec10a,* whereas the second group of macrophages that were labelled as $CD11b^{+}CD24^{-}$ expressed genes such as *Fn1, Ctss, Hexb, Gatm, Ctsl* and *Runx3* (Figure 26). Firstly, I looked to see if there was any inflammatory response change based on different degrees of CIN in both cohorts. Interestingly I discovered that both subsets showed expression of *Tnf* superfamily genes like *Tnf, Tnfrsf1a* and *Tnfrsf1b*. Similarly, gene sets activated in response to inflammation triggered by the activation of *Tnf* pathway such as *Il1b, Traf2, Nlrp3, Tlr2, Nfkb1* and *Tmem173* were also upregulated in both cohorts regardless of their ploidy status, with no discernible differences (Figure 30 A&B).

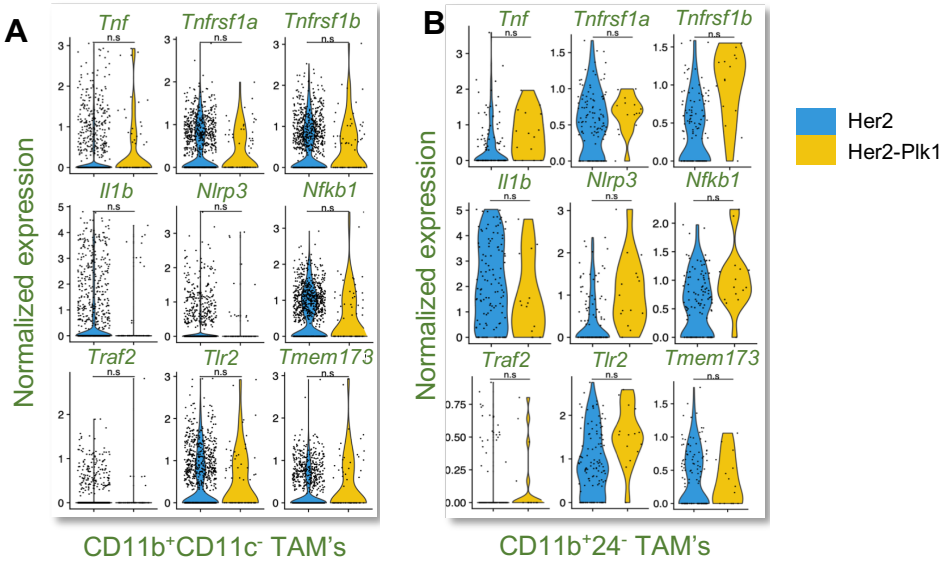

Figure 30: Violin plots displaying normalized gene expression values of Tnf and other genes involved in Tnf mediated inflammatory signaling. **(A)** $CD11b^{+}CD11c^{-}$and **(B)** $CD11b^{+}CD24^{-}$macrophages respectively.

Subsequently, from the differential expression of genes in $CD11b^{+}24^{-}$ TAM subset, I saw upregulation of genes such as *Gpnmb, Adam8, Fam20c, Fcgr2b, Pdpn, Ahnak* (Figure 31) and *Arg1, Il1rn, Pltp, Nrp2 and Timp1* etc in the Her2-Plk1 group as shown in the heatmap below (Figure 32). Other genes from toll like receptor family, Myd88 signaling, chemokines, super oxide family members, endoplasmic reticulum genes etc are also displayed in the heatmap (Figure 32). *Arg1, Nrp2* mediate immunosuppressive functions through catabolizing arginine required for T cell activation/proliferation and regulating efferocytosis of apoptotic tumor cells (Rodriguez et al., 2007; Bronte & Zanovello., 2005; Fadok et al., 2001) respectively. Similarly, other overexpressed genes such as *Gpnmb, Adam8, Fam20c, Pdpn, Ahnak* also play a critical role in angiogenesis, migration and invasion of tumor cells (Rose et al., 2007; Rose et al., 2010; Schwab et al., 2021; Bieniasz-Krzywiec et al., 2019; Sohn et al., 2018). Additionally, these macrophage subsets displayed decrease in expression of the MHCII-related genes *H2-ab1, H2-Aa,* and *H2-Dma* that affect their antigen presentation (Figure 32). Altogether, the phenotype of these macrophages show decrease in effector functions, thereby dampening their cytotoxic ability.

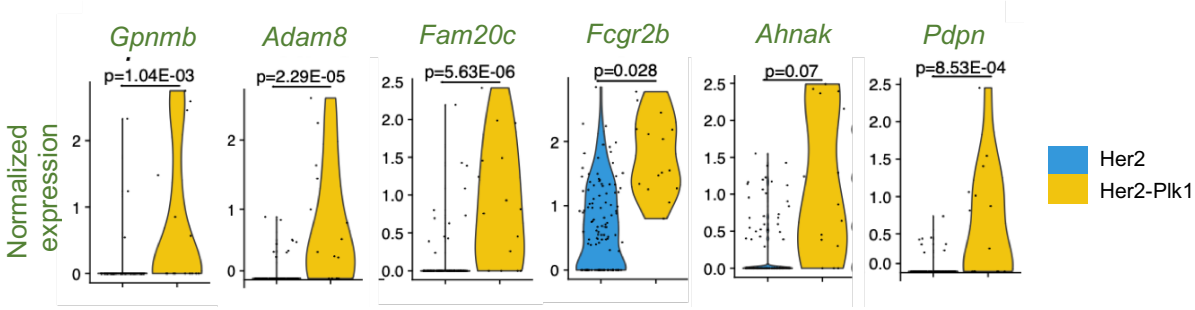

Figure 31: Violin plots displaying normalized gene expression values (along with Adjusted p-values) in $CD11b^{+}CD24^{-}$ macrophages for selected genes *Gpnmb, Adam8, Fam20c, Fcgr2b, Ahnak, Pdpn.* Each dot represents an individual cell.

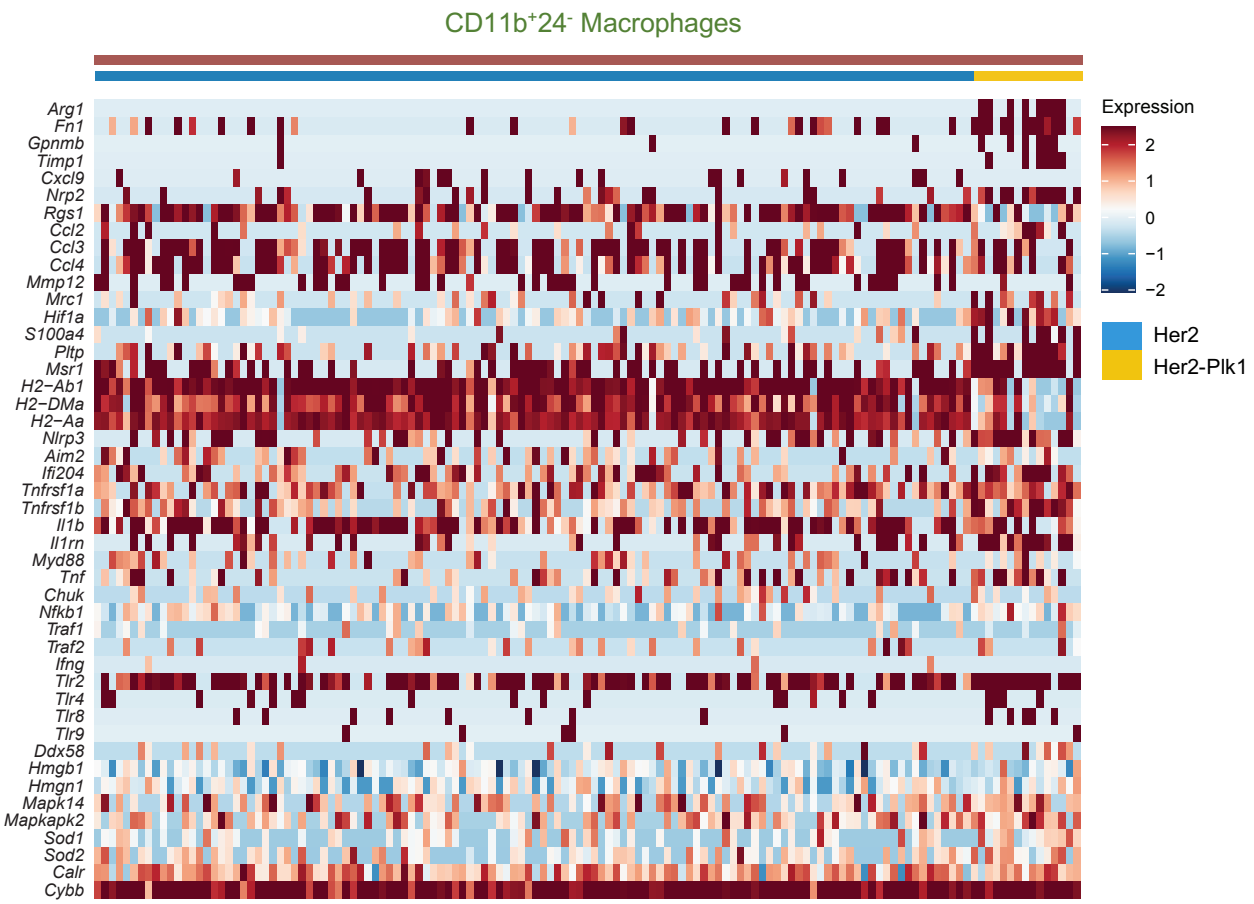

Figure 32: Heatmap showing the normalized gene expression levels of antigen presentation, anti-inflammatory and EMT related genes in CD11b^{+}CD24^{-} macrophages. Her2 samples are displayed in blue and Her2-Plk1 samples in yellow.

Lastly, differential expression analysis from the CD11b^{+}11c^{-} subset revealed downregulation of genes such as *S100a8/S100a9, Ltb, Tpt1, Smad7, Crip1, Ccl24* and *Ccl6* in Her2-Plk1 cohort (Figure 33A). These genes are known to be primarily involved in the transcriptional activation of inflammatory signaling. However, there was no significant difference in the phenotype between both the groups. Finally, angiogenesis and Epithelial-Mesenchymal Transition pathways were shown to be elevated in Her2-Plk1 samples according to GSEA analysis of CD11b+24- macrophages (Figure 33B). This section gives a detailed overview in terms of the phenotype of various innate immune cells (NK cells and Macrophages) in the context of CIN. In conclusion, early differentiation of macrophages to Arg1^{+} TAMs and restraining effector NK cell cytotoxicity contributes towards reduced anti-tumor responses in tumors displaying high levels of CIN.

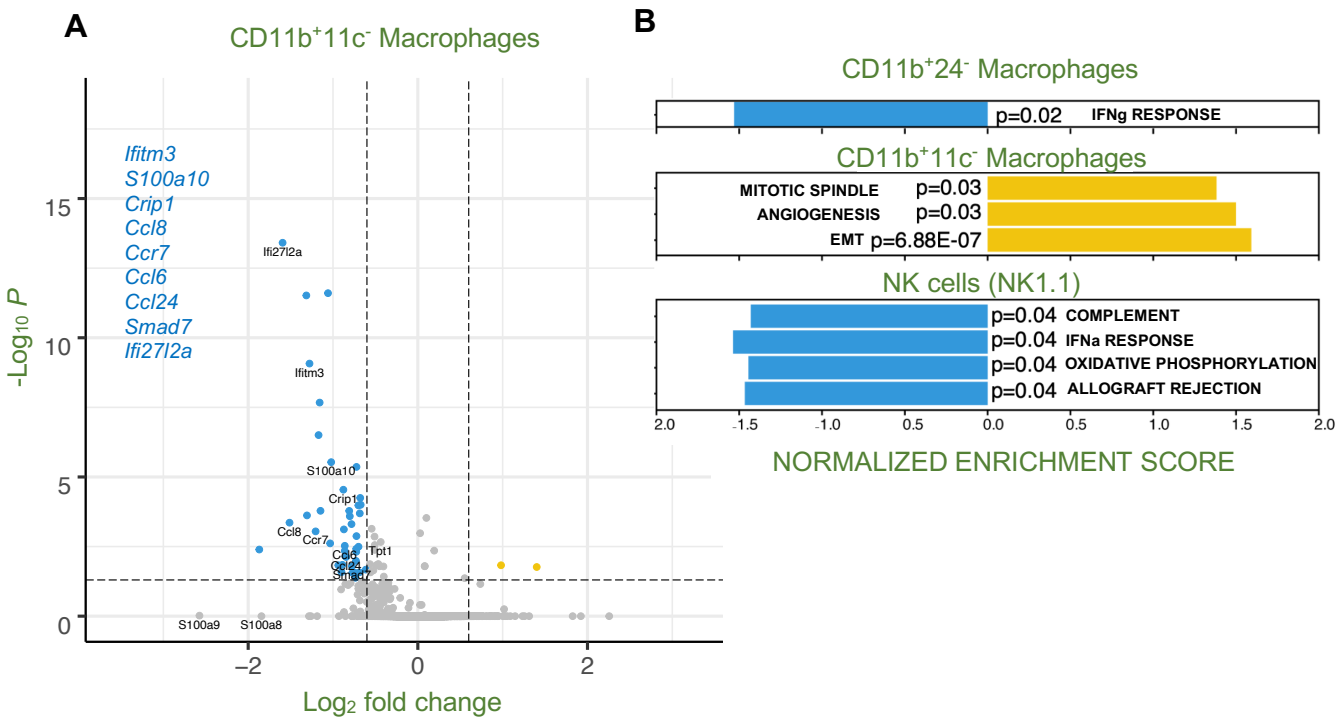

Figure 33: **A)** Volcano plot displaying differentially expressed genes in the CD11b^{+}CD11c^{-} macrophage group. Up/downregulated genes in Her2-Plk1 group with respect to Her2 are plotted on the graph (fold change of ±0.6 and adjusted p-value of ≤0.05). **B)** Bar plots displaying pathways enriched from gene set enrichment analysis in both macrophage groups and NK cells. Y-axis: hallmark signatures and X-axis: normalized enrichment scores

4.3.6 Impact of CIN on cells of the Adaptive immune system – B cells

B lymphocytes are cells of the adaptive immune system that play an important role in humoral immunity. They express clonally diverse cell surface immunoglobulin receptors with the capability to recognize various antigenic epitopes and aid in inhibiting tumor development. However, due to their ability to produce autoantibodies (Lee et al., 2021) and differentiate into regulatory B (He et al., 2014) cells, they can aid in the formation of tumors. To characterize the phenotype of B cells in both Her2 and Her2-Plk1 cohorts, I performed differential expression and found reduced expression of genes *Mzb1, Ltb, Ccl6, Ighg1, C1qa, Myl12b, Cd47, S100a10, Ptpn6, Rgs1, Gimap1, Irf8, Ptpn22, Cd3g, Scd1* and *Cd79b* in Her2-Plk1 early stage mammary glands (Figure 34). Additionally, prior research also demonstrated a close correlation between *Cd79, Mzb1, Scd1, Ptpn22* with altered B cell receptor (BCR) signaling, autoantibody production and modified lipid metabolism (Hardy et al., 2014; Miyagawa-Hayashino et al., 2018; Zhang et al., 2021). I have not done further validations on the phenotype, but it remains interesting to see if Plk1 overexpression results in anti-dsDNA production and an autoimmune phenotype.

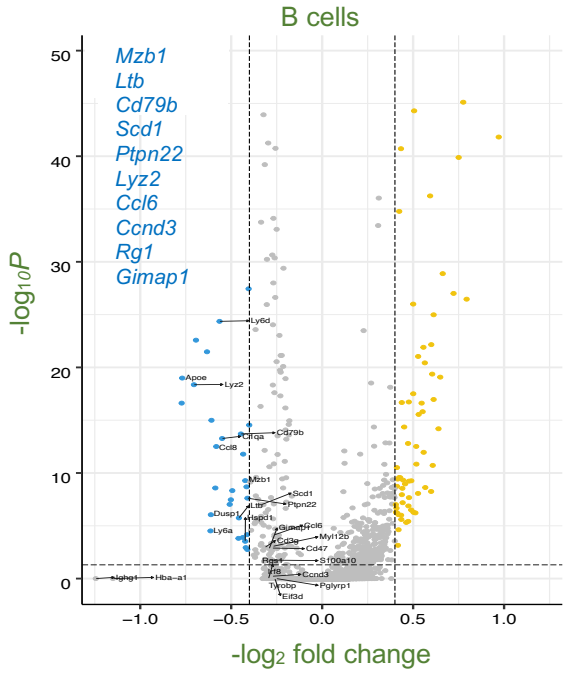

Figure 34: Volcano plots showing differentially expressed genes in the B cell subset of Her2 and Her2-Plk1 mammary glands. Up/downregulated genes in Her2-Plk1 cohort with respect to Her2 are plotted on the graph (by a fold change of ±0.4 and an adjusted p-value of ≤0.05).

4.3.7 Impact of CIN on cells of the Adaptive immune system –Regulatory T cells (Tregs)

Finally, I performed sub-clustering of T cells at higher resolution in Her2 and Her2-Plk1 samples to evaluate T cell infiltration in high CIN samples. I found five unique T cell subsets (Treg cells, CD4+ helper T cells, CD8+ cytotoxic T cells, CD8+ memory T cells, and CD8+ nave T cells) as well as two additional sub clusters (γδT cells) with no definitive information due to their extremely low cell numbers and relative proportions (Figure 35A).

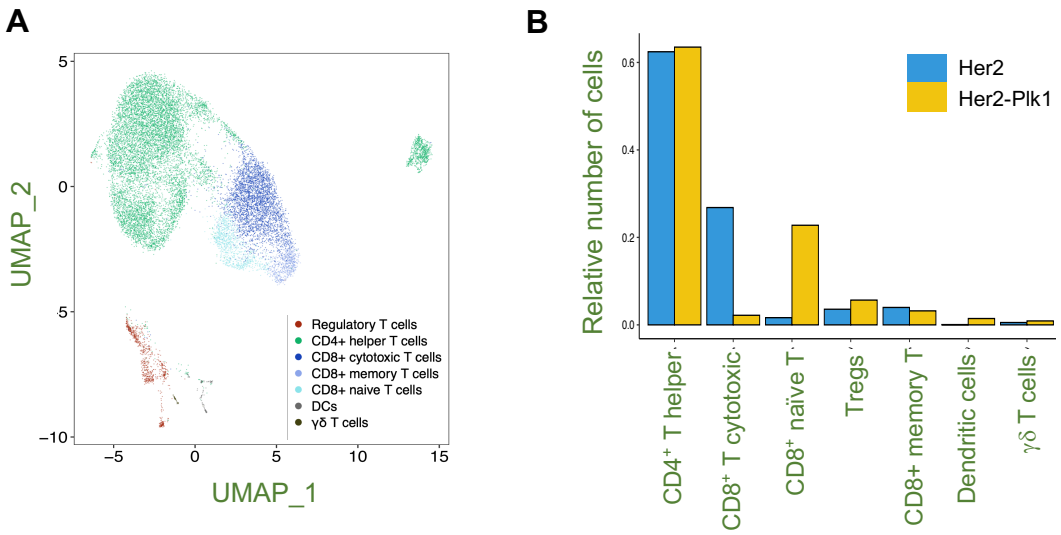

Figure 35: UMAP showing different sub-clusters of T cells. **A)** Cell type annotation reveals the presence of seven different clusters. **B)** Relative distribution of the number of cells in each of the T cell sub-cluster with Her2 in blue and Her2-Plk1 in yellow.

In the Her2-Plk1 samples, I found that the relative proportion of $CD8^+$ naive T cells, regulatory T cells, and $CD4^+$ helper T cells increased while the proportion of $CD8^+$ cytotoxic T cells decreased (Figure 35B). Regulatory T cells play an important role in maintaining self-tolerance but can also suppress the recruitment and proliferation of effector T cells, thereby mitigating antitumor immune responses (Mougiakakos et al., 2010). Surface expression of *Ccr7* and *Cd62L (Sell)* in mouse Tregs defines their activation status thereby being classified as central/resting Tregs ($Cd62L^{high}Ccr7^{high}$) or effector Tregs ($Cd62L^{low}Ccr7^{low}$). When I compared Tregs from Her2 and Her2-Plk1 mammary glands, I found slight upregulation of *Sell* (FC=0.5, p_{adj}=0.4) and *Ccr7* (FC=0.6, p_{adj}=0.02) in Her2-Plk1 cohort, suggesting an increase in the resting phenotype (Figure 36A). Similarly, I observed reduction in gene expression of *Ccr2*, *Ccl5*, and *Ccl8* which are found to affect Treg function (Zhan et al., 2020), compared to Her2 tumors. In high CIN tumors expressing Plk1, my data points towards a decrease in Treg activity and an overall rise in the relative number of resting Tregs very early during tumor development.

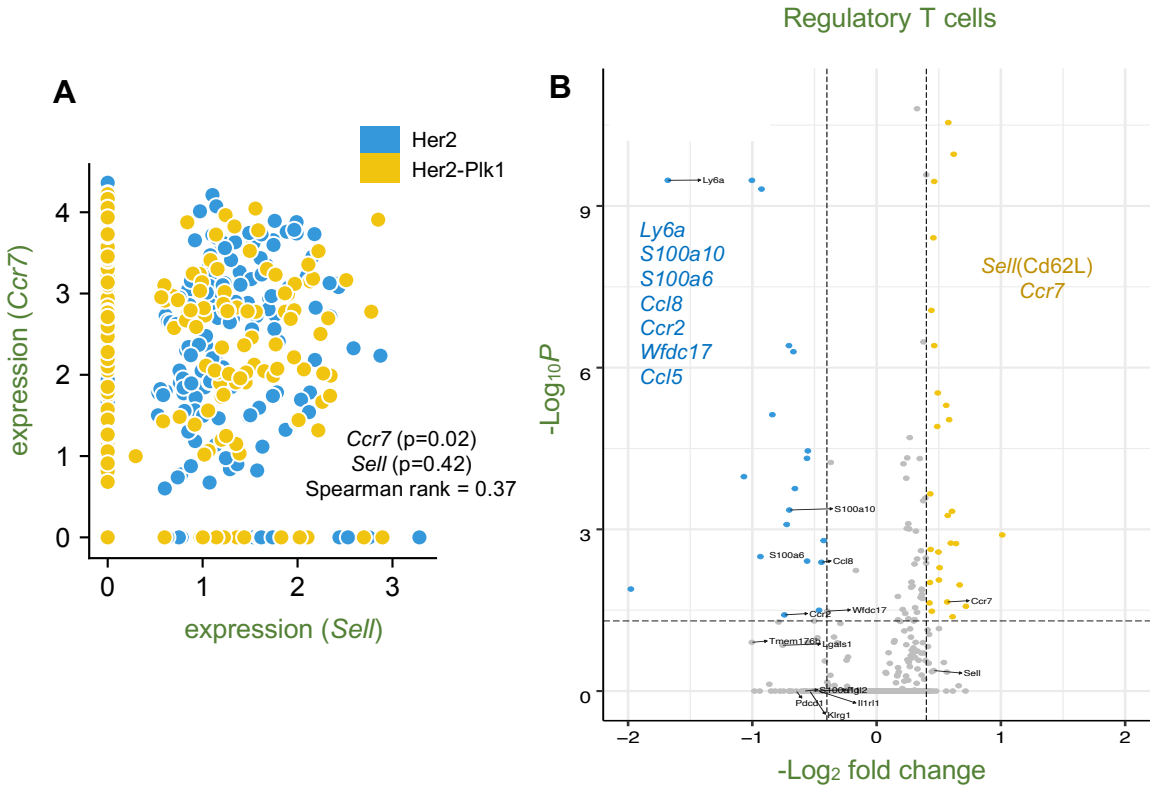

Figure 36: **A)** Normalized gene expression of *Ccr7* versus *Sell* (Cd62L) at single cell level. The Spearman rank correlation coefficient and p-adjusted values for differential expression between Her2 and Her2-Plk1 samples are displayed. **B)** Volcano plot showing differentially expressed genes in Tregs of Her2 and Her2-Plk1 mammary glands. Up/downregulated genes in Her2-Plk1 group with respect to Her2 are plotted on the graph (with a fold change of ±0.4 and an adjusted p-value of ≤0.05).

For the remaining subset of T cells, there was no significant difference in terms of the phenotype (genes expressed), specially CD4 T cells and CD8 T cells. The single cell sequencing at early stages gave a quantitative insight with regards to total numbers and gene sets that were predominant in each of the cell type. Similarly, for the phenotype presented in other cell types (Macrophages/Tregs/B cells/NK cells) *invivo* validation for different activation and suppression markers is presently in progress. In conclusion, induction of CIN in mammary tumors by expressing Plk1 affects the development of both innate and adaptive immune cells leading to immune suppression.

4.4 Understanding the impact of high PLK1 expression in human breast cancers

4.4.1 Human BRCA tumors segregated into two cohorts based on the expression of PLK1

To deepen our investigation into how immune responses of human breast cancers relate to PLK1 expression, I obtained gene expression and copy number data from 1098 human breast tumors (TCGA, PanCancer Atlas). Gene expression data was obtained from Xena Browser (xenabrowser.net) as Log2(normalized counts+1)) and the copy number data in the form of chromosome losses and gains for each chromosome arm from cBioPortal (cbioportal.org). Tumors were segregated into two cohorts based on the expression of PLK1 as PLK1-high and PLK1-low tumors (Figure 37A). PLK1-high tumors had a Z-score of > +1 and PLK1-low tumors had a Z-score of < -1. The average expression of PLK1 in the cohort was 8.817 with a Standard Deviation of 1.32. Individual Z scores are calculated by the formula $Z = x-\mu/\sigma$, where Z is the standard score, x is the expression of PLK1 in the particular sample, μ is the mean of PLK1 expression in the data set and σ is the standard deviation of the dataset.

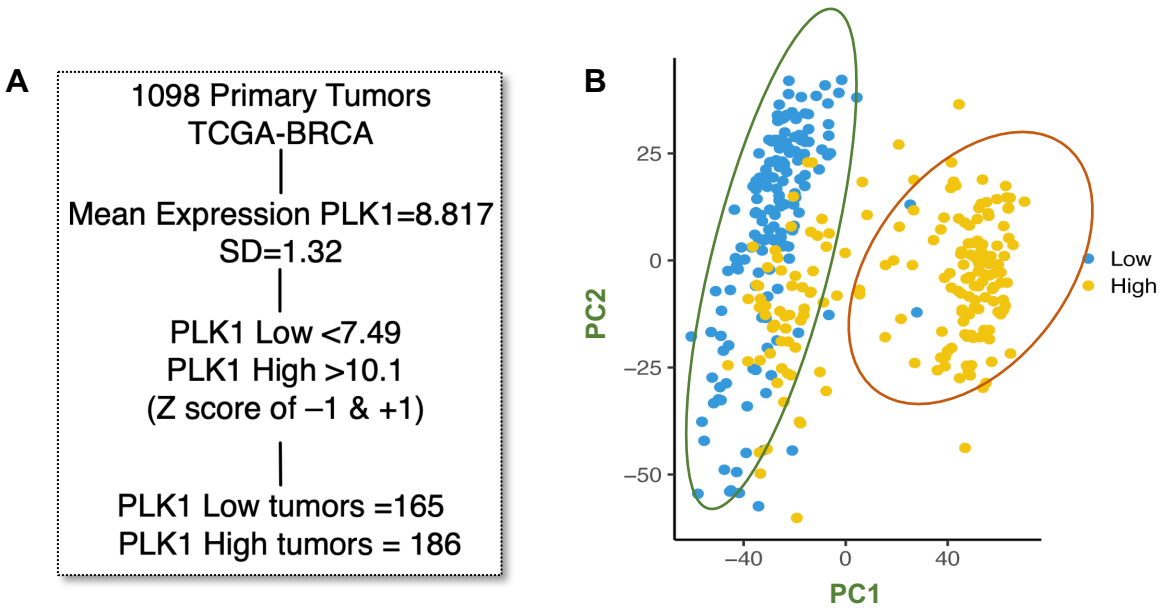

Figure 37: A) Schematic of the segregation strategy used for identifying PLK1-high and PLK1-low tumors from TCGA-BRCA cohort. **B)** Scatter plot showing unsupervised clustering of PLK1-low and PLK1-high tumors using principle component analysis (PCA). Samples are color coded.

Next, to show the separation between the two cohorts, I employed unsupervised clustering using principle component analysis (PCA) to identify key variables in the data set (Figure 37B). The two cohorts showed clear separation, with high PLK1 levels correlating majorly with aggressive basal like breast cancers (triple negative) and low PLK1 levels with luminal subtype. PLK1-high group has 92.9% of basal tumors (171 out of 184 tumors) and PLK1-low group has 52.2% (84 out of 161 tumors) luminal subtype tumors and 47.8% (68 out of 161 tumors) basal tumors (Table 3). Basal like breast cancers pose a major clinical challenge often associated with poor outcomes, frequent relapses and early resistance to chemotherapy (Rakha et al., 2006; Li et al., 2017; Nedelijkovic et al., 2019; Soares et al., 2021).

Tumor Type – PLK1 High	***Total number***
Breast invasive ductal carcinoma (basal tumors)	171
Breast invasive lobular carcinoma (luminal tumors)	7
Basal cell carcinoma	1
Metaplastic breast cancer	3
Breast invasive ductal + luminal carcinoma	2
Tumor Type - PLK1 Low	***Total number***
Breast invasive ductal carcinoma (basal tumors)	68
Breast invasive lobular carcinoma (luminal tumors)	84
Basal cell carcinoma	-
Metaplastic breast cancer	-
Breast invasive ductal + luminal carcinoma	9

Table 3: Total number of basal and luminal subtypes present in PLK1-high and PLK1-low TCGA-BRCA tumors.

These findings showing PLK1 to be mostly expressed by basal tumors confirm earlier research that identified PLK1 inhibition as a possible target for treating triple negative breast malignancies (Giordano et al., 2019; Nieto-Jimenez et al., 2020).

4.4.2 PLK1-high human BRCA tumors experience higher degree of somatic copy number alterations

Furthermore, to corroborate our previous findings from the *in vivo* model, I checked to see if there was any correlation between PLK1 levels and somatic copy number alterations in human BRCA tumors. As predicted, tumors with high levels of PLK1 showed elevated levels of chromosome gains and losses compared to PLK1-low tumors (Figure 38A).

High levels of PLK1 distinctively resulted in loss of chromosome arms 5p, 5q, 7p, 16p and 16q while gain of 1p, 2p, 2q, 10q, 17p and 22q (Figure 38B). Among other regions that were amplified in the high PLK1 cohort, chromosome 9p is of particular interest as it harbors the Cd274 (PD-L1) gene. Budczies et.al, 2017 showed that TCGA tumors with chromosome 9p amplifications are associated with proliferation and immune modulation signatures involving the activation of PLK1 and other proliferation related kinases. This finding goes hand in hand with the previous result where PLK1 overexpressing tumors showed elevated levels of PD-L1 (Figure 16). However, the gene dosage effects resulting from specific chromosome loss or gain and its impact on the phenotype remains to be elucidated.

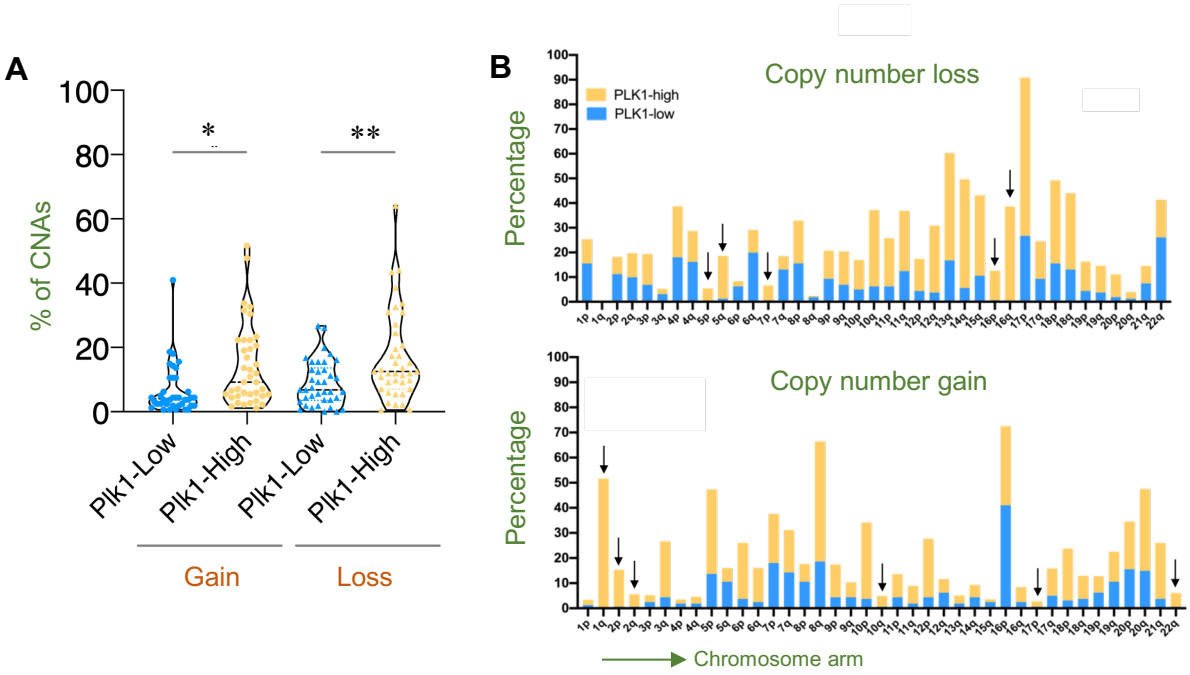

Figure 38: A) Violin plots showing the overall percentage of copy number gains or losses in PLK1-low and PLK1-high tumors of the TCGA-BRCA cohort. Each arm of the chromosome is represented by a dot. *, P<0.05; **, P<0.005, Oneway ANOVA, Tukey's multiple comparison test. **B)** Bar graphs showing percentage gains or losses on each arm of the chromosome in both PLK-high and PLK-low groups. Arrows show chromosomal regions that are gained or lost specifically in high PLK1 tumors.

4.4.3 PLK1-high human BRCA tumors show higher expression of signatures associated with immune suppression, senescence and T-cell exhaustion

Earlier in the thesis, I have shown that PLK1 overexpression resulted in a senescence associated secretory phenotype (SASP) with upregulation of non-canonical NF-kB (RELB) signaling, increased expression of immune suppression markers PDL1 and CD206, infiltration of Tregs and decreased number of cytotoxic NK cells. To validate whether, such a phenotype exists in

human tumors expressing high levels of PLK1, I grouped a set of genes into three different signatures. *ARG2, CD274, IL10, PDCD1LG2 ,IDO1, PDCD1, TGFB1, VEGFB, VEGFA* and *CTLA4* (associated with immune suppression), *TNF, CDKN2A, CDKN1A, MAPK14, HMGB1 IL1A, IL1B, MMP12, MMP13, MMP1, TIMP1, IFNG* and *NFKB1* (associated with SASP) and *TNFRSF18/GITR, HAVCR2, LAG3, TCF7 and TIGIT* (associated with T-cell exhaustion). Interestingly, PLK1 expression directly correlates with expression of gene signatures associated with immune suppression, senescence and T cell exhaustion (Figure 39). Some studies also show how high CIN tumors alter tumor antigens and facilitating cancer immunoediting (Duijf & Benezra., 2013). However, aspects related to antigen presentation, neo antigen burden were not explored in detail in this study. Altogether, the data suggest that elevated PLK1 expression inhibits antitumor immunity. Accumulation of pro-inflammatory cytokines, expression of PD-L1 and infiltration of T cell (Tregs) makes these high CIN tumors "HOT" and also highlights the need for immune checkpoint inhibitors as an adjuvant therapy alongside first line treatment.

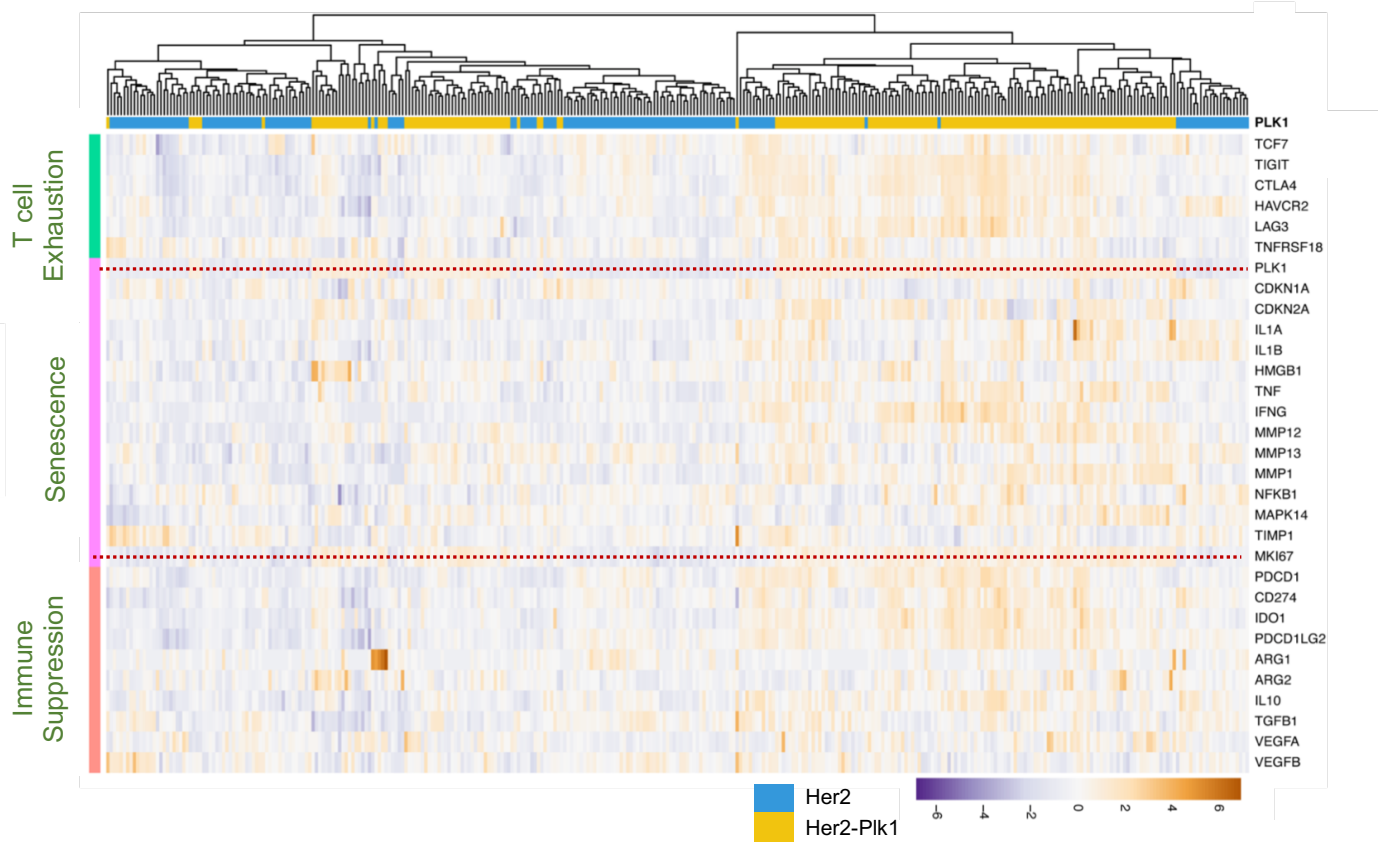

Figure 39: Heatmap showing gene expression data (log2norm_counts+1) from three different signatures associated with T- cell exhaustion, senescence and immune suppression in both PLK1-high (yellow) and PLK1-low (blue) TCGA-BRCA tumor cohorts. *Analysis done with assistance from Anand Mayakonda.

4.4.4 PLK1-high human BRCA tumors show increased infiltration of Tregs

To analyze the enrichment levels of various immune cell types, I used the deconvolution tool CIBERSORTx (cibersortx.stanford.edu), which is designed to quantify infiltrating immune cells obtained from high-throughput sequencing data extracted from bulk tissues. I estimated

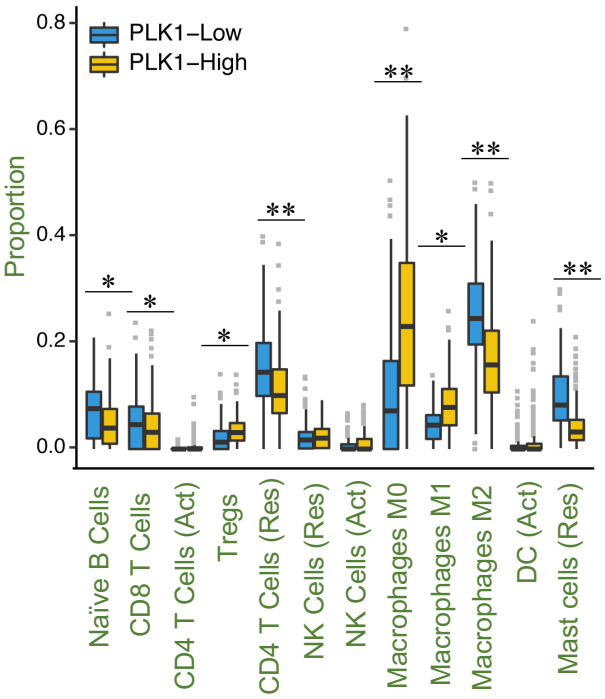

Figure 40: Percentage of different innate and adaptive immune cell types in PLK1-high and PLK1-low tumor samples using CIBERSORT. *, P<0.05; **, P<0.01.
*Res = resting, *Act= Activated
*Analysis done with assistance from Anand Mayakonda.

the relative number of tumor infiltrating lymphocytes (TIL's), macrophages, dendritic cells and NK cells (Figure 40). Tumors expressing high PLK1 showed elevated levels of Tregs, M0/M1 macrophages and reduced infiltration of CD4/CD8, M2 macrophages and naïve B cells. However, it is interesting to note that the effect of PLK1 expression on immune cell infiltration is tissue-dependent (Li et al., 2018). PLK1 expression negatively correlates with immune cell infiltration in 10 different cancer types (LUSC, TGCT, STAD, GBM, ESCA etc) while positively correlating in 4 different cancers (KIRC, THCA, THYM, LGG). Similarly, PLK1 expression correlates negatively with Treg recruitment in 16 different cancer types (THYM, LUSC, GBM, TCGT, LUAD, STAD etc) while positively correlating in 5 different cancer types (BRCA, THCA, KIRC, BLCA, LIHC). The above findings highlight how high levels of PLK1 mediate immune cell infiltration in mammary tumors.

4.4.5 TCGA-BRCA tumors expressing high levels of Plk1 are predicted to respond better to adjuvant therapies involving PD-L1 inhibition

To understand the correlation between PLK1 levels and PD-L1 specifically in Her2$^+$ tumors, myself together with my colleague Lena Voith von Voithenberg, used the METABRIC cohort (Pereira et al., 2016; Curtis et al., 2012) to segregate the tumors into basal (335 samples) and non-basal tumors which includes luminal (1865 samples) and Her2$^+$ subtypes (247 samples). We then looked at the gene expression levels of ERBB2 (Neu), CD274 (PD-L1) and PLK1 in all the three subtypes (Figure 41). Similar to the TCGA PanCancer Atlas, basal tumors have highest expression of PLK1 followed by Her2$^+$ subtype. Likewise, Her2$^+$ tumors also expressed higher levels of PD-L1 compared to luminal subtype but lower compared to luminal tumors.

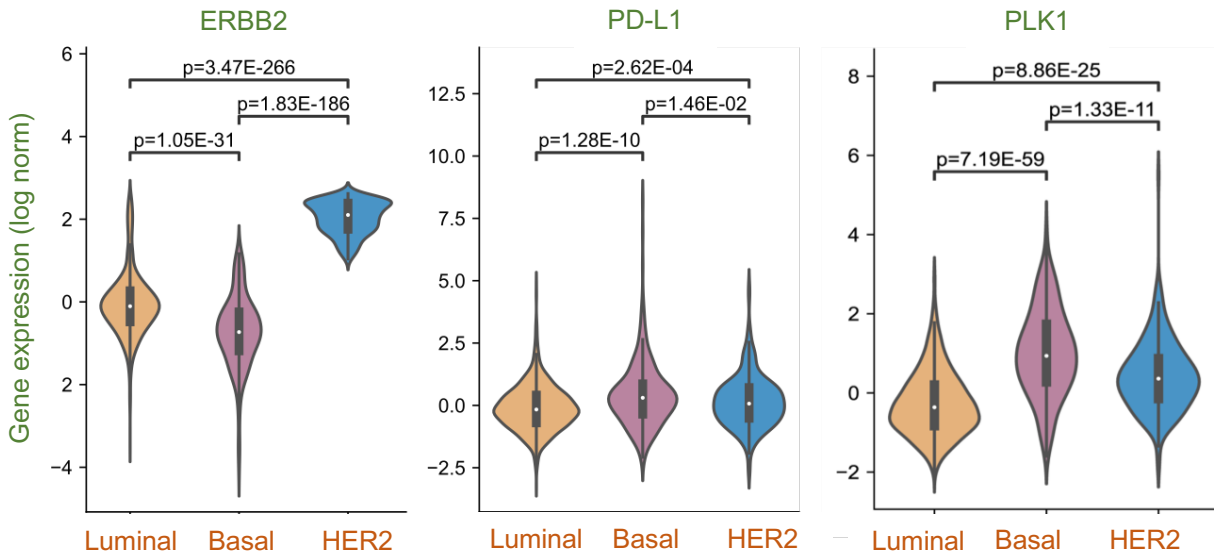

Figure 41: Violin plots showing gene expression levels of ERBB2 (Her2), PD-L1 and PLK1 from three different tumor subtypes, luminal, basal and Her2$^+$ of the Metabric study from TCGA. Welch t-test was performed to determine the significance. * Analysis done in assistance with Lena Voithenberg

Finally, the data presented here sheds light on different immune suppression markers expressed by high PLK1 tumors and highlights additional vulnerabilities that can be exploited. Although, I have successfully demonstrated the non-cell autonomous effects of PLK1 expression in mammary tumors using our mouse model, there are certain limitations to using this model for therapeutic interventions. Firstly, Trastuzumab (Herceptin) a monoclonal antibody that specifically binds Her2 receptor does not bind to rat or mouse ErbB2/Her2/neu (Phillips et al., 2022).

Secondly, doxycycline induction drives long lasting transcription of target genes which mitigates the effect of alternate drugs like Lapatinib (dual inhibitor of HER2 and EGFR pathways). Therefore, further experiments involving the use of immune checkpoint inhibitors (PD-L1, CTLA4), senolytic inhibitors (drugs that remove senescent cells) and non-canonical NF-kB inhibitors as adjuvant therapies need to be explored in an alternative mice model in the context of high CIN tumors expressing PLK1.

5. Summary of Results

The following are the main findings from this thesis:

- Overexpression of Plk1 results in a Senescence Associated Secretory Phenotype (SASP).

- Plk1 overexpression leads to the upregulation of both canonical and non-canonical NF-kB signaling.

- High CIN tumors express immune suppression markers such as PD-L1 as a consequence of non-cell autonomous effects of chromosomal instability induced by Plk1.

- NK cells from early stage Her2-Plk1 mammary glands characterized as $CD11b^{-}CD27^{+}$ have reduced cytotoxic abilities.

- Early stage Her2-Plk1 mammary glands have increased infiltration of $Arg1^{+}$ TAM's and resting Tregs.

- Human BRCA tumors expressing high levels of PLK1 also show signatures of SASP, immune suppression along with T cell exhaustion markers.

- Immune checkpoint blockade with anti-PD-L1, RELB/ Senolytic inhibitors could prove to be effective as adjuvant treatment of high CIN tumors expressing PLK1.

6. Discussion

The role of the immune system in the context of chromosomal instability has been in limelight for the last few years. Several studies have used *in vitro* models to demonstrate the effect of CIN on human cells (Santaguida et al., 2017; Alice et al., 2012; Wang et al., 2021; Lukow et al., 2021). However, the missing pieces in the puzzle are the random missegregation events/gene dosage effects induced by CIN (no voluntary control on the ploidy status) and the presence of an active immune system in this context. Therefore, we used a Plk1 overexpressing animal model to address the issue. Plk1 is a prominent kinase which plays a key role in cell cycle regulation, is known to induce CIN and is overexpressed in many cancer types. Our work using *in vivo* models to address how different innate and adaptive immune cell respond to CIN (Plk1 overexpression) will add to existing knowledge in the field and becomes resourceful for any upcoming clinical trials involving immunotherapy and other adjuvant therapies for the treatment of high CIN tumors.

6.1 SASP induction and role of NK cells in high CIN environment

CIN as a result of somatic copy number alterations is a hallmark of cancer and drives immune evasion. On the contrary, the innate immune system helps in sensing chromosomally unstable cells. Therefore, it remains important to understand the role of immune cells in the context of tumor development *in vivo* as many other factors have been taken into consideration to address this question. we used the tetracycline-inducible-model to study the effects of CIN induced by Plk1 expression on the immune system.

Innate immune responses mediated by NK cells aids in the elimination of cells with complex karyotypes by activating NKG2D receptors (Santaguida et al., 2017), NF-kB signaling (Wang et al., 2021) or responding to a SASP like gene expression signature (Raulet & Guerra., 2009). SASP signatures shown in our study are associated with chronic inflammation and immune suppression markers (pro-tumorigenic) compared to signatures from *in vitro* studies (IL6, IL8 and CCL2) that show the expression of inflammatory cytokines and chemokines that recruit various immune cells (anti-tumorigenic). This brings us to the idea that SASP could be dynamic and changes over time during the process of tumor development under the influence of CIN. Functional validation of the importance of NK cells in aneuploid tumor microenvironment by blocking NK cells *in vivo* displayed reduction in overall survival of Plk1 expressing tumors compared to Her2 alone, suggesting that NK cells besides triggering immune sensing, also plays

an opposite role. Future experiments showing the interaction between NK cells at different stages of SASP could explain the dual role of NK cells in the context of aneuploidy. Moreover, the cytotoxic activity of NK cells is reduced through the exposure of inhibitory receptors in an immunosuppressive microenvironment (Cózar et al., 2021). Even though the activation of NKG2D (activating receptors) showed no significant differences, Plk1 expression during the early phases of tumor development causes NK cells to remain in a mature state ($CD11b^{-}CD27^{+}$) with diminished effector capacities in comparison to tumors with low levels of CIN. We identified important molecules such as *Socs3, Irf8 and Cx3cr1* that could influence the cytotoxic abilities and infiltration of these cells. These findings corroborate with some of the previous studies that have shown the importance of these genes (Meisam et al., 2018; Mace et al., 2016; Ponzetta et al., 2013) in the development of effector NK cells. Although, the findings presented previously emphasize the importance of NF-kB signaling in eliminating chromosomally unstable cells (Wang et al., 2021), we predict that the constituents of SASP could actually drive the functional capabilities of NK cells *in vivo*. This is primarily because of SASP being under tight regulation of NF-kB.

6.2 PD-L1 upregulation: a consequence of Plk1 overexpression

PD-L1 expression correlates with aggressive behavior and poor prognosis in many cancer types (Carlsson et al., 2020; Gu et al., 2019; Noronha et al., 2022; Yu et al., 2020) and immune checkpoints are exploited as key targets for anti-cancer therapies. Furthermore, PD-L1 expression in the tumors is used as a biomarker for initiating immunotherapy (Doroshow et al., 2021). My results show that Her2-Plk1 tumors besides upregulating both canonical and non-canonical NF-kB signaling also show increased expression of PD-L1. Although a direct link between NF-kB and PD-L1 was not established in the present study, we hypothesize that activated NF-kB regulates PD-L1 expression in the context of high chromosomal instability. Previous studies show that PD-L1 is under tight regulation of NF-kB either directly, at transcriptional level, where different binding sequences of NF-kB have been found at the promoter region of PD-L1 (Chen et al., 1999). Similarly, inflammatory cytokines like TNFa and IFNg acting via NF-kB pathway also regulate PD-L1 expression indirectly (Ju et al., 2020). what is more interesting is that fact that chromosome 9p copy number gains involving PD-L1 upregulate proliferation related kinases and genes like PLK1, TTK, MELK etc across major cancer types (Budczies et al., 2017). Apart from NF-kB, PD-L1 upregulation is also associated with the infiltration of immunosuppressive macrophages and neutrophils which induce a EMT phenotype (Taki M et al., 2021). EMT at gene level is known to be regulated by non-canonical

NF-kB signaling (Asgarova et al., 2018) with TNFα and TGFβ as key players in driving this phenotype (Thiery & Sleeman., 2006). It also remains interesting to see if CIN induced (with different drivers) in various other tissues elevate PD-L1 expression as this information could aid in a better understanding of the relationship between non-canonical NF-kB and PD-L1 in high CIN tumors.

6.3 Macrophages, Tregs and other targets in high CIN tumors

Essential innate immune cells that dominate in the aneuploid tumor microenvironment are macrophages. (Thorsson et al., 2018). Macrophages play a dual role in the development of tumors, either by aiding the phagocytosis of tumor cells (M1) or by stimulating angiogenesis and mediating tumor invasion (M2) (Tamura et al., 2018). It is interesting to note that the results from my research demonstrate an enrichment of the *Arg1*$^{+}$ TAMs subset in Her2-Plk1 tumors. These Tumor associated macrophages are also implicated in TGF-β , reactive oxygen species (ROS), and EMT signaling, which promote early modulation of immune responses. Although Her2 tumors grow faster and are aneuploid, to a lesser extent compared to Her2-Plk1 tumors, the *Arg1*+ subsets never appeared in the early stages of tumor development. Therefore, targeting *Arg1* and other related EMT-related proteins simultaneously may offer a promising method for repolarizing macrophages and boosting the effectiveness of checkpoint inhibition in high CIN malignancies. Another interesting finding, is the early infiltration of resting Treg cells in Plk1 tumors. Tregs contribute to tumor development and progression through suppression of T effector cell functions (Zou et al., 2006; Curiel et al., 2008). As an extrinsic strategy to maintain immunological homeostasis in settings of chronic inflammation, Tregs are attracted to the inflamed tissue to prevent excessive immune responses to self-antigen (Gouirand et al., 2009). This could be the primary reason for Treg infiltration in Plk1 overexpressing tumors. In contrary, second line of thought shows sustained activation of STING signaling enhances Treg infiltration in certain cancer types (Ni et al., 2022; Liang et al., 2015). However, i saw that there was no difference in gene expression levels of STING among macrophage susbsets of both the groups from my study. Therefore, it can be concluded that Treg infiltration in Plk1 expressing tumors is a result of ongoing CIN and sustained chronic inflammation.

Another crucial phase of immune response during stress-induced inflammation is cytokine production, which has a negative effect on autoimmune diseases and cancer (Elenkov et al., 2002). Plk1 is upregulated in splenic B220+ cells of lupus mice and also contributes to the

progression of Systemic lupus erythematosus by activating Aurora-A/PLK1/mTOR signaling and further producing autoantibodies (Li et al., 2022). The study underlines the importance of several genes such as *Cd79*, *Mzb1*, *Scd1* and *Ptpn22* affiliated with defective metabolism and dysregulated B cell signaling in high CIN tumors. Although, autoimmunity remains out of context in the scope of this thesis, it remains interesting to see the relation between CIN and autoimmunity. In summary, below is a schematic of immune regulation in high CIN tumors expressing Plk1 (Figure 42).

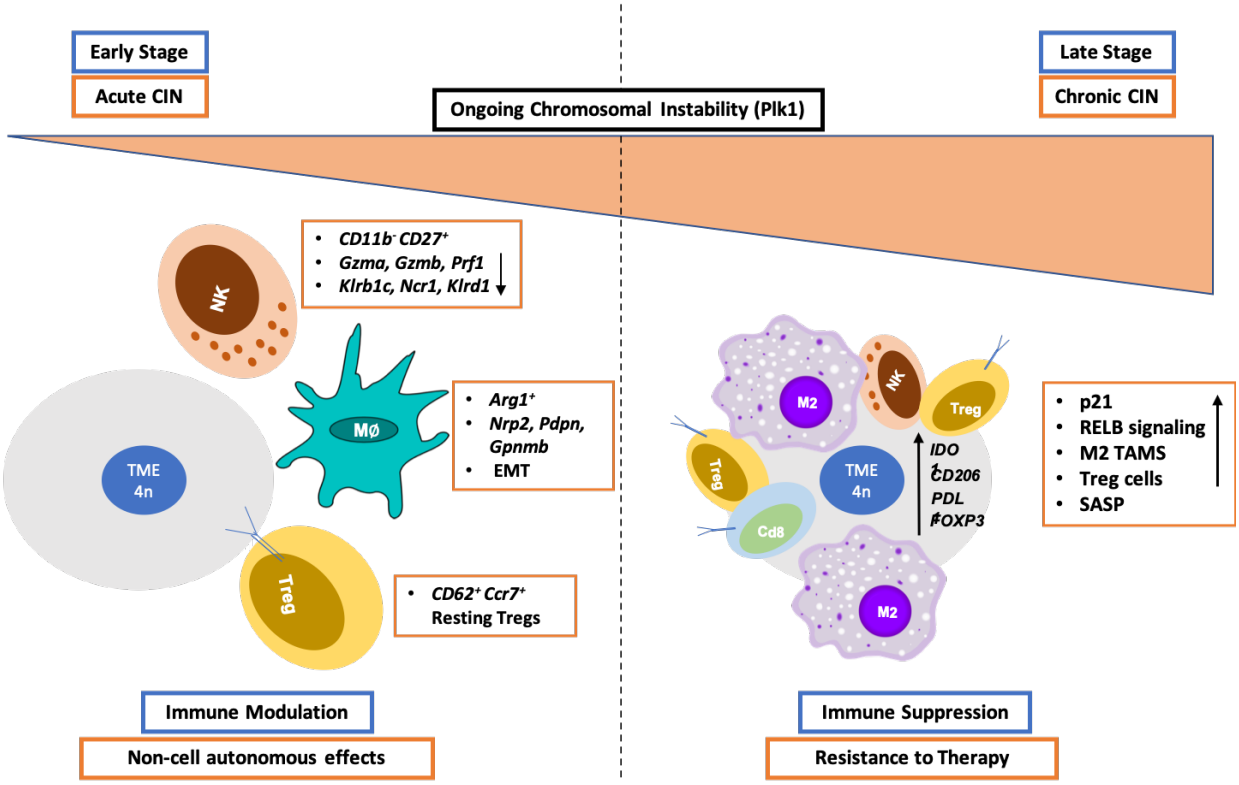

Figure 42: Schematic showing the consequences of acute and chronic CIN in early and late stage Her2-Plk1 tumors during the course of development.

6.4 Concluding remarks:

During the course of this PhD project, I have investigated the phenotype of various immune cells as a consequence of non-cell autonomous effects induced by CIN. Interestingly, not only did overexpression of Plk1 result in an immunosuppressive phenotype, but also led to early modulation of immune cells affecting their cytotoxicity, inspite of previous data pointing towards a good prognosis as a result of increased survival time of these tumors (de Carcer et

al., 2018). Moreover, some of the presented results like upregulation of NF-kB/p38MAPK signaling remain in consensus with previously published data but additionally the study also highlights key molecules like PD-L1, RELB and cells such as *Arg1*$^{+}$ TAMs and Tregs that can be targeted in high CIN breast cancers. In conclusion, it can be postulated that SASP remains upstream of NF-kB signaling while PD-L1 expression is a downstream effect of sustained inflammation and NF-kB signaling.

It is to be understood that the conclusions presented in the thesis do not undermine the importance of using Plk1 inhibitors for the treatment of cancer, as kinase inhibition during tumor cell division produces anti-tumor effects. Moreover, targeting immune suppression markers, repolarization of macrophages and activation of cytotoxic NK cells can be explored in the context of high CIN. Furthermore, the effect of CIN induced by Plk1 expression in different tissues also need to be explored. Therefore, the study is directed to provide alternate adjuvant strategies alongside existing first line treatments for high CIN breast cancers.

7. References

Abel, A. M., Yang, C., Thakar, M. S., & Malarkannan, S. (2018). Natural killer cells: development, maturation, and clinical utilization. *Frontiers in Immunology*, 9, 1869.

Andriani, G. A., Almeida, V. P., Faggioli, F., Mauro, M., Tsai, W. L., Santambrogio, L., & Vijg, J. (2016). Whole Chromosome Instability induces senescence and promotes SASP. *Scientific reports*, 6(1), 1-17.

Antonangeli, F., Natalini, A., Garassino, M. C., Sica, A., Santoni, A., & Di Rosa, F. (2020). Regulation of PD-L1 expression by NF-κB in cancer. *Frontiers in Immunology*, 11, 584626.

Apel, K., & Hirt, H. (2004). Reactive oxygen species: metabolism, oxidative stress, and signaling transduction. *Annual review of plant biology*, 55, 373.

Aran, D., Looney, A. P., Liu, L., Wu, E., Fong, V., Hsu, A., & Abate, A. R. (2019). Reference-based analysis of lung single-cell sequencing reveals a transitional profibrotic macrophage. *Nature immunology*, 20(2), 163-172.

Asgarova, A., Asgarov, K., Godet, Y., Peixoto, P., Nadaradjane, A., Boyer-Guittaut, M., & Perrard, J. (2018). PD-L1 expression is regulated by both DNA methylation and NF-kB during EMT signaling in non-small cell lung carcinoma. *Oncoimmunology*, 7(5), e1423170.

Ashford, N. A., Bauman, P., Brown, H. S., Clapp, R. W., Finkel, A. M., Gee, D., & Sass, J. B. (2015). Cancer risk: role of environment. *Science*, 347(6223), 727-727.

Baker, D. J., Dawlaty, M. M., Wijshake, T., Jeganathan, K. B., Malureanu, L., Van Ree, J. H., & Shapiro, V. (2013). Increased expression of BubR1 protects against aneuploidy and cancer and extends healthy lifespan. *Nature cell biology*, 15(1), 96-102.

Bakhoum, S. F., & Cantley, L. C. (2018). The multifaceted role of chromosomal instability in cancer and its microenvironment. *Cell*, 174(6), 1347-1360.

Bakhoum, S. F., Danilova, O. V., Kaur, P., Levy, N. B., & Compton, D. A. (2011). Chromosomal instability substantiates poor prognosis in patients with diffuse large B-cell lymphoma. *Clinical Cancer Research*, 17(24), 7704-7711.

Bakhoum, S. F., Ngo, B., Laughney, A. M., Cavallo, J.-A., Murphy, C. J., Ly, P., & Taunk, N. K. (2018). Chromosomal instability drives metastasis through a cytosolic DNA response. *Nature*, 553(7689), 467-472.

Barr, F. A., Silljé, H. H., & Nigg, E. A. (2004). Polo-like kinases and the orchestration of cell division. *Nature reviews Molecular cell biology*, 5(6), 429-441.

Beard, C., Hochedlinger, K., Plath, K., Wutz, A., & Jaenisch, R. (2006). Efficient method to generate single-copy transgenic mice by site-specific integration in embryonic stem cells. *Genesis,* 44(1), 23-28.

Ben-Baruch, A. (2006). Inflammation-associated immune suppression in cancer: the roles played by cytokines, chemokines and additional mediators. *Paper presented at the Seminars in cancer biology.*

Bielski, C. M., Zehir, A., Penson, A. V., Donoghue, M. T., Chatila, W., Armenia, J., & Bandlamudi, C. (2018). Genome doubling shapes the evolution and prognosis of advanced cancers. *Nature genetics*, 50(8), 1189-1195.

Bieniasz-Krzywiec, P., Martín-Pérez, R., Ehling, M., García-Caballero, M., Pinioti, S., Pretto, S., & Prenen, H. (2019). Podoplanin-expressing macrophages promote lymphangiogenesis and lymphoinvasion in breast cancer. *Cell metabolism*, 30(5), 917-936. e910.

Bray, N. L., Pimentel, H., Melsted, P., & Pachter, L. (2016). Near-optimal probabilistic RNA-seq quantification. *Nature biotechnology*, 34(5), 525-527.

Bronte, V., & Zanovello, P. (2005). Regulation of immune responses by L-arginine metabolism. *Nature Reviews Immunology*, 5(8), 641-654.

Budczies, J., Denkert, C., Győrffy, B., Schirmacher, P., & Stenzinger, A. (2017). Chromosome 9p copy number gains involving PD-L1 are associated with a specific proliferation and immune-modulating gene expression program active across major cancer types. *BMC Medical Genomics*, 10(1), 1-8.

Burrell, R. A., McGranahan, N., Bartek, J., & Swanton, C. (2013). The causes and consequences of genetic heterogeneity in cancer evolution. *Nature*, 501(7467), 338-345.

Burstein, H. J., Temin, S., Anderson, H., Buchholz, T. A., Davidson, N. E., Gelmon, K. E., & Solky, A. J. (2014). Adjuvant endocrine therapy for women with hormone receptor–positive breast cancer: American Society of Clinical Oncology clinical practice guideline focused update. *Journal of clinical oncology*, 32(21), 2255.

Butler, A., Hoffman, P., Smibert, P., Papalexi, E., & Satija, R. (2018). Integrating single-cell transcriptomic data across different conditions, technologies, and species. *Nature biotechnology*, 36(5), 411-420.

Campbell, J. J., Qin, S., Unutmaz, D., Soler, D., Murphy, K. E., Hodge, M. R., & Butcher, E. C. (2001). Unique subpopulations of CD56+ NK and NK-T peripheral blood lymphocytes identified by chemokine receptor expression repertoire. *The Journal of Immunology*, 166(11), 6477-6482.

Cánovas, B., Igea, A., Sartori, A. A., Gomis, R. R., Paull, T. T., Isoda, M., & Stracker, T. H. (2018). Targeting p38α increases DNA damage, chromosome instability, and the anti-tumoral response to taxanes in breast cancer cells. *Cancer cell*, 33(6), 1094-1110. e1098.

Carlsson, J., Sundqvist, P., Kosuta, V., Fält, A., Giunchi, F., Fiorentino, M., & Davidsson, S. (2020). PD-L1 expression is associated with poor prognosis in renal cell carcinoma. *Applied Immunohistochemistry & Molecular Morphology,* 28(3), 213-220.

Carter, S. L., Cibulskis, K., Helman, E., McKenna, A., Shen, H., Zack, T., & Weir, B. A. (2012). Absolute quantification of somatic DNA alterations in human cancer. *Nature biotechnology*, 30(5), 413-421.

Chen, F. E., & Ghosh, G. (1999). Regulation of DNA binding by Rel/NF-κB transcription factors: structural views. *Oncogene*, 18(49), 6845-6852.

Colaprico, A., Silva, T. C., Olsen, C., Garofano, L., Cava, C., Garolini, D., & Castiglioni, I. (2016). TCGAbiolinks: an R/Bioconductor package for integrative analysis of TCGA data. *Nucleic acids research,* 44(8), e71-e71.

Coppé, J.-P., Desprez, P.-Y., Krtolica, A., & Campisi, J. (2010). The senescence-associated secretory phenotype: the dark side of tumor suppression. *Annual review of pathology*, 5, 99.

Cózar, B., Greppi, M., Carpentier, S., Narni-Mancinelli, E., Chiossone, L., & Vivier, E. (2021). Tumor-Infiltrating Natural Killer Cells. *Cancer discovery*, 11(1), 34-44.

Cuadrado, A., & Nebreda, A. R. (2010). Mechanisms and functions of p38 MAPK signalling. *Biochemical journal*, 429(3), 403-417.

Cuenda, A., & Rousseau, S. (2007). p38 MAP-kinases pathway regulation, function and role in human diseases. *Biochimica et Biophysica Acta (BBA)-Molecular Cell Research*, 1773(8), 1358-1375.

Curiel, T. J. (2008). Regulatory T cells and treatment of cancer. *Current opinion in immunology*, 20(2), 241-246.

Curtis, C., Shah, S. P., Chin, S.-F., Turashvili, G., Rueda, O. M., Dunning, M. J., & Yuan, Y. (2012). The genomic and transcriptomic architecture of 2,000 breast tumours reveals novel subgroups. *Nature*, 486(7403), 346-352.

Dang, S.-C., Fan, Y.-Y., Cui, L., Chen, J.-X., Qu, J.-G., & Gu, M. (2018). PLK1 as a potential prognostic marker of gastric cancer through MEK-ERK pathway on PDTX models. *OncoTargets and therapy*, 11, 6239.

Davalos, A. R., Coppe, J.-P., Campisi, J., & Desprez, P.-Y. (2010). Senescent cells as a source of inflammatory factors for tumor progression. Cancer and Metastasis Reviews, 29(2), 273-283.

Davoli, T., Uno, H., Wooten, E. C., & Elledge, S. J. (2017). Tumor aneuploidy correlates with markers of immune evasion and with reduced response to immunotherapy. *Science,* 355(6322), eaaf8399.

De Cárcer, G., Venkateswaran, S. V., Salgueiro, L., El Bakkali, A., Somogyi, K., Rowald, K., de Martino, A., Mcgranahan, N., & Sotillo, R. (2018). Plk1 overexpression induces chromosomal instability and suppresses tumor development. *Nature communications*, 9(1), 1-14.

Decout, A., Katz, J. D., Venkatraman, S., & Ablasser, A. (2021). The cGAS–STING pathway as a therapeutic target in inflammatory diseases. *Nature Reviews Immunology*, 21(9), 548-569.

Deng, L., Liang, H., Xu, M., Yang, X., Burnette, B., Arina, A., & Darga, T. (2014). STING-dependent cytosolic DNA sensing promotes radiation-induced type I interferon-dependent antitumor immunity in immunogenic tumors. *Immunity*, 41(5), 843-852.

Deshaies, R. J. (2014). Proteotoxic crisis, the ubiquitin-proteasome system, and cancer therapy. *BMC biology*, 12(1), 1-14.

Donnelly, N., & Storchová, Z. (2015). Aneuploidy and proteotoxic stress in cancer. *Molecular & cellular oncology*, 2(2), e976491.

Doroshow, D. B., Bhalla, S., Beasley, M. B., Sholl, L. M., Kerr, K. M., Gnjatic, S., & Hirsch, F. R. (2021). PD-L1 as a biomarker of response to immune-checkpoint inhibitors. *Nature reviews Clinical oncology*, 18(6), 345-362.

Dou, Z., Ghosh, K., Vizioli, M. G., Zhu, J., Sen, P., Wangensteen, K. J., & Zhou, Z. (2017). Cytoplasmic chromatin triggers inflammation in senescence and cancer. *Nature*, 550(7676), 402-406.

Duijf, P., & Benezra, R. (2013). The cancer biology of whole-chromosome instability. *Oncogene,* 32(40), 4727-4736.

Dürrbaum, M., Kuznetsova, A. Y., Passerini, V., Stingele, S., Stoehr, G., & Storchová, Z. (2014). Unique features of the transcriptional response to model aneuploidy in human cells. *BMC genomics*, 15(1), 1-14.

Elenkov, I. J., & Chrousos, G. P. (2002). Stress hormones, proinflammatory and antiinflammatory cytokines, and autoimmunity. *Annals of the New York Academy of Sciences*, 966(1), 290-303.

Fadok, V. A., Bratton, D. L., & Henson, P. M. (2001). Phagocyte receptors for apoptotic cells: recognition, uptake, and consequences. *The Journal of Clinical Investigation*, 108(7), 957-962.

Fischer, U., Yang, J. J., Ikawa, T., Hein, D., Vicente-Dueñas, C., Borkhardt, A., & Sánchez-García, I. (2020). Cell Fate Decisions: The Role of Transcription Factors in Early B-cell Development and Leukemia, Lineage Restriction in Normal and Leukemia B Cells. *Blood cancer discovery*, 1(3), 224-233.

Georgoudaki, A.-M., Prokopec, K. E., Boura, V. F., Hellqvist, E., Sohn, S., Östling, J., & Klevebring, D. (2016). Reprogramming tumor-associated macrophages by antibody targeting inhibits cancer progression and metastasis. *Cell reports*, 15(9), 2000-2011.

Giordano, A., Liu, Y., Armeson, K., Park, Y., Ridinger, M., Erlander, M., & Yeh, E. (2019). Polo-like kinase 1 (Plk1) inhibition synergizes with taxanes in triple negative breast cancer. *PloS one*, 14(11), e0224420.

Goel, S., Wang, Q., Watt, A. C., Tolaney, S. M., Dillon, D. A., Li, W., & Varadan, V. (2016). Overcoming therapeutic resistance in HER2-positive breast cancers with CDK4/6 inhibitors. *Cancer cell*, 29(3), 255-269.

Goldman, M. J., Zhang, J., Fonseca, N. A., Cortés-Ciriano, I., Xiang, Q., Craft, B., & Barrera, E. (2020). A user guide for the online exploration and visualization of PCAWG data. *Nature communications*, 11(1), 1-9.

Gorgoulis, V., Adams, P. D., Alimonti, A., Bennett, D. C., Bischof, O., Bishop, C., & Ferbeyre, G. (2019). Cellular senescence: defining a path forward. *Cell,* 179(4), 813-827.

Gouirand, V., & Rosenblum, M. D. (2021). Tregs and inflammation—bring it on! *Science Immunology*, 6(64), eabm5116.

Gu, X., Dong, M., Liu, Z., Mi, Y., Yang, J., Zhang, Z., & Dong, S. (2019). Elevated PD-L1 expression predicts poor survival outcomes in patients with cervical cancer. *Cancer cell international*, 19(1), 1-9.

Gunther, E. J., Belka, G. K., Wertheim, G. B., Wang, J., Hartman, J. L., Boxer, R. B., & Chodosh, L. A. (2002). A novel doxycycline-inducible system for the transgenic analysis of mammary gland biology. *The FASEB Journal*, 16(3), 283-292.

Gupta, J., & Nebreda, A. R. (2015). Roles of p38α mitogen-activated protein kinase in mouse models of inflammatory diseases and cancer. *The FEBS journal*, 282(10), 1841-1857.

Hadjantonakis, A.-K., & Papaioannou, V. E. (2004). Dynamic in vivo imaging and cell tracking using a histone fluorescent protein fusion in mice. *BMC biotechnology*, 4(1), 1-14.

Hardy, I. R., Anceriz, N., Rousseau, F., Seefeldt, M. B., Hatterer, E., Irla, M., & Fletcher, A. (2014). Anti-CD79 antibody induces B cell anergy that protects against autoimmunity. *The Journal of Immunology*, 192(4), 1641-1650.

Hassan, Q. N., Alinari, L., & Byrd, J. C. (2018). PLK1: a promising and previously unexplored target in double-hit lymphoma. *The Journal of Clinical Investigation*, 128(12), 5206-5208.

Hayden, M. S., & Ghosh, S. (2008). Shared principles in NF-κB signaling. *Cell*, 132(3), 344-362.

He, Q., Au, B., Kulkarni, M., Shen, Y., Lim, K., Maimaiti, J., & Lim, E. H. (2018). Chromosomal instability-induced senescence potentiates cell non-autonomous tumourigenic effects. *Oncogenesis*, 7(8), 1-18.

He, Y., Qian, H., Liu, Y., Duan, L., Li, Y., & Shi, G. (2014). The roles of regulatory B cells in cancer. *Journal of immunology research*, 2014.

Hoevenaar, W. H., Janssen, A., Quirindongo, A. I., Ma, H., Klaasen, S. J., Teixeira, A., & Offerhaus, G. J. A. (2020). Degree and site of chromosomal instability define its oncogenic potential. *Nature communications*, 11(1), 1-11.

Holland, A. J., & Cleveland, D. W. (2009). Boveri revisited: chromosomal instability, aneuploidy and tumorigenesis. *Nature reviews Molecular cell biology*, 10(7), 478-487.

Ippolito, M. R., Martis, V., Martin, S., Tijhuis, A. E., Hong, C., Wardenaar, R., & Fachinetti, D. (2021). Gene copy-number changes and chromosomal instability induced by aneuploidy confer resistance to chemotherapy. *Developmental cell*, 56(17), 2440-2454. e2446.

Ishikawa, H., & Barber, G. N. (2008). STING is an endoplasmic reticulum adaptor that facilitates innate immune signalling. *Nature,* 455(7213), 674-678.

Janssen, A., & Medema, R. (2013). Genetic instability: tipping the balance. *Oncogene*, 32(38), 4459-4470.

Ju, X., Zhang, H., Zhou, Z., & Wang, Q. (2020). Regulation of PD-L1 expression in cancer and clinical implications in immunotherapy. *American journal of cancer research*, 10(1), 1.

Karlin, K. L., Mondal, G., Hartman, J. K., Tyagi, S., Kurley, S. J., Bland, C. S., & Migliaccio, I. (2014). The oncogenic STP axis promotes triple-negative breast cancer via degradation of the REST tumor suppressor. *Cell reports*, 9(4), 1318-1332.

Konno, H., Yamauchi, S., Berglund, A., Putney, R. M., Mulé, J. J., & Barber, G. N. (2018). Suppression of STING signaling through epigenetic silencing and missense mutation impedes DNA damage mediated cytokine production. *Oncogene,* 37(15), 2037-2051.

Lee, A. J., Endesfelder, D., Rowan, A. J., Walther, A., Birkbak, N. J., Futreal, P. A., & Howell, M. (2011). Chromosomal instability confers intrinsic multidrug resistance. *Cancer research*, 71(5), 1858-1870.

Lee, D. S., Rojas, O. L., & Gommerman, J. L. (2021). B cell depletion therapies in autoimmune disease: advances and mechanistic insights. *Nature reviews Drug discovery*, 20(3), 179-199.

Lewis Phillips, G., Guo, J., Kiefer, J. R., Proctor, W., Bumbaca Yadav, D., Dybdal, N., & Shen, B.-Q. (2022). Trastuzumab does not bind rat or mouse ErbB2/neu: implications for selection of non-clinical safety models for trastuzumab-based therapeutics. *Breast cancer research and treatment*, 191(2), 303-317.

Li, L., Xu, L., Yan, J., Zhen, Z.-J., Ji, Y., Liu, C.-Q., & Xu, J. (2015). CXCR2–CXCL1 axis is correlated with neutrophil infiltration and predicts a poor prognosis in hepatocellular carcinoma. *Journal of Experimental & Clinical Cancer Research,* 34(1), 1-10.

Li, M., Liu, Z., & Wang, X. (2018). Exploration of the combination of PLK1 inhibition with immunotherapy in cancer treatment. *Journal of oncology*, 2018.

Li, X., Yang, J., Peng, L., Sahin, A. A., Huo, L., Ward, K. C., & Meisel, J. L. (2017). Triple-negative breast cancer has worse overall survival and cause-specific survival than non-triple-negative breast cancer. *Breast cancer research and treatment*, 161(2), 279-287.

Li, Z., Li, J., Bi, P., Lu, Y., Burcham, G., Elzey, B. D., & Kuang, S. (2014). Plk1 phosphorylation of PTEN causes a tumor-promoting metabolic state. *Molecular and cellular biology*, 34(19), 3642-3661.

Liang, D., Xiao-Feng, H., Guan-Jun, D., Er-Ling, H., Sheng, C., Ting-Ting, W., & Ya-Yi, H. (2015). Activated STING enhances Tregs infiltration in the HPV-related carcinogenesis of tongue squamous cells via the c-jun/CCL22 signal. *Biochimica et Biophysica Acta (BBA)-Molecular Basis of Disease*, 1852(11), 2494-2503.

Lin, M.-C., Chen, S.-Y., He, P.-L., Luo, W.-T., & Li, H.-J. (2017). Transfer of mammary gland-forming ability between mammary basal epithelial cells and mammary luminal cells via extracellular vesicles/exosomes. *JoVE (Journal of Visualized Experiments)*(124), e55736.

Liu, A. M., Qu, W. W., Liu, X., & Qu, C.-K. (2012). Chromosomal instability in in vitro cultured mouse hematopoietic cells associated with oxidative stress. *American journal of blood research,* 2(1), 71.

Liu, B., Meng, L.-B., Su, J.-Z., Fan, B., Zhao, S.-B., Wang, H.-Y., & Ni, X.-C. (2022). PLK1 as one novel target for the poor prognosis of bladder cancer: An observational study. *Medicine*, 101(39), e30723.

Liu, H., Zhang, H., Wu, X., Ma, D., Wu, J., Wang, L., & Tan, R. (2018). Nuclear cGAS suppresses DNA repair and promotes tumorigenesis. *Nature*, 563(7729), 131-136.

Liu, X. S., Song, B., & Liu, X. (2010). The substrates of Plk1, beyond the functions in mitosis. *Protein & cell,* 1(11), 999-1010.

Liu, Z., Sun, Q., & Wang, X. (2017). PLK1, a potential target for cancer therapy. *Translational oncology,* 10(1), 22-32.

Love, M. I., Huber, W., & Anders, S. (2014). Moderated estimation of fold change and dispersion for RNA-seq data with DESeq2. *Genome biology*, 15(12), 1-21.

Luecke, S., Holleufer, A., Christensen, M. H., Jønsson, K. L., Boni, G. A., Sørensen, L. K., & Paludan, S. R. (2017). cGAS is activated by DNA in a length-dependent manner. *EMBO reports*, 18(10), 1707-1715.

Lukow, D. A., Sausville, E. L., Suri, P., Chunduri, N. K., Wieland, A., Leu, J., & Kendall, J. (2021). Chromosomal instability accelerates the evolution of resistance to anti-cancer therapies. Developmental cell, 56(17), 2427-2439. e2424.

Luo, W., & Brouwer, C. (2013). Pathview: an R/Bioconductor package for pathway-based data integration and visualization. *Bioinformatics,* 29(14), 1830-1831.

Mace, E. M., Bigley, V., Gunesch, J. T., Chinn, I. K., Angelo, L. S., Care, M. A., & Watkin, L. B. (2017). Biallelic mutations in IRF8 impair human NK cell maturation and function. *The Journal of Clinical Investigation*, 127(1), 306-320.

Maleki, S. S., & Röcken, C. (2017). Chromosomal instability in gastric cancer biology. *Neoplasia*, 19(5), 412-420.

Mazouzi, A., Velimezi, G., & Loizou, J. I. (2014). DNA replication stress: causes, resolution and disease. *Experimental cell research*, 329(1), 85-93.

McGranahan, N., & Swanton, C. (2017). Clonal heterogeneity and tumor evolution: past, present, and the future. *Cell*, 168(4), 613-628.

McLean, A. C., Valenzuela, N., Fai, S., & Bennett, S. A. (2012). Performing vaginal lavage, crystal violet staining, and vaginal cytological evaluation for mouse estrous cycle staging identification. *JoVE (Journal of Visualized Experiments)*(67), e4389.

Metzger-Filho, O., Tutt, A., De Azambuja, E., Saini, K. S., Viale, G., Loi, S., & Ellis, P. (2012). Dissecting the heterogeneity of triple-negative breast cancer. *Journal of clinical oncology*, 30(15), 1879-1887.

Miyagawa-Hayashino, A., Yoshifuji, H., Kitagori, K., Ito, S., Oku, T., Hirayama, Y., & Yamada, N. (2018). Increase of MZB1 in B cells in systemic lupus erythematosus: proteomic analysis of biopsied lymph nodes. *Arthritis research & therapy*, 20(1), 1-11.

Moasser, M. M., & Krop, I. E. (2015). The evolving landscape of HER2 targeting in breast cancer. *JAMA oncology*, 1(8), 1154-1161.

Moody, S. E., Sarkisian, C. J., Hahn, K. T., Gunther, E. J., Pickup, S., Dugan, K. D., & Chodosh, L. A. (2002). Conditional activation of Neu in the mammary epithelium of transgenic mice results in reversible pulmonary metastasis. *Cancer cell,* 2(6), 451-461.

Morimoto, R. I. (2008). Proteotoxic stress and inducible chaperone networks in neurodegenerative disease and aging. *Genes & development*, 22(11), 1427-1438.

Mougiakakos, D., Choudhury, A., Lladser, A., Kiessling, R., & Johansson, C. C. (2010). Regulatory T cells in cancer. *Advances in cancer research*, 107, 57-117.

Mukai, K., Konno, H., Akiba, T., Uemura, T., Waguri, S., Kobayashi, T., & Taguchi, T. (2016). Activation of STING requires palmitoylation at the Golgi. *Nature communications*, 7(1), 1-10.

Naeimi Kararoudi, M., Elmas, E., Lamb, M., Chakravarti, N., Trikha, P., & Lee, D. A. (2018). Disruption of SOCS3 promotes the anti-cancer efficacy of primary NK cells. *In: American Society of Hematology Washington, DC.*

Nedeljković, M., & Damjanović, A. (2019). Mechanisms of chemotherapy resistance in triple-negative breast cancer—how we can rise to the challenge. *Cells*, 8(9), 957.

Ni, H., Zhang, H., Li, L., Huang, H., Guo, H., Zhang, L., & Li, K. (2022). T cell-intrinsic STING signaling promotes regulatory T cell induction and immunosuppression by upregulating FOXP3 transcription in cervical cancer. *Journal for immunotherapy of cancer*, 10(9), e005151.

Nieto-Jimenez, C., Galan-Moya, E. M., Corrales-Sanchez, V., del Mar Noblejas-Lopez, M., Burgos, M., Domingo, B., . . . Esparis-Ogando, A. (2020). Inhibition of the mitotic kinase PLK1 overcomes therapeutic resistance to BET inhibitors in triple negative breast cancer. *Cancer Letters*, 491, 50-59.

Noronha, C., Ribeiro, A. S., Taipa, R., Leitão, D., Schmitt, F., Reis, J., & Paredes, J. (2022). PD-L1 tumor expression is associated with poor prognosis and systemic immunosuppression in glioblastoma. *Journal of neuro-oncology*, 156(3), 453-464.

Ohashi, A., Ohori, M., Iwai, K., Nakayama, Y., Nambu, T., Morishita, D., & Okaniwa, M. (2015). Aneuploidy generates proteotoxic stress and DNA damage concurrently with p53-mediated post-mitotic apoptosis in SAC-impaired cells. *Nature communications*, 6(1), 1-16.

Pavelka, N., Rancati, G., Zhu, J., Bradford, W. D., Saraf, A., Florens, L., & Li, R. (2010). Aneuploidy confers quantitative proteome changes and phenotypic variation in budding yeast. *Nature,* 468(7321), 321-325.

Pereira, B., Chin, S.-F., Rueda, O. M., Vollan, H.-K. M., Provenzano, E., Bardwell, H. A., & Sammut, S.-J. (2016). The somatic mutation profiles of 2,433 breast cancers refine their genomic and transcriptomic landscapes. *Nature communications*, 7(1), 1-16.

Petrucelli, N., Daly, M. B., & Pal, T. (2016). BRCA1-and BRCA2-associated hereditary breast and ovarian cancer.

Ponzetta, A., Sciumè, G., Benigni, G., Antonangeli, F., Morrone, S., Santoni, A., & Bernardini, G. (2013). CX3CR1 regulates the maintenance of KLRG1+ NK cells into the bone marrow by promoting their entry into circulation. *The Journal of Immunology*, 191(11), 5684-5694.

Raab, M., Sanhaji, M., Matthess, Y., Hörlin, A., Lorenz, I., Dötsch, C., & Firestein, R. (2018). PLK1 has tumor-suppressive potential in APC-truncated colon cancer cells. *Nature communications,* 9(1), 1-17.

Rakha, E. A., Abd El-Rehim, D., Paish, C., Green, A. R., Lee, A. H., Robertson, J. F., & Ellis, I. O. (2006). Basal phenotype identifies a poor prognostic subgroup of breast cancer of clinical importance. *European journal of cancer*, 42(18), 3149-3156.

Ramani, P., Nash, R., Sowa-Avugrah, E., & Rogers, C. (2015). High levels of polo-like kinase 1 and phosphorylated translationally controlled tumor protein indicate poor prognosis in neuroblastomas. *Journal of neuro-oncology*, 125(1), 103-111.

Rancati, G., Pavelka, N., Fleharty, B., Noll, A., Trimble, R., Walton, K., & Li, R. (2008). Aneuploidy underlies rapid adaptive evolution of yeast cells deprived of a conserved cytokinesis motor. *Cell,* 135(5), 879-893.

Raulet, D. H., & Guerra, N. (2009). Oncogenic stress sensed by the immune system: role of natural killer cell receptors. *Nature Reviews Immunology*, 9(8), 568-580.

Ricke, R. M., Jeganathan, K. B., & van Deursen, J. M. (2011). Bub1 overexpression induces aneuploidy and tumor formation through Aurora B kinase hyperactivation. *Journal of Cell Biology*, 193(6), 1049-1064.

Rodriguez, P. C., Quiceno, D. G., & Ochoa, A. C. (2007). L-arginine availability regulates T-lymphocyte cell-cycle progression. *Blood*, 109(4), 1568-1573.

Roschke, A. V., & Rozenblum, E. (2013). Multi-layered cancer chromosomal instability phenotype. *Frontiers in oncology*, 3, 302.

Rose, A. A., Annis, M. G., Dong, Z., Pepin, F., Hallett, M., Park, M., & Siegel, P. M. (2010). ADAM10 releases a soluble form of the GPNMB/Osteoactivin extracellular domain with angiogenic properties. *PloS one*, 5(8), e12093.

Rose, A. A., Pepin, F., Russo, C., Abou Khalil, J. E., Hallett, M., & Siegel, P. M. (2007). Osteoactivin promotes breast cancer metastasis to bone. *Molecular Cancer Research*, 5(10), 1001-1014.

Rosenthal, R., Cadieux, E. L., Salgado, R., Bakir, M. A., Moore, D. A., Hiley, C. T., & Joshi, K. (2019). Neoantigen-directed immune escape in lung cancer evolution. *Nature,* 567(7749), 479-485.

Rowald, K., Mantovan, M., Passos, J., Buccitelli, C., Mardin, B. R., Korbel, J. O., & Sotillo, R. (2016). Negative selection and chromosome instability induced by Mad2 overexpression delay breast cancer but facilitate oncogene-independent outgrowth. *Cell reports*, 15(12), 2679-2691.

Roylance, R., Endesfelder, D., Gorman, P., Burrell, R. A., Sander, J., Tomlinson, I., & Birkbak, N. J. (2011). Relationship of Extreme Chromosomal Instability with Long-term Survival in a Retrospective Analysis of Primary Breast Cancer. Relationship of Extreme CIN with Breast Cancer Prognosis. *Cancer epidemiology, biomarkers & prevention*, 20(10), 2183-2194.

Santaguida, S., Richardson, A., Iyer, D. R., M'Saad, O., Zasadil, L., Knouse, K. A., & Amon, A. (2017). Chromosome mis-segregation generates cell-cycle-arrested cells with complex karyotypes that are eliminated by the immune system. *Developmental cell,* 41(6), 638-651. e635.

Sawant, K. V., Sepuru, K. M., Lowry, E., Penaranda, B., Frevert, C. W., Garofalo, R. P., & Rajarathnam, K. (2021). Neutrophil recruitment by chemokines Cxcl1/KC and Cxcl2/MIP2: Role of Cxcr2 activation and glycosaminoglycan interactions. *Journal of leukocyte biology*, 109(4), 777-791.

Sawant, K. V., Xu, R., Cox, R., Hawkins, H., Sbrana, E., Kolli, D., & Rajarathnam, K. (2015). Chemokine CXCL1-mediated neutrophil trafficking in the lung: role of CXCR2 activation. *Journal of innate immunity*, 7(6), 647-658.

Schmitt, C., Ktorza, S., Sarun, S., Verpilleux, M.-P., Blanc, C., Deugnier, M.-A., & Debrea, P. (1995). CD34-positive early stages of human T-cell differentiation. *Leukemia & lymphoma*, 17(1-2), 43-50.

Schwab, M., Lohr, S., Schneider, J., Kaiser, M., Krunic, D., Helbig, D., & Angel, P. (2021). Podoplanin is required for tumor cell invasion in cutaneous squamous cell carcinoma. *Experimental Dermatology*, 30(11), 1619-1630.

Sheltzer, J. M., Ko, J. H., Replogle, J. M., Burgos, N. C. H., Chung, E. S., Meehl, C. M., & Amon, A. (2017). Single-chromosome gains commonly function as tumor suppressors. *Cancer cell*, 31(2), 240-255.

Shi, C., & Pamer, E. G. (2011). Monocyte recruitment during infection and inflammation. *Nature Reviews Immunology*, 11(11), 762-774.

Silk, A. D., Zasadil, L. M., Holland, A. J., Vitre, B., Cleveland, D. W., & Weaver, B. A. (2013). Chromosome missegregation rate predicts whether aneuploidy will promote or suppress tumors. *Proceedings of the National Academy of Sciences*, 110(44), E4134-E4141.

Soares, R. F., Garcia, A. R., Monteiro, A. R., Macedo, F., Pereira, T. C., Carvalho, J. C., & Póvoa, S. (2021). Prognostic factors for early relapse in non-metastatic triple negative breast cancer—real world data. *Reports of practical Oncology and radiotherapy*, 26(4), 563-572.

Sohn, M., Shin, S., Yoo, J.-Y., Goh, Y., Lee, I. H., & Bae, Y. S. (2018). Ahnak promotes tumor metastasis through transforming growth factor-β-mediated epithelial-mesenchymal transition. *Scientific reports*, 8(1), 1-10.

Song, B., Liu, X. S., Davis, K., & Liu, X. (2011). Plk1 phosphorylation of Orc2 promotes DNA replication under conditions of stress. *Molecular and cellular biology*, 31(23), 4844-4856.

Sotillo, R., Hernando, E., Díaz-Rodríguez, E., Teruya-Feldstein, J., Cordón-Cardo, C., Lowe, S. W., & Benezra, R. (2007). Mad2 overexpression promotes aneuploidy and tumorigenesis in mice. *Cancer cell,* 11(1), 9-23.

Soto, M., Raaijmakers, J. A., Bakker, B., Spierings, D. C., Lansdorp, P. M., Foijer, F., & Medema, R. H. (2017). p53 prohibits propagation of chromosome segregation errors that produce structural aneuploidies. *Cell reports*, 19(12), 2423-2431.

Stingele, S., Stoehr, G., Peplowska, K., Cox, J., Mann, M., & Storchova, Z. (2012). Global analysis of genome, transcriptome and proteome reveals the response to aneuploidy in human cells. *Molecular systems biology*, 8(1), 608.

Sun, L., Wu, J., Du, F., Chen, X., & Chen, Z. J. (2013). Cyclic GMP-AMP synthase is a cytosolic DNA sensor that activates the type I interferon pathway. *Science*, 339(6121), 786-791.

Swanton, C., Nicke, B., Schuett, M., Eklund, A. C., Ng, C., Li, Q., & East, P. (2009). Chromosomal instability determines taxane response. *Proceedings of the National Academy of Sciences*, 106(21), 8671-8676.

Taki, M., Abiko, K., Ukita, M., Murakami, R., Yamanoi, K., Yamaguchi, K., & Mandai, M. (2021). Tumor Immune Microenvironment during Epithelial–Mesenchymal Transition. The Review of the Loop Between EMT and Immunosuppression. *Clinical Cancer Research*, 27(17), 4669-4679.

Tamura, R., Tanaka, T., Yamamoto, Y., Akasaki, Y., & Sasaki, H. (2018). Dual role of macrophage in tumor immunity. *Immunotherapy*, 10(10), 899-909.

Tanaka, Y., & Chen, Z. J. (2012). STING specifies IRF3 phosphorylation by TBK1 in the cytosolic DNA signaling pathway. *Science signaling*, 5(214), ra20-ra20.

Thiery, J. P., & Sleeman, J. P. (2006). Complex networks orchestrate epithelial–mesenchymal transitions. *Nature reviews Molecular cell biology*, 7(2), 131-142.

Thompson, S. L., Bakhoum, S. F., & Compton, D. A. (2010). Mechanisms of chromosomal instability. *Current biology,* 20(6), R285-R295.

Thompson, S. L., & Compton, D. A. (2010). Proliferation of aneuploid human cells is limited by a p53-dependent mechanism. *Journal of Cell Biology*, 188(3), 369-381.

Thorsson, V., Gibbs, D. L., Brown, S. D., Wolf, D., Bortone, D. S., Yang, T.-H. O., & Eddy, J. A. (2018). The immune landscape of cancer. *Immunity*, 48(4), 812-830. e814.

Torres, E. M., Sokolsky, T., Tucker, C. M., Chan, L. Y., Boselli, M., Dunham, M. J., & Amon, A. (2007). Effects of aneuploidy on cellular physiology and cell division in haploid yeast. *Science*, 317(5840), 916-924.

Torres, N. P., Ho, B., & Brown, G. W. (2016). High-throughput fluorescence microscopic analysis of protein abundance and localization in budding yeast. *Critical reviews in biochemistry and molecular biology*, 51(2), 110-119.

Trakala, M., Partida, D., Salazar-Roa, M., Maroto, M., Wachowicz, P., de Cárcer, G., & Malumbres, M. (2015). Activation of the endomitotic spindle assembly checkpoint and thrombocytopenia in Plk1-deficient mice. *Blood, The Journal of the American Society of Hematology*, 126(14), 1707-1714.

Tripathi, R., Modur, V., Senovilla, L., Kroemer, G., & Komurov, K. (2019). Suppression of tumor antigen presentation during aneuploid tumor evolution contributes to immune evasion. *Oncoimmunology*, 8(11), 1657374.

Turner, M. D., Nedjai, B., Hurst, T., & Pennington, D. J. (2014). Cytokines and chemokines: At the crossroads of cell signalling and inflammatory disease. *Biochimica et Biophysica Acta (BBA)-Molecular Cell Research*, 1843(11), 2563-2582.

Tut, T. G., Lim, S., Dissanayake, I., Descallar, J., Chua, W., Ng, W., & Lee, C. S. (2015). 14. Upregulated PLK1 expression confers radiation resistance and poor patient survival outcomes in rectal cancer. *Pathology*, 47, S104-S105.

Uetake, Y., & Sluder, G. (2010). Prolonged prometaphase blocks daughter cell proliferation despite normal completion of mitosis. Current biology, 20(18), 1666-1671.

Van Allen, E. M., Miao, D., Schilling, B., Shukla, S. A., Blank, C., Zimmer, L., & Goldinger, S. M. (2015). Genomic correlates of response to CTLA-4 blockade in metastatic melanoma. *Science,* 350(6257), 207-211.

Vitale, M., Chiesa, M. D., Carlomagno, S., Romagnani, C., Thiel, A., Moretta, L., & Moretta, A. (2004). The small subset of CD56brightCD16–natural killer cells is selectively responsible for both cell proliferation and interferon-γ production upon interaction with dendritic cells. *European journal of immunology*, 34(6), 1715-1722.

Vitre, B. D., & Cleveland, D. W. (2012). Centrosomes, chromosome instability (CIN) and aneuploidy. *Current opinion in cell biology*, 24(6), 809-815.

Waltman, L., & Van Eck, N. J. (2013). A smart local moving algorithm for large-scale modularity-based community detection. *The European physical journal* B, 86(11), 1-14.

Wang, H., Hu, S., Chen, X., Shi, H., Chen, C., Sun, L., & Chen, Z. J. (2017). cGAS is essential for the antitumor effect of immune checkpoint blockade. *Proceedings of the National Academy of Sciences*, 114(7), 1637-1642.

Wang, R. W., Vigano, S., Ben-David, U., Amon, A., & Santaguida, S. (2021). Aneuploid senescent cells activate NF-κB to promote their immune clearance by NK cells. *EMBO reports*, 22(8), e52032.

Waskom, M. L. (2021). Seaborn: statistical data visualization. *Journal of Open Source Software*, 6(60), 3021.

Watkins, T. B., Lim, E. L., Petkovic, M., Elizalde, S., Birkbak, N. J., Wilson, G. A., & Dewhurst, S. M. (2020). Pervasive chromosomal instability and karyotype order in tumour evolution. *Nature,* 587(7832), 126-132.

Wickham, H. (2016). Data analysis. In ggplot2 (pp. 189-201): *Springer.*

Wierer, M., Verde, G., Pisano, P., Molina, H., Font-Mateu, J., Di Croce, L., & Beato, M. (2013). PLK1 signaling in breast cancer cells cooperates with estrogen receptor-dependent gene transcription. *Cell reports*, 3(6), 2021-2032.

Williams, B. R., Prabhu, V. R., Hunter, K. E., Glazier, C. M., Whittaker, C. A., Housman, D. E., & Amon, A. (2008). Aneuploidy affects proliferation and spontaneous immortalization in mammalian cells. *Science*, 322(5902), 703-709.

Woo, S.-R., Fuertes, M. B., Corrales, L., Spranger, S., Furdyna, M. J., Leung, M. Y., & Fitzgerald, K. A. (2014). STING-dependent cytosolic DNA sensing mediates innate immune recognition of immunogenic tumors. *Immunity*, 41(5), 830-842.

Wu, T., Hu, E., Xu, S., Chen, M., Guo, P., Dai, Z., . . . Zhan, L. (2021). clusterProfiler 4.0: A universal enrichment tool for interpreting omics data. *The Innovation*, 2(3), 100141.

Xian, S., Dosset, M., Almanza, G., Searles, S., Sahani, P., Waller, T. C., & Zanetti, M. (2021). The unfolded protein response links tumor aneuploidy to local immune dysregulation. *EMBO reports,* 22(12), e52509.

Xu, D., Li, J., Li, R.-Y., Lan, T., Xiao, C., & Gong, P. (2019). PD-L1 expression is regulated by NF-κB during EMT signaling in gastric carcinoma. *OncoTargets and therapy*, 12, 10099.

Xun, R., Lu, H., & Wang, X. (2020). PLK1 Is Implicated in the Poor Prognosis of Hepatocellular Carcinoma. *Yangtze Medicine*, 4(03), 193.

Yu, W., Hua, Y., Qiu, H., Hao, J., Zou, K., Li, Z., & Sui, S. (2020). PD-L1 promotes tumor growth and progression by activating WIP and β-catenin signaling pathways and predicts poor prognosis in lung cancer. *Cell death & disease*, 11(7), 1-16.

Zasadil, L. M., Britigan, E. M., Ryan, S. D., Kaur, C., Guckenberger, D. J., Beebe, D. J., & Weaver, B. A. (2016). High rates of chromosome missegregation suppress tumor progression but do not inhibit tumor initiation. *Molecular biology of the cell*, 27(13), 1981-1989.

Zasadil, L. M., Britigan, E. M., & Weaver, B. A. (2013). 2n or not 2n: Aneuploidy, polyploidy and chromosomal instability in primary and tumor cells. *Paper presented at the Seminars in cell & developmental biology.*

Zhan, Y., Wang, N., Vasanthakumar, A., Zhang, Y., Chopin, M., Nutt, S. L., & Lew, A. M. (2020). CCR2 enhances CD25 expression by FoxP3+ regulatory T cells and regulates their abundance independently of chemotaxis and CCR2+ myeloid cells. *Cellular & molecular immunology*, 17(2), 123-132.

Zhang, R., Shi, H., Ren, F., Liu, H., Zhang, M., Deng, Y., & Li, X. (2015). Misregulation of polo-like protein kinase 1, P53 and P21WAF1 in epithelial ovarian cancer suggests poor prognosis. *Oncology Reports*, 33(3), 1235-1242.

Zhang, Y., Gui, M., Wang, Y., Mani, N., Chaudhuri, S., Gao, B., & Dumas, S. N. (2021). Inositol-Requiring Enzyme 1α–Mediated Synthesis of Monounsaturated Fatty Acids as a

Driver of B Cell Differentiation and Lupus-like Autoimmune Disease. *Arthritis & Rheumatology*, 73(12), 2314-2326.

Zheng, G. X., Terry, J. M., Belgrader, P., Ryvkin, P., Bent, Z. W., Wilson, R., & Zhu, J. (2017). Massively parallel digital transcriptional profiling of single cells. *Nature communications*, 8(1), 1-12.

Zierhut, C., Yamaguchi, N., Paredes, M., Luo, J.-D., Carroll, T., & Funabiki, H. (2019). The cytoplasmic DNA sensor cGAS promotes mitotic cell death. *Cell*, 178(2), 302-315. e323.
Zou, W. (2006). Regulatory T cells, tumour immunity and immunotherapy. *Nature Reviews Immunology*, 6(4), 295-307.

8. Publications

The following manuscript contains contributions that were not a part of this thesis

Acquisition of chromosome instability is a mechanism to evade oncogene addiction

Lorena Salgueiro[1], Christopher Buccitelli[2], Konstantina Rowald[1], Kalman Somogyi[1], Sridhar Kandala[1], Jan O Korbel[2] & Rocio Sotillo[1,3]

[1]Division of Molecular Thoracic Oncology, German Cancer Research Center (DKFZ), Im Neuenheimer Feld 280, 69120 Heidelberg, Germany
[2] Genome Biology Unit, European Molecular Biology Laboratory (EMBL), Heidelberg, Germany
[3] Translational Lung Research Center Heidelberg (TRLC), German Center for Lung Research (DZL)

EMBO Molecular Medicine. DOI: **https://doi.org/10.15252/emmm.201910941**

9. Acknowledgements

I would like to use this opportunity to express my sincere gratitude to everyone who helped me during these four and half years. Without the continuous support and encouragement from the people around me, this would have never been possible. Through all of it, my supervisor Dr. Rocio Sotillo has been very supportive without giving up on me. I would like to pay my gratitude for that. I also want to thank her for giving me an opportunity to work in her lab. I am also extremely grateful to my TAC members Dr. Hans-Reimer Rodewald, Dr. Benedikt Brors, Dr. Sylvia Erhardt and Dr. Guoliang Cui for their valuable insights and feedback during my TAC meetings.

I am very much indebted to our collaborators Dr. Benedikt Brors, Dr. Charles Imbusch, Dr. Lena Voith von Voithenberg for agreeing to help me with the analysis of the single cell data and providing very valuable inputs. A special thanks to Lena again for making sure that we stayed on time for the meetings, manuscript submission and for handling the single cell analysis part. I am also grateful to Simone Kraut, Dr. Kalman Somogyi and Vanessa Neubauer for their technical assistance in the lab. The Helmholtz association that funded my research and the DKFZ graduate school headed by Dr. Lindsay Murrells who supported me during my time as a PhD student also deserve my appreciation.

Furthermore, I want to convey my gratitude to Dr. Anand Mayakonda for teaching me the basics of bioinformatics and introducing me to the world of high throughput sequencing data analysis. It has been a privilege of getting to know him during this journey and will remain one of my best friends for life. A big thank you to Ms. Hilary Davies-Rück for helping me with the proofreading and German translations and for all the office support during my stay at Heidelberg.

I would like to acknowledge all the members of the Sotillo lab who have helped me during this endeavor. I would especially like to mention Dr. Yuanyuan Chen, Rangeet Manna Dr. Lorena Salgueiro, Pan Fan, Sara Chocarro, Alicia Alonso, Alberto Diaz and Maria.

This section would not be finished without mentioning my wife Ms. Susmitha Nettu who has been a pillar of support. Last but definitely not the least, I want to thank my brother Dr. Bhargava Kandala who has been an inspiration both as a graduate student and as a scientist, and my parents Mr. Satyanarayana Murthy Kandala and Mrs. Nagamani Kandala (back home in India) who gave their unconditional support through these four years.